

Master's thesis

**Electric vehicle fast charging
with energy storage and
generation capabilities -
Simulations based on real
charging data**

Lena Rohde

ie3-number : ie3-20.005
Supervisor : Prof. Dr.-Ing. Christian Rehtanz
Prof. Dr.-Ing. Pertti Järventausta
Dr.-Ing. Kalle Rauma
Submitted : February 3rd 2020

Acknowledgements

I would like to express my very great appreciation to Prof. Pertti Järventausta for the possibility of visiting Tampere University as part of my thesis. I would like to thank Prof. Rehtanz to make this visit possible. My grateful thanks are extended to Kalle Rauma for his advice and assistance especially during the writing process. I would like to thank the company Fortum Charge and Drive for the provided charging data. My special thanks are extended to the colleges I met at Tampere University and my friends from Dortmund and Tampere.

Abstract

The increasing use of electric vehicles (EV) brings up the need to invest in the charging infrastructure and extend the number of charging sites and stations. Especially the integration of fast charging sites increases the convenience for the user. The growing utilization of charging sites is also a chance to learn about charging behaviour and future needs. In this thesis, usage data of a charging site in Norway is processed by a self-developed modelling tool, to create charging profiles based on the measured energy data. Additionally an optimized peak-shaving approach is examined. The capabilities and influence of an integrated battery electric storage (BES) system and a photovoltaic (PV) system on the charging profiles are analysed. The peak-shaving reaches values between 30 % and 60 % depending on the BES and PV configuration. Based on the results, differences and patterns in the charging behaviour are visible on a weekly and monthly basis. The results of the peak-shaving indicate a correlation of higher peak-shaving with a increasing BES capacity. The PV system introduces more flexibility to the charging site that implies more independence of the grid.

Contents

1. Introduction	1
1.1. Goal of the thesis	5
2. State-of-the-art	6
2.1. Electric vehicle charging and design of a charging Site	6
2.2. Comparison of common battery types and their application and operation	10
2.2.1. Renewable energy on demand by using energy storage systems	11
2.2.2. Diversity of energy storage systems	12
2.2.3. Electrochemical energy storages	12
2.3. Optimization technologies in power systems	14
2.3.1. Optimization problems	14
2.3.2. Common optimization problem solving algorithms and their applications	16
2.4. Programming in Python	20
3. Charging Profile Modelling tool	21
3.1. Used <i>Python</i> modules	22
3.1.1. <i>matplotlib</i>	22
3.1.2. <i>NumPy</i>	23
3.1.3. <i>pandas</i>	23
3.1.4. <i>SciPy</i>	24
3.1.5. <i>sqlite3</i>	24
3.2. Process in the Charging Profile Modelling tool	25
3.2.1. Properties of measurement database	26
3.2.2. Modelling of the charging profiles	28
3.2.3. Writing charging profiles to a database	30
3.3. Structure of the Charging Profile Modelling tool	31

4. Extension of the Charging Profile Modelling tool with a peak-shaving optimization of a BES and a PV system	36
4.1. Optimization problem for using a BES system to supply a DC charging site	37
4.1.1. Objective function	38
4.1.2. Constraints and boundaries	38
4.2. Optimization problem for using a PV and BES system to supply a DC charging site	39
4.2.1. Objective function	40
4.2.2. Boundaries and constraints	40
4.2.3. Modelling of the solar power output	41
4.3. Developed optimization for peak-shaving and the used algorithm in <i>Python</i>	43
5. Use Case: Evaluation of Charging Profile Modelling tool and three DC charging sites in Norway	46
5.1. Results of the Charging Profile Modelling tool	48
5.1.1. Evaluation of the results on each weekday	48
5.1.2. Evaluation of the results on monthly basis	51
5.2. Results of the peak-shaving optimization	55
5.2.1. Results of the BES-only peak-shaving optimization	55
5.2.2. Results of the combined BES and PV peak-shaving optimization	66
6. Discussion	79
6.1. Discussion of the results of the Charging Profile Modelling tool	79
6.1.1. Discussion of the results on each weekday	79
6.1.2. Discussion of the results on monthly basis	80
6.2. Discussion of the peak-shaving optimization	81
6.2.1. Discussion of the results of the BES system optimization for peak-shaving	81
6.2.2. Discussion of the results of the combined BES and PV system optimization for peak-shaving	82
6.3. Summary of the discussion	83
7. Conclusion	85

8. Future Work	86
8.1. Analysing more data	86
8.2. Vary the peak-shaving optimization	86
8.3. Improving the Charging Profile Modelling	87
8.4. Accuracy of the charging profiles	88
A. Appendix	89
A.1. Cases for the peak-shaving optimization	89
A.2. Results of weekly evaluation of charging sites A&B	93
A.3. results of monthly evaluation of charging sites A&B	96
A.4. Results of peak-shaving optimization with the BES for charging sites A & B	101
A.5. Results of peak-shaving optimization with BES and PV system for charging sites A & B	107
Bibliography	113

List of Figures

2.1. Setup of a common charging site containing several chargers, electric vehicles (EV) as well as a grid connection	7
3.1. Process in the Charging Profile Modelling divided into three parts: the pre-process, the main process, the data visualization	25
3.2. Measured charging profile of a Tesla Model S for modelling charging profiles from energy data	29
3.3. Structure of the Charging Profile Modelling	32
4.1. Setup of a charging site containing several chargers, several EVs, a grid connection, and a battery energy storage (BES) system	37
4.2. Setup of a charging site containing several chargers, EV, a grid connection, a BES system, and photovoltaic (PV) panels	40
4.3. Parameter for the solar irradiance model	42
4.4. Program process extended with the Optimization of PV and/or BES system as well as plotting the output	43
4.5. Optimization flow diagram with the charging profiles as input database	44
5.1. Mean of all Mondays to Fridays in the observation period from charging site C	49
5.2. Mean of all Saturdays and Sundays in the observation period from charging site C	50
5.3. Monthly evaluation of the charging profiles on a daily basis (Charging Site C)	53
5.4. Monthly evaluation of the charging profiles on a 24h basis (Charging Site C)	54
5.5. Evaluation of the peak-shaving optimization with the BES system in a low demand scenario (Charging Site C; 25 & 50 kWh)	58
5.6. Evaluation of the peak-shaving optimization with the BES system in a low demand scenario (Charging Site C; 100 & 150 kWh)	59

5.7. Evaluation of the peak-shaving optimization with the BES system in a medium demand scenario (Charging Site C; 25 & 50 kWh)	61
5.8. Evaluation of the peak-shaving optimization with the BES system in a medium demand scenario (Charging Site C; 100&150 kWh)	62
5.9. Evaluation of the peak-shaving optimization with the BES system in a high demand scenario (Charging Site C; 25 & 50 kWh)	64
5.10. Evaluation of the peak-shaving optimization with the BES system in a high demand scenario (Charging Site C; 100 & 150 kWh)	65
5.11. Evaluation of the peak-shaving optimization with the BES combined with a PV system in a low irradiance scenario (Charging Site C; 25 kWh, 20 & 40 kW)	69
5.12. Evaluation of the peak-shaving optimization with the BES combined with a PV system in a low irradiance scenario (Charging Site C; 150 kWh, 20 & 40 kW)	70
5.13. Evaluation of the peak-shaving optimization with the BES combined with a PV system in a medium irradiance scenario (Charging Site C; 25 kWh, 20 & 40 kW)	72
5.14. Evaluation of the peak-shaving optimization with the BES combined with a PV system in a medium irradiance scenario (Charging Site C; 150 kWh, 20 & 40 kW)	73
5.15. Evaluation of the peak-shaving optimization with the BES combined with a PV system in a high irradiance scenario (Charging Site C; 25 kWh, 20 & 40 kW)	76
5.16. Evaluation of the peak-shaving optimization with the BES combined with a PV system in a high irradiance scenario (Charging Site C; 150 kWh, 20 & 40 kW)	77
A.1. Mean of all Mondays to Fridays in the observation period from charging site A	93
A.2. Mean of all Saturdays and Sundays in the observation period from charging site A	94
A.3. Mean of all Mondays to Fridays in the observation period from charging site B	94
A.4. Mean of all Saturdays and Sundays in the observation period from charging site B	95

A.5. Monthly evaluation of the charging profiles on a daily basis (Charging Site A)	97
A.6. Monthly evaluation of the charging profiles on a 24h basis (Charging Site A)	98
A.7. Monthly evaluation of the charging profiles on a daily basis (Charging Site B)	99
A.8. Monthly evaluation of the charging profiles on a 24h basis (Charging Site B)	100
A.9. Monthly evaluation of the charging profiles with BES system on a 24h basis (Charging Site A, low demand)	101
A.10. Monthly evaluation of the charging profiles with BES system on a 24h basis (Charging Site A, medium demand)	102
A.11. Monthly evaluation of the charging profiles with BES system on a 24h basis (Charging Site A, high demand)	103
A.12. Monthly evaluation of the charging profiles with BES system on a 24h basis (Charging Site B, low demand)	104
A.13. Monthly evaluation of the charging profiles with BES system on a 24h basis (Charging Site B, medium demand)	105
A.14. Monthly evaluation of the charging profiles with BES system on a 24h basis (Charging Site B, high demand)	106
A.15. Monthly evaluation of the charging profiles with BES and PV system on a 24h basis (Charging Site B, low PV power)	107
A.16. Monthly evaluation of the charging profiles with BES and PV system on a 24h basis (Charging Site B, medium PV power)	108
A.17. Monthly evaluation of the charging profiles with BES and PV system on a 24h basis (Charging Site B, high PV power)	109
A.18. Monthly evaluation of the charging profiles with BES and PV system on a 24h basis (Charging Site A, low PV power)	110
A.19. Monthly evaluation of the charging profiles with BES and PV system on a 24h basis (Charging Site A, medium PV power)	111
A.20. Monthly evaluation of the charging profiles with BES and PV system on a 24h basis (Charging Site A, high PV power)	112

List of Tables

2.1. Charger types for direct current (DC) and alternating current (AC) charging of electric vehicles (EVs) listed by region	8
3.1. Examples for input database entries. Charging event at index 1) general, 2) until after midnight, 3), and 4) split of 2)	26
3.2. Possible output format and the time resolution of 24 hours	28
3.3. Example for the <i>SQLite</i> database regarding the merging of two charging events at one charging station	30
3.4. Example for the <i>SQLite</i> database regarding the merging of two charging stations at one charging site	30
3.5. Properties of the parent classes <i>BatteryElectricVehicle</i> and <i>DCCharger</i>	33
3.6. Properties of the child class <i>ChargingStationBatteryElectricVehicle</i> .	34
3.7. Properties of the <i>DBSQLite</i> class including a <i>pandas</i> DataFrame (see sec. 3.1.3)	35
4.1. Calculation of Factor p to model the solar irradiance seasonally . . .	42
5.1. Key data of the analysed charging sites that are located in Norway .	46
5.2. Statistical analysis of the mean value of charging profiles per week-day, in <i>kWh</i>	50
5.3. Statistical analysis of the mean value of charging profiles per month, in <i>kWh</i>	52
5.4. Peak-decrease with the BES system in different sizes of Capacity and power for each demand scenario (Charging site C)	66
5.5. Peak-decrease with BES and PV system over the examined scenarios	78
A.1. All cases for BESS and PV optimization of different PV irradiance, PV Power, BESS capacity and BESS power	92

List of Acronyms

AC	alternating current
BES	battery electric storage
CCS	Combined Charging System
CHAdeMO	CHArge de MOve
CHP	combined heat and power
CPM	charging profile modelling
DC	direct current
DP	dynamic programming
EV	electric vehicle
HV	high voltage
LP	linear programming
LV	low voltage
MV	medium voltage
N-dim	multi-dimensional
NP	Non-Linear Programming
OO	object-oriented
PV	photovoltaic
QP	quadratic programming
SoC	state of charge
SQL	Structured Query Language

1. Introduction

The key targets for 2020 in the EU climate action are "20% less greenhouse gas emissions compared with 1990, a total of 20% energy consumption from renewable energy, 20% increase of energy efficiency" [1]. These goals embrace the annually growing consumption of electrical energy world wide [2]. The European society failed the 2020 goals in transportation sector by increasing by 26% [3], and those for 2040 are higher: at least 40% less emissions (1990), 32% renewable energy of the total consumption, and 32.5% more energy efficiency. [1]

To reach the 2040 targets the development and research of new technologies is ongoing as well as the combination of existing technologies. Those energy solutions need to be more sustainable, efficient, and produce less emissions. Around 24.6% percent of the total emissions are from the transportation sector [3]. To reduce the amount caused by transportation one of the most emerging technologies is the electric vehicle (EV).

Used as transportation in cities EVs reduce the emission of pollution caused by traffic. This is mostly desirable in large cities where huge amounts of people live and many cars are used. This does not only include private cars but also taxis and buses. To reduce the carbon dioxide (CO_2) and nitrogen oxides (NO_x) emissions EVs are interesting for Germany as well. They reduce the CO_2 and NO_x emissions in cities so the legal limits are satisfied. Of course the fine dust by tire abrasion is still existent. [4]

EVs are of interest because they do not have a combustion engine. Basically a battery supplies a most often gear-less DC-motor, which drives the vehicle. Electricity is the fuel, and it has the advantage that it is possible to use renewable energy sources (p.e. Solar, Wind, Water). The reduction of pollution during driving an EV makes it more sustainable and environmentally friendly than driving with combustion engines. On the down side most electricity is still generated in conventional power plants that are burning fossil fuels to produce electric energy. When an EV charges this conventionally generated electricity, another conversion step is added instead of directly using fossil fuel. This reduces the overall efficiency and the energy that is

gained from the fossil fuel. It also eliminates the advantage of less CO_2 emission. Conventional generated electricity has higher CO_2 emissions than renewable generated electricity and results therefore in higher emissions mitigation costs. [5]

Due to this fact it is preferable to use renewable sources to produce the charging power of EVs. This adds another problem: The power grid can suffer under high penetration of renewable sources. Changing weather conditions (solar, wind) are causing an intermittent energy supply. A difference between supplied energy and load causes an power imbalance in the grid. This imbalance causes frequency stability problems in the power grid. To prevent such an imbalance between demand and supply due to the intermittent renewable generation an energy buffer is needed in the grid. This can flatten the intermittent power. Such an energy buffer is an energy storage system. There are many different systems (see sec. 2.2).

The development and research in the field of EVs impacts the research and improvement of larger-scale battery systems. One objective to improve the efficiency of EVs is to develop lighter batteries and/or increase capacity. The development of more efficient batteries is forwarding the research on battery electric storage (BES) in general. The increasing efficiency and capacity in batteries of EVs leads to increasing efficiency and capacity in stationary battery systems as well. The price of the technologies is related. Due to higher production margins of each component EVs battery prices are decreasing. The price of the components for similar energy systems of different size than the EVs battery decreases as well.

Instead of gas stations the EV is 'refuelled' at a charging station. There are different kinds of charging stations. The two categories of charging possibilities are: DC (fast, medium) and AC (slow, medium) charging. In each category are several charger types, charging power or possible locations for charging sites (see. chap. 2.1).

A limitation of EVs compared with combustion engines is the range an EV is able to drive with one charge. The maximum range can differ between 60 to 610 *km* depending on the manufacturer, the model, and the installed battery [6]. The range that can be reached maximally is also dependent on the temperature. The outside temperature influences the charging energy of the battery.

A solution to determine the range issue of EVs is the use of a range extender in the vehicle itself or to have a Plug-in-hybrid vehicle. Both types still use an amount of gasoline to extend the range. The dependency on fossil fuel is continuing. The extension of the range can be up to 500 *km*. The charging of the battery is still required. alternating current (AC) charging is often related with long charging times

when charging at home or at work. This is another drawback compared to the short time of refilling a conventional vehicle. The longer charging times are inconvenient especially for long-distance travels.

One approach to have a full battery within several minutes is a battery swap at a swapping station. This idea is only working when there is an economical battery recycling system that is in the best case also environment friendly and resource saving. [7, 8]

Another approach is direct current (DC) fast charging. The most common fast charging types are *CHArge de MOve (CHAdeMO)* and *Combined Charging System (CCS)* (see. chap. 2.1). To make this more attractive for the user an increasing number and density of DC fast charging sites is needed. Those charging stations can charge between 120 and 480V [9]. This is resulting in charging times of 40min to 80% with 480V fast charging, and more than 11.5h to charge to 100% for 240V charging or less. The range limitation forces the driver to stop for a break. Breaks during long distance travels are anyway necessary for the driver to ensure safe driving. Fast charging enables to reduce the break to under one hour.

The location of those charging sites can be in city centres to offer a public fast recharge of EVs. These are useful for people who do not have access to EV charging at home or at work. Those fast charging sites can be located outside the cities as well. Next to the highways they provide charging to people who need to travel distances beyond cities. It is not needed to be present while the EV charges. This enables the EV user to spent the time on different purposes during the charging process. One concrete example is grocery shopping after work in a store next to the charging site. Therefore it is more attractive to users if there are places nearby the charging station where the charging time can be spent usefully.

There is a problem with fast charging sites and charging sites in general. The amount of energy consumption is adding up with other loads located in the grid. Charging sites are mostly needed and can be economically feasible in areas where many people live or passing by. The grid in highly populated areas may have transformer capacity additionally to the daily load. In rural areas for example near highways where many people are passing by the capacity of the transformers may not be enough to supply also the charging of EVs. [10]

If many EVs are charged, it can cause an additional peak time that causes stress to the grid. In addition to the previous daily consumption the EV load stresses the grid and its components to its voltage and frequency limits. This can cause overloads of transformers and cables.

If a transformer is not able to deliver the demanded energy without overloading, the grid suffers under great stress and assets may be destroyed. If there is an imbalance between demanded and supplied energy, it can cause an instability in the grid. If the caused frequencies are below 49.9Hz , the primary operating reserve in the grid is fully activated. The overall grid stability would be in danger if the other reactions to restore the frequency stability failed. [11]

If there is an increasing number of charging sites, the impact on the grid may not be in a desired way. To prevent an instability one solution is to make costly investments in transformers with a higher capacity and cables that are designed for higher power. This makes sure that the demanded energy can be transported by the grid without a bottleneck.

Most of the time the demanded energy is within the components limits, but there is a peak time every day. To cover this peak, a transformer with higher capacity may be needed, but the surplus capacity is unnecessary during non-peak time. There are components which can make the grid more flexible.

Those components are for example decentralized energy generation systems. Energy generation systems can be small-scale combustion engines like micro turbines or fuel cells. The generation systems have often a higher efficiency when they are used in combined heat and power (CHP). In CHP systems the waste heat is used from the combustion systems. One example for an application is the heating of a building that is co-located to the charging site. If there are charging sites without any co-located buildings that need to be heated, a CHP system is less efficient and therefore infeasible. The combustion engines are using mostly fossil fuels or hydrogen, which is also mostly produced from fossil materials. [12]

Another technology that provides flexibility to a power grid is a stationary energy storage systems. They are flexible in the sense that they can store energy in times of low utilisation of the station and can supply the charging site during high peaks. This is called "peak-shaving". The most know storage system is the electro-chemical, which has the operational principle like a conventional battery used as power source for small electronic devices. [13]

For supportive systems, battery systems may be most feasible. There are different solutions (see sec. 2.2). The most used kind of battery system is the Lithium-Ion battery. They are available in different sizes. They are used for mobile electric devices as well as for EVs. There are several other types of battery storage systems. Another system used in power grids are Redox-Flow battery systems (see sec. 2.2)

1.1. Goal of the thesis

In this thesis the main objectives are to develop a tool in *Python* (see Sec. 2.4) that is able to model charging profiles from real measurement data of a DC fast charging site for EVs¹ and a peak shaving optimization to show the impacts of integrated energy sources on the charging profiles.

The real data is processed by the developed tool from the single energy values into the charging profiles over the given charging time. This enables an overview how much energy is charged at each time of the day. Monthly and weekly observations are possible as well. In this shape the charging data can be analysed and used for further applications. For charging site operators it is helpful to know what kind of charging profile each station has, to plan the operation and also know the impact of a site on the grid. The less a fast charging site impacts the power grid the cheaper is the operation of the site. This charging profile modelling (CPM) Tool is completed with the peak-shaving optimization that integrates a photovoltaic (PV) and a BES system into the charging site. This shows how both systems impact the grid demand of the charging site regarding peak-shaving. Both tools are evaluated (Chap. 5) and validated (Chap. 6) later on with examples from the real charging data kindly provided by Fortum Charge & Drive. Finally the results are concluded (Chap. 7) and future perspectives are suggested (Chap. 8).

The thesis is based on the idea from [14]. In that thesis a tool is implemented to model the charging profiles in Java. He also implemented a peak-shaving optimization with a BES system in *Matlab*. He also approached to add a PV system to the site. In contrast, in this thesis the approach is the development of a holistic tool set in *Python*. The tool set includes modelling of the charging profiles, optimizing the peak-decrease, and plotting the results in a general way. The tool set is implemented as scripts and classes so that they could be easily used as back-end for a GUI application.

¹In the context of the thesis the EV means a electric vehicle that contains only a battery system as energy source.

2. State-of-the-art

Today new technologies are developing fast. To give an overview on EV charging this chapter presents the state of the art of related topics. Firstly charging of EV and different architectures of charging sites are presented. In the second section battery types are compared and their different applications examined. Furthermore optimization technologies are evaluated and presented how they are used to improve power systems. Finally programming in *Python* is introduced firmly.

2.1. Electric vehicle charging and design of a charging Site

There are two options to charge a EV. The first option is the charging via AC. The advantage with AC charging is that it is possible at normal plugs in households. The batteries inside the EV need DC. During charging, the AC from the plug is converted to DC inside the EV. AC is transmitted in today's meshed grids. The transport over long distances is possible with a small amount of losses due to the high voltage (HV) levels in the transmission grid. This method of charging usually takes several hours depending on the battery size of the EV. The AC chargers require power between $16A(3.7kWh)$ and $63A(43kWh)$. This method is suitable for places where the car is parked longer than $20min$ for example next to offices and accommodations. The installation and operational costs are lower which is reflected in the charging price. [15]

The alternative is DC charging also often referred to as "fast charging". The AC from the grid is converted inside the charging station into DC. ¹ A DC charging station requires around $125A$. With a voltage level of around $400V$ a station can provide $50kW$ power in one hour to the EV. This enables a quick recharge especially interesting for long-distant trips. Their location is most feasible next to highways. The charging costs are in general higher due to higher operational and installation costs. [15]

¹The term "charging station" in this context means a single charging station (pole). To draw a difference to more than one charging station respectively a group of charging stations, which is comparable to a classic filling station for fossil fuel, the term "charging site" is used.

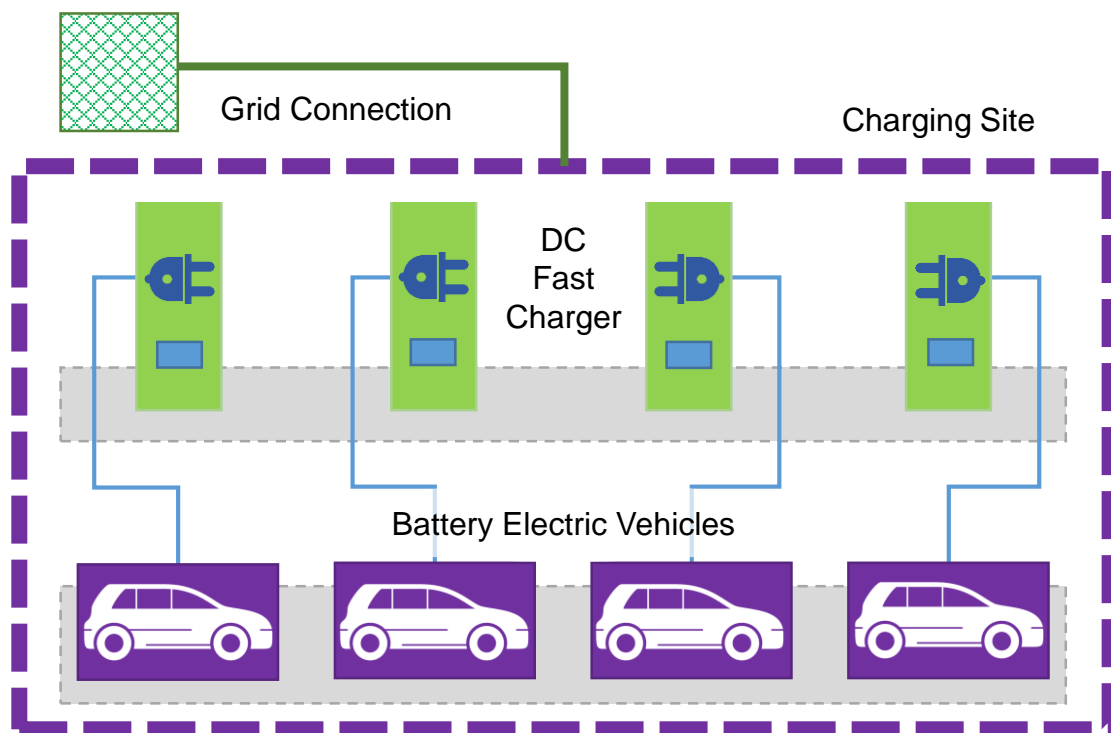


Figure 2.1.: Setup of a common charging site containing several chargers, electric vehicles (EV) as well as a grid connection

The different types of charger are listed in Table 2.1. There are basically four regions with different charger types: Japan, America, Europe (and other countries) as well as China. The typical charger types depend on the standards in the countries as well as on the regional manufacturers of EVs. EVs from Japan have AC charger of "Type 1" and DC charger of type "CHAdeMO". In America it is common to use for AC charging also "Type 1" but for DC charging "CCS1" is used. It looks similar to "Type 1" but has added the DC connection below. In Europe and the rest of the world the commonly used charger is "Type 2" for AC charging and "CCS2" for DC charging. Here is also a similarity to the "Type 2" charger and also to "CCS1". In China the charger for both charging types is called "GB/T" although they have a different structure. This thesis focusses on the public DC fast charging. A structural example of an charging site is given in Figure 2.1. Depending on the number of chargers, one or more EV can charge at a DC fast charging station. It is also possible to have different charger types (see Tab. 2.1) at one charging station. This enables more flexibility for the operator as well as for the customer. The customer can charge independently despite which model his EV is and from which manufacturer. The operator supplies as many customers as possible by providing them flexibility and convenience. The fast charging can be used for a few minutes, to charge energy to reach the

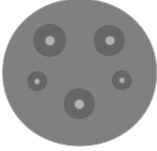
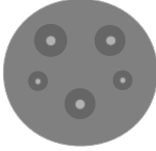
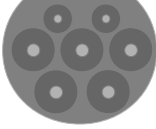


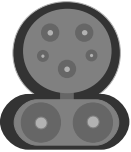
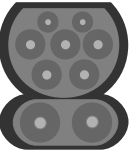
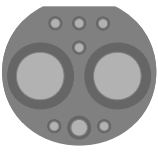
	Region			
Current type	Japan	America	Europe, rest of world	China
AC				
Plug name	Type1 (or J1772)	Type1 (or J1772)	Type2 (or Mennekes)	GB/T
DC				
Plug name	CHAdeMO	CCS1	CCS2	GB/T

Table 2.1.: Charger types for direct current (DC) and alternating current (AC) charging of electric vehicles (EVs) listed by region

destination or it can be used to fully charge the EV. This can take up to an hour depending on the state of charge (SoC) and the model of the EV. Every model has its own charging profile, which depends on the used battery and the charging control. As power supply fast charging sites are often connected to the medium voltage (MV) grid that is operated between $10kV$ and $30kV$ and can handle maximum power up to $1000kVA$ [16]. Such an afford is needed to make sure the grid can supply the high power demand. Normally the MV grid supplies large grid customers as industry, which have a constant and high demand of energy every working day, and the low voltage (LV) grid. The LV grid is the lowest voltage level and supplies the rest of the cities as households, public services and businesses.

Obtain an access to the MV grid, the customer must get an usage authorisation from the grid operator. To establish the connection, a fee has to be paid for the construction as well as connection charges. There are possible expenses for grid extensions that guarantee the security of supply. Those grid extensions can be the replacement of a transformer that is one of the most expensive assets in a power grid. At the same time it is one of the most likely assets that need an upgrade to mitigate the impact of fast-charging on the power grid stability. [10] Additionally to the grid connection, it is also possible to supply the charging station with different kinds of electrical energy sources. The additional source enables the charging station to operate temporarily independent of the grid or it contributes in the charging station

at least supportive. That can have a positive impact for the operator regarding the grid connection. If the operator is able to generate some of the energy on-site at the charging site, it will influence the needed power grid modifications. [13] A problem is that the most feasible locations for consumers are not the best options from a grid utility perspective, because in city centres and areas with a high population density is also a high grid utilisation. That is especially high, when EVs users charge their vehicles at home. If fast charging sites are built in areas with high grid capacity, the high stress of the grid in certain areas can be relocated, so the stress is significantly reduced. [10]

Possible sources are different kinds of storage systems, fossil driven generators as well as renewable sources [13, 10]. Most interesting are storage systems and renewable sources because fossil driven generators are still depending on fuel. Renewable sources like PV power plants are feasible in small-scale like on roof tops of residential or commercial buildings. Storage systems have the advantage that energy can be stored during low utilisation of the charging site and the grid, when the price is usually lower than during high-peak times. During high utilisation of the station the storage system can release the stored energy to the charging stations to support or avoid charging from the grid. This leads to peak-shaving. [13] This combined system is especially advantageous for the operator if the operation of the charging site would cause a change to a higher power transformer. In theory a storage system will enable the operator to avoid a transformer replacement if the storage is has enough capacity to cover the exceed peak-demand at high utilisation of the charging site. Also during operation there are significant savings for the charging site operator if a combination of storage system and PV system is used [10].

The current research is already exploring the combination of charging sites with different kinds of (renewable) energy sources and storage systems. In the following a selection of studies is presented briefly.

One example for a charging system with on-site generation is presented in the study [17] from California. They created a nano-grid that is consisting of several charging stations, a PV system and a BES system. Those are combined with a smart-inverter and several control algorithms to optimise the operation. However in contrast to this thesis the study did not consider DC fast charging but AC charging. Another example for an micro-grid with integrated charging site for EV is given in [18]. The system consists of a PV and a wind generation unit, a Diesel generator, a charging site, a load, the grid connection, which can be set off, and a voltage controller. The main focus here lays on the control algorithms of the voltage controller to gain the voltage

stability in the micro-grid. In [19] the focus is on the "design of an EV fast-charging station". Those stations also include renewable sources (PV and wind generation units) as well as a storage system. The charging energy and time is modelled with the Monte Carlo method. Later on the installation and operation of the system is optimised based on the charging model and economic factors. In contrast this thesis uses real world charging data. The behaviour of the charging profile is modelled and the optimisation used for peak-shaving is linear instead of non-linear. In [20] a modelled charging system is presented that contains a BES system, a Diesel generator, PV panels, and a grid connection. The charging site contains fast, medium and slow charging facilities. It is demonstrated that the hourly power model and the optimisation successfully reduce the costs and the peak-load. In this thesis the model and optimisation can have various time intervals from seconds to hours. No cost optimisation is done.

In most papers the design of charging sites is done from an economic point of view based on modelled charging data. The objective of this thesis is to explore the technological feasibility in connection with real world charging data. The peak-shaving optimisation problem (4) for the BES system and the combination with a PV is quadratic. It shows the impact on the real charging data. Summed up the charging site design proposed in this thesis is already proven by various models in combination with economic feasibility. In the chapters 3 and 4 the real charging data processing and the optimization are presented. In Chapter 5 the results of the real data processing and the influence of the optimized peak-shaving operation of BES system and the PV system are presented.

2.2. Comparison of common battery types and their application and operation

Nowadays many people are emerged by the climate change and its probable amplifiers CO_2 and other greenhouse gases produced also by humans. The politicians try to agree on climate goals to stop the critical temperature rise. That include limits and goals of reducing the production of greenhouse gas emissions. The use of renewable and sustainable energy sources becomes the focus of attention once again. The power plants that harvest those energy resources do not emit greenhouse gases during the production of energy. Popular sources are solar, hydro, geothermal and wind power. Those sources are not needed to be grown as for ex-

ample the sources for biomass power plants.

Hydro power is used preferably because there is either the chance to store energy or the power plant is based on a constant flow of water that provides energy at all time. The storage is in form of potential energy by keeping an water reservoir filled that is located in a high position. Hydro power plants are highly dependent on the the geological structure. This is the reason why Germany has not many hydro power plants. The regions with those geological structures are already utilized. Norway on the other hand has a huge geological advantage which they used since the 70's. Nowadays Norway has around 95% of their energy demand covered by hydro power.[21]

As constant the use of hydro power can be as intermittent solar and wind power are due to the not constant availability. Both sources are dependent on weather. That makes the power production unpredictable on longer term and harder to plan in advance. It is not available on demand.

2.2.1. Renewable energy on demand by using energy storage systems

In the recent years the idea of combining energy storage systems with renewable and intermittent energy sources made progress. A large-scale energy storage that can provide a grid with enough power on demand should be efficient, reliable, controllable, and affordable. It does not always has to be one large-scale storage system. Also a combination of small-scale storages can be feasible if the control is implemented in a desirable way.

Distributed energy generation is another topic that comes with renewable energies. Since many private house owners installing small solar power plants on roofs there is a distributed generation besides the centralised generation by huge power plants. Distributed generation has the advantage of lesser transmission losses but comes with challenges. The grid system in Germany for example is build for centralized generation that is delivered from the highest voltage level to the lowest. The PV power plants used by house owners not delivering power from the lowest level against the usual power flow. This makes it harder to control the stability of the grid system [22]. [23, 24, 17]

For those solar systems there is already a solution with storage systems which make it possible for the owner to store the surplus power that is produced by the PV systems. This makes it possible to store the power produced during the day and use it by night. This results in a lower export of energy to the grid system as well as

less importing back power from the system. This makes the PV power plant system more efficient for the owner. [23, 25]

2.2.2. Diversity of energy storage systems

The diversity of energy storage systems on the market or currently in research are huge. For storing electrical energy in most cases it is converted into other types of energy. This means there are different ways to store energy. So in the following the different possibilities are shortly explained.

Mechanical energy storages use potential energy, angular momentums or utilize compression. Chemical energy storage use the energy within chemical reactions. For example the production of hydrogen via electrolyse, that split up water (H_2O) into oxygen (O_2) and hydrogen H_2 by using electrical energy. If the two components are brought back together in a fuel the used energy to split the chemical binding is released as electrical and thermal energy. Thermal energy storages using heat energy. The electrical energy is converted into heat. There are currently three ways how it is done. One way is to stored the energy in a phase shift of the storing material. Another is heating the storage material that is keeping the heat or store the heat in a thermochemical reversible reaction. With electrostatic or electromagnetic storage systems the energy is stored in electric fields. This does not need a energy conversion. Besides the other storage possibilities electrochemical energy storages are known by everybody. They are basically batteries therefore also called BESs.

2.2.3. Electrochemical energy storages

Electrochemical energy storages are used in the daily life as energy sources for smart-phones, cameras, laptops but also for EVs. The electric energy is stored in electrochemical energy. [22, 24]

Lead-acid battery

The oldest version is the lead-acid battery. It was invented in 1859. Those technology is cheaper than other BESs. The low energy and power densities with $50 - 80Wh/kg$ and $150 - 300W/kg$ is a huge disadvantage for mobile applications that require a lot of energy or static applications in limited spaces. The charging time is long as well. [22, 24, 7]

Lithium-ion battery

The most common system today is the lithium-ion battery. It is deployed in almost every portable electronic device. In larger scale the application are EV and stationary storage systems in power system. The energy density ($100 - 200Wh/kg$) and the power density ($1000 - 2000W/kg$) are larger compared with lead-acid batteries. This makes it possible to find a compromise between weight and energy supply. The charging cycle is fast and the self-discharge is very low. The energy efficiency is between $85\% - 95\%$. Besides a disadvantage is poor heat handling that leads to premature ageing. With increasing scale the economic viability decreases. Therefore a large-scale application is costly with lithium-ion batteries. [22, 24]

Flow battery energy storage systems

A flow battery is not a battery in the classical way that they are consisting of two electrodes that are immersed in an electrolyte medium. When there is a closed circuit between the electrodes the energy stored in the electrochemical reaction is released. In flow batteries there are two electrodes but also two liquid electrolytes. Those are stored in two separate tanks. In between the electrodes is a membrane to separate the electrolytes. To release or to store the energy the electrolytes are pumped through the system. A negative electrolyte on the negative electrode and a positive electrolyte at the positive electrode. One type of flow battery is the reduction-oxidation (redox) flow battery. The vanadium redox battery for example utilises dissolved vanadium ions in different state pairs as electrolyte.

Their energy density is $35 - 60Wh/kg$. The energy that can be provided varies with the size of the electrolyte tanks. The power density is $75 - 150W/kg$. It is connected to the design of the electrochemical cell where the chemical process takes place. Due to the electrical pumps needed to move the electrolytes the efficiency lies only by 85% . The self-discharge is low. In contrast to Lithium-ion batteries redox-flow batteries can be discharged fully without harming the functionality of the system. The electrolyte is maintenance-free but the membrane needs to be replaced two to three times in a life-span of 15 to 20 years. This membrane is costly due to low commercialization this leads to an economic disadvantage. Less costly membranes are in development stage.[24, 7, 26, 22]

2.3. Optimization technologies in power systems

Energy is a high demanded good and will become more and more valuable and on demand in the future. The amount of technology and machines is growing which leads to a higher energy consumption as well as the use of EV. Research is focussing on energy efficiency in different ways. In the past the optimization was more based on experience and assumptions than on mathematical calculations. The computation of mathematical problems becomes faster with the evolving computer technology. The optimization of complex problems with fitting algorithms is state-of-the-art in many disciplines.

2.3.1. Optimization problems

There is a broad variety of optimization algorithms. The goal of every optimization algorithm is to get the optimal solution to a problem. The optimal solution is often the result of weighting different needs and demands to a problem. [27] The optimal solution is mostly defined as a minimum or a maximum of an objective function. The objective function also called cost function describes what has to be optimized. So it is a model of the real-world problem. One easy example is to minimize a cost of sweets. There are three kinds of sweets that have three different prices and you want the most sweets for the least cost. So it needs to be found out how many of each sweet can be bought to have the lowest price.

The design parameters give the values, that can be changed during the optimization to reach the optimal solution. They describe real-world parameters that can be changed and that are not fixed. In the example the number of each sweet are the design parameters. In the simplest case a optimal solution is to buy the cheapest sweet.

There are constraints and boundaries in an optimization. Constraints are requirements that need to be fulfilled in the optimal solution. In the sweets example, one constraint is that the number of sweets is greater 10 and less than 20. Those are inequality constraints. There are also equality constraints. It is a possible equality constraint that the number of sweets shall equal 15. Constraints makes it more difficult to find a solution with the least cost.

Boundaries give the limits for the design parameters. There are lower boundaries and upper boundaries for each parameter. Those are the minimal and maximum values that each design parameter shall have in the optimal solution. In the sweets

example possible boundaries are that sweet type 1 needs to be bought at least 1 time and at most 5 times. The boundaries can have individual ranges and units all depending on the design parameters and the real-world problem.

There are basically three types of optimization problems: Linear, quadratic and non-linear programming. All types are described in the following three subsections. All decision variables are continuous. For discontinuous decision variables there are mixed-integer programs. Those are not elaborated in this thesis. Afterwards three of the most used solving algorithms approaches in the energy section are explained briefly.

Linear Programming

When the objective function and all constraints are linear the optimization problem is called a *linear programming (LP)* problem. Such a problem has usually a form like in Equation 2.1. [28]

$$\begin{aligned} \min_x f(x) &= c^T x \\ Ax &\leq b; x \geq 0 \end{aligned} \quad (2.1)$$

The vectors c and b are real and have different sizes. c is n -size and b is m size. The matrix A is real and has the size $m \times n$. [27, 28]

$f(x)$ is the objective function, x is hereby a possible solution. $Ax \leq b$ are the (in)equality constraints and $x \geq 0$ depicts the boundaries. Solutions of linear problems are easier to determine and the computations are based on less complex mathematics than non-linear problems. The formulation and analysis of a problem has in many cases naturally a linear form. It is possible to solve *LP* problems analytical but there are also numerical solving algorithms that are also used for *LP*. [27, 28, 29]

Quadratic Programming

For *quadratic programming (QP)* the objective function is quadratic and the decision variables and constraints are all linear. It is a special form of a *Non-Linear Programming (NP)* problem. A general quadratic problem formulation with boundaries is presented in 2.2. [28, 30]

$$\begin{aligned} \min_x f(x) &= \frac{1}{2} x^T A x + b^T x + c \\ Cx &\leq d \end{aligned} \quad (2.2)$$

Non-Linear Programming

When the objective functions or the constraints are non-linear the optimization problem is a *NP*. *NP* problems are not solvable by analytical calculations but need to be approximated by the solving algorithms. In many cases *NP* problems can be linearised and solved like *LP* problems. [27, 28, 29]

2.3.2. Common optimization problem solving algorithms and their applications

There are various optimization algorithms but in the following only the common algorithms used recently in the power system field are used are described. To those count evolutionary algorithms, *dynamic programming (DP)* and gradient-based algorithms. [31]

Dynamic Programming

Dynamic Programming is a gradient free optimization method. It was developed by the mathematician Bellman [32]. In the *DP* approach a complex problem is broken down into smaller parts of the original problem. It works with discrete values of time, state and decision variables. In every stage a new optimum for the next stage is chosen depending on the objective function and the decision variables. The method is not sensitive to linearity, continuity or the absence of both. It cannot be trapped into a local minimum which means it always finds the global minimum. One downside is that it is more calculation intensive for complex problems. One application Bellman himself thought of was adaptive control. [32, 33, 34]

In energy generation systems *DP* is used for decision making in the operation and control of the system. In [34] it is proposed to use *DP* for real-time energy management. This application targets optimal energy efficiency by using the *DP* solution to find the optimal distribution of the demanded power to the generation units. In [35] *DP* is used for the optimal management of CHP power plants. In this case backward *DP* is used to determine the optimal state of the plant from an economical point of view. To increase the efficiency of the distribution grid they approach in [36] to add energy storage devices into the grid. The optimal placement of the storage devices and their control strategy is determined by Dynamic Programming.

Gradient-based algorithms

As the name says they use derivatives to solve an optimization problem. They have two sub-problems to solve. A search direction in the n -space needs to be computed, along which the search starts or continues in each iteration. The step size, which is a positive scalar, needs to be computed as well. There are various algorithms. They are efficient but complex algorithms, that can be trapped in local optima. Not always are information of derivatives available. In the following there are two of the interior point methods and the trust region method explained briefly. [32]

Interior point methods are often used for convex problems that have only one global minimum. The Steepest Descent Method the gradient vector is calculated at each point of the function. In each iteration the gradient is used as the search direction. At each point the search direction is also where the rate of change reaches its maximum. [27, 37, 38, 39]

Newton's Method differs to the Steepest Decent Method only in the calculation of the search direction. Newton's Method is using as a second-order information of the function the second-order Taylor series expansion. This means the objective function is approximated by a quadratic function. This approximation is minimized exactly. The Newton's Method converges quadratically for a non-linear function. It is also possible that the method does not guarantee convergence for some non-linear functions. This method has another disadvantage. It not only needs the gradient calculated but also the Hessian to compute the search direction. The Hessian must be symmetric and positive definite. Advanced methods based on the Newton's method are the Davidon-Fletcher-Powell (DFP) Method and the Broyden-Fletcher-Goldfarb-Shanno (BFGS) Method. It is problem depending what method performs better. [27, 29, 37, 38, 39]

Trust Region Methods are a different approach. It tries to remove the drawbacks of the Newton's method. They are originating from highly non-linear functions or the restrictions for the Hessian. The problem that occurs is that the region, where the quadratic approximation is suitable, is left during the optimization steps. This can be resolved by minimizing the quadratic function. This is done in a region around the design variables. In this region the quadratic model can be trusted so this is called the trust region. In every iteration the trust region is calculated again depending on the accuracy of the quadratic model. [27, 37, 38, 39]

Newton-like algorithms are popular in the field of energy dispatch optimization [35]. But gradient based algorithms are also used for solar power plants to reach the opti-

mal design and the optimal management [31]. Interior-point methods in general are also used for state estimation when it comes to power grids [40]. In [41] *LP* is used to obtain an optimal schedule for Distributed Energy Resources including a BES system. The objective function is dual and combines economics and peak-shaving. It is said that the *LP* solver of *Matlab* is used which can be a Simplex or an Interior-Point algorithm [42].

Evolutionary algorithms

Evolutionary Algorithms draw inspiration from phenomena in nature. This method does not need information about the gradient. They are easy to implement and have a higher chance of reaching the global optimum and do not get trapped in local optima. They also hold diversity during the optimization process [43]. Evolutionary Algorithms seem suitable to find solutions for multi-objective optimization problems as well because of the simultaneous processing of possible solutions [44]. There are also drawbacks. The computational cost are high [28] and the constraint-handling is difficult. The solutions are usually bases on stochastic so every time the algorithm is executed the result is different. [32]

In Genetic Algorithms a solution to a specific problem depicts a chromosome. A group of chromosomes is called a population. This population represents a part of the solution space. The optimal solution is assumed to be in the search space, which is defined as the solution space. Each possible solution is represented by an chromosome. The initial set of randomly chosen chromosomes is the first generation, the initial population. All chromosomes are compared based on their fitness. This is measured by the objective function of the optimization problem. At the end of every iteration genetic search operators are applied on the chromosomes. The operators are selection, mutation and crossover. A new generation of chromosomes is created and be expected to have over all a better quality than the previous generation. The fittest chromosome in the last generation is the obtained solution. When the termination criteria is met the process is stopped. [45]

Particle Swarm algorithms are another evolutionary approach. They are also population base, and stochastic as well as heuristic. Particle Swarm does not imitate evolution but it copies the concept of schooling. Possible solutions to the optimization problem are depicted as particles. Those particles move through the solution space with each velocity and a moving direction. All particles are attracted by the best global solution of the last iteration and move towards it. Additionally each par-

ticle has a kind of a memory that recognises regions that were found to have a positive impact. This influences the way of the particle as well. The iterations go on until certain criteria are met to stop the process. Those criteria are for example stalling of the particles or reaching the number of iterations that were set as maximum. [45, 46]

In [47] a Genetic Algorithm has been used to coordinate the charging of EV taking into account the limits of the charging and grid infrastructure. The aim is to create optimal load pattern to ensure reliability of the charging site. In the study the resulting algorithm is applied in a low-voltage charging system. The results show a positive effect of smart charging on the load profile. In [48] a Genetic Algorithm and a Particle Swarm Optimization is used to optimize control parameters of a SoC feed control scheme. It is used to control the output power dispatch of a PV farm to charge a BES system. To find the optimal design of an EV fast-charging site a Genetic Algorithm is used in [49]. It optimizes the installation of charger, renewable generation units and a storage system. The fitness function is here the profitability which takes installing costs, energy incomes and cost as well as maintenance costs into account. In [31] there are several applications of Evolutionary Algorithms listed which mostly try to minimize the operational costs. The design parameters are depending on the energy system that is optimized. Mostly those systems contain renewable power plants that need to be scaled. In [50] a multi-objective optimization problem is solved with an Evolutionary Algorithm. The energy management of an CHP is optimised so that total operational cost are minimized.

Hybrid approaches

Hybrid approaches mean that different optimization methods are combined. The aim is to eliminate drawbacks and create an algorithm that has the strength of each method. Not only algorithms of different solving method types mentioned above are joined together but also from the same type. For example in [45] the two evolutionary optimization techniques, Particle Swarm Optimization and Genetic Algorithms, are combined. The aim is to create an algorithm that finds the global minimum more reliably than each of the both algorithms alone. A combination of a Genetic Algorithm and Dynamic Programming is purposed in [51]. The Dynamic Programming is used to obtain the optimal control rules for a combined ultra-capacitor-battery-storage system. The optimal parameters under different load cycles are gained by the Genetic Algorithm.

2.4. Programming in Python

Python is a programming language that is often used for scientific programming and data analysis but it is also a powerful scripting language [52]. The project is Open-Source. This means the download and use of the programming language is free of charge. [53] Furthermore it is available on the operating systems Windows, Unix and Mac OS X. *Python* is a high-level language that has a high abstraction level compared with low-level and hardware-related languages like *Assembler*. *Python* is also an interpreted language. This means the code is translated at run time by an interpreter to machine code. [54] This makes development faster but it is also a downside of *Python*. Interpreting at runtime is slower than executing a pre-compiled program. Such fully-compiled languages are *C* and *C++*. [55]

Python belongs to the object-oriented (OO) programming languages. Similar examples are *Java*, *Perl*, *Ruby* or *Scheme*. As typical for OO programming, *Python* supports classes, polymorphism as well as multiple inheritances. [53, 54, 56, 57]

Basic data types are numbers (`int`, `float`, `long` and `complex`), sequence types (`string`, `list`) and containers (`dictionary`). Advanced features are generators and list comprehensions. There are additional data types available in modules and packages. Those can be installed in addition to the basic *Python* distribution. This features also enable more functionality in form of methods and functions. [53][56][54] *Python* has a syntax that is easy to read and to write. That makes it easier to learn and faster to develop applications than in languages like *C* or *C++*. Never the less *Python* has modules that makes it possible to interface *C* code and it is possible to write extension modules in *C*. [58][53][54]

For this thesis *Python* version 3.7 is used on Windows with the IDE *PyCharm Community Edition*.

3. Charging Profile Modelling tool

In many countries all over the world the utilization of EV is desired instead of driving vehicles with combustion engines that consume fossil fuel. It is desired because it is one step to reach the countries climate goals by reducing the CO_2 emissions in the transport sector. Another effect is the reduction of smog in cities if the density of EV is high enough.

To supply the rising amount of EV with energy the charging infrastructure is enhanced. Either the amount of chargers in an existing charging sites increase or the density of charging sites rises in high populated areas. Nowadays many assets in power grids have a measurement systems on-board to establish a connection with the central unit via communication technologies. This enables the operators of those assets to have a real-time monitoring system. This makes statistical data about the power grid available and helps to improve the operators planning and business. Predictions based on real data are more precise than predictions that are based on artificial models. Those artificial data sets are created with the assumption that they are realistic. The amount of gathered data is growing together with the number of observed assets. In the case of charging sites the amount of data grows with every charger, every site, and every charging event. That means the operator needs to invest more time in editing the gathered data to use the advantage of having real data.

As part of this thesis a tool is developed that eases the process of editing the data. It enables the user to create a modelled charging profile from charging data that includes only start and end time as well as the consumed energy over the charging duration. Additionally information about the charging point and the charger type are available. Those modelled load curves improve the gain of information about charging behaviour of the customers in a visual way.

3.1. Used *Python* modules

Python has many built-in functions which cover a wide field of possible applications. In many cases an application needs additional data types or methods which exceed the built-in functions. Those functionalities are brought to *Python* by modules, libraries and packages. Those are not necessarily programmed in *Python* but also in *C/C++*. The use of those extensions lead to faster execution, less code and more readability in many cases. This can be very useful and time efficient. The modules contain elements that obviate the need for implementing such functionality yourself and extend the possibilities of *Python*.

The modules that are used in this thesis are listed and explained in the following. All modules are known in different fields of expertise like data science, data analysis, numeric modelling or scientific programming [28, 46]. This is also seen in the comprehensive documentations that contain different examples of application. The modules are capable of operating together. They often have special functions to provide better compatibility to other modules, libraries and packages. [53, 57, 58]

3.1.1. *matplotlib*

matplotlib is a library in *Python* that uses *NumPy* (see chap. 3.1.2) and other modules as well. The objective of this library is to enable the user to create 2D plots based on *Python* arrays. Originally the library was implemented for emulating *Matlab* graphic commands. Although it is fully independent of *Matlab* and can be used in the object oriented way that is typical for *Python*.

The documentation provides many examples how to display diagrams and modify the kind and appearance of the plot. Examples for diagram types are line plots, bar charts, scatter plots, contour plots, box plots, pie charts and 3D plots. It is possible to plot two and more diagrams in one figure which is a so called `subplot`.

Each plot can be configured in a wide range. It ranges from none to an advanced degree of modification depending on purpose and demand of the figures. With *matplotlib* the generated plots can be stored as graphical images in different file types like *Scalable Vector Graphics (SVG)*, *Portable Network Graphics (PNG)* or *Portable Document Format (PDF)* to mention the most common ones. [59]

In this thesis *matplotlib* is used to plot the figures for presenting the results which are acquired from the real charging data by the CPM . This includes creating, modifying and saving the plots in figures.

3.1.2. *NumPy*

NumPy is a package for scientific programming. Beside the detailed reference the documentation provides a guide for *Matlab* users. It explains the main differences as well as the equivalents to *NumPy*. This supports easy migration to *NumPy* for developers with *Matlab* experience. In general *NumPy* can be used for similar applications as *Matlab*. Like *Python* itself, *NumPy* is open source and free of charge. In context of this work the most useful functionality of this package is the introduction of the multi-dimensional (N-dim) array object. It is a N-dim container that enables nesting of arrays. The N-dim array enables linear algebra operations in N-dims as well as other routines like polynomial operations, statistics and Fourier transformations to mention a few possibilities.

The creation of N-dim arrays is almost as easy as the creation of conventional *Python* arrays and lists. The access to each element of the N-dim array is comparably easy. The basic operations include slicing, indexing reshaping, repeating, sorting, adding and various others [60].

The use of a N-dim array has limitations. It emerges that all items in the array must have the same data-type. Data types are for example integers or floating point numbers. Including a column of integer type and floating point type in one array is not viable. That prevents the bundling of the measurement data series in one N-dim array when the data types differ. [60]

In this thesis *NumPy* is used for calculation and internally processing the data within different classes.

3.1.3. *pandas*

pandas is an open source package for *Python*. It provides additional data structures that are called *DataFrame* and *Series*. Those enable the user to have heterogeneously-typed columns in one data structure. The library also includes data analysis tools for use in *Python*.

The primary used data structure in this thesis is *DataFrame*. It is a two-dimensional data structure and can be compared with a table. The *DataFrame* has columns and rows as well. Each row has an index. All elements are accessible by column and row identifiers, which makes it easy to access elements. It is possible to import data to *DataFrames* from Structured Query Language (SQL) data bases, EXCEL sheets and other common types. The original data types are converted to the correspond-

ing *pandas* data type. [52]

In this thesis *pandas* is used for processing the huge amount of measuring data and writing this data to *SQLite* data bases directly without using the *sqlite3* module (see chap. 3.1.5). The advantage with *pandas* is that it can load/store whole *pandas* data frames filled with the measurement data from/to *SQLite* data bases without any adding of column headers, data conversions or modification in the table structure.

3.1.4. *SciPy*

SciPy is built on the *NumPy* module (see chap. 3.1.2). The user can use high-level commands and classes to manipulate and visualise data. It encloses various mathematical algorithms for example in the optimization and clustering sub-packages. So called convenience functions appear in signal processing or statistical sub-package. The functionality can compete with *Matlab* or *Octave*, both strong scientific tools for data-processing and system-modelling. It is beneficial that *SciPy* is based on the language *Python* because it enables the user to create specialized applications by making use of the open source and efficient development in *Python*. *SciPy* has a detailed documentation with examples and tutorials which makes it easily accessible for beginners in *SciPy* and *Python* as well. [61]

In this thesis the `optimize` sub-package of *SciPy* is used for the optimization of the BES and PV systems. The optimization process is explained in 4.3.

3.1.5. *sqlite3*

sqlite3 is a module that is based on the *C* library *SQLite*. *SQLite* is a database that is disk-based which means that it does not require a server to run on. It enables the user to access the database with a version of the SQL query language.

The module provides methods to connect with a database, create databases and execute SQL queries and get data from the database by fetching it. There are more methods for advanced use as well. Important is that *SQLite* natively supports five types to store data (`NULL`, `INTEGER`, `REAL`, `TEXT`, `BLOB`). The *sqlite3* library automatically maps the following *Python* data types: `None`, `int`, `float`, `str`, `bytes`. Other data types in *Python* must be adapted into a matching type. [62]

In this thesis the module is used for minor tasks related to the *SQLite* database. It is used for reading and returning the column names for further usage. There is a method that changes the decimal format from `”,` to `”.` because the notation for

decimal numbers in *Python* is a dot. This differs from the usual European convention to use a comma for decimal numbers and thus needs to be changed in the database with the measurement data before the database is read by the CPM .

3.2. Process in the Charging Profile Modelling tool

In the following the process within the CPM tool will be explained. The process is divided into three parts: The pre-processing, the main process, and the plot process. Figure 3.1 depicts the process from pre-processing the input measurement data to plotting the output data.

The input data is a *SQLite* database. An example for the database schema is

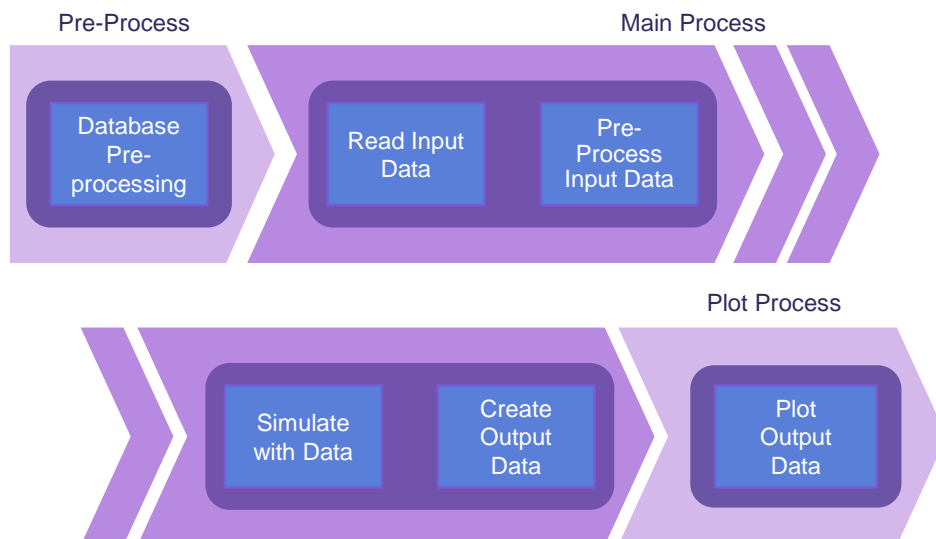


Figure 3.1.: Process in the Charging Profile Modelling divided into three parts: the pre-process, the main process, the data visualization

given in Table 3.1. The database contains the DC charging measurement data. The flow in Figure 3.1 is interrupted before and after the main process to show that it is independent of the first step, the pre-processing and the last step, the plotting.

The main process starts with reading the measurement data from the pre-processed *SQLite* database. Before the actual modelling of the charging profile begins, the input data needs to be pre-processed internally. That means every charging event is assigned to an object which has the attributes of an EV that charges at the time of the event.

Every charging station that appears in the charging events is assigned to an object with the attributes of a charging station. With this data the charging profiles for each event and therefore each day are modelled. The acquired charging profiles are exported to a *SQLite* database. Different formats and time resolutions are possible (see Tab. 3.2).

In the last step it is possible to plot the output data if needed. It is not necessary and can be left out or done from the output data later as well. There are different kinds of plots possible. The main process is completed when the results are written.

3.2.1. Properties of measurement database

The DC charging measurement database has a special format that is explained in the following. It contains the start and end time of the charging process, the charged energy during this event, the charging point and the charger type (CCS, CHADEMO). The format of the time is a time stamp `DD.MM.YYYY hh:mm:ss:uuuu` and the unit of the energy is *Wh*.

In Table 3.1 at index 1 is a general charging event with start and end time as time

index	start time	end time	energy [Wh]	charging point	charging type
1	10.10.2010 10:10:10:1000	10.10.2010 11:11:11:1100	1234	Charging Point 007	CHADEMO
2	10.10.2010 23:10:10:1000	11.10.2010 01:11:11:1100
3	10.10.2010 23:10:10:1000	11.10.2010 00:00:00:0000
4	11.10.2010 00:00:00:0000	11.10.2010 01:11:11:1100
...

Table 3.1.: Examples for input database entries. Charging event at index 1) general, 2) until after midnight, 3), and 4) split of 2)

stamp, the energy, as well as the information about the charger. At index 2 it is shown how charging events until after midnight looks like in the original data set. It appears as one charging event. This is problematic because the results are required to be in a period of 24 hours. Those start at midnight and end 24 hours later as well at midnight. Each day needs to be separately observable.

The solution is to split the charging event at midnight. How this looks like is shown at index 3 and 4 of Table 3.1. The start time at index 3 is the same as at index 2. At index 3 the end time changes to midnight of the following day. The start time at

index 4 equals the end time of index 3. The end time in 4 equals the end time from index 2. Finally there are two charging events from start time to midnight and from midnight to end time.

Furthermore it is problematic if charging events appear more than once in the database with the exact same values in all columns. This would mean to have two cars charging in one time interval that is exactly the same up to microseconds. In reality it is very unlikely to have such a situation. This is often resulting from an error while saving the measurement data at the charging station.

To solve this issue the first appearance is recognised and all following 'exact copies' are deleted. Empty rows or entries with missing values are removed from the database as well. This is done in order to guarantee that only relevant charging events appear in the pre-processed database.

Those problems are handled in the pre-processing with the *Python* script *Clean-DataBaseAndSplit.py*. This script belongs to the developed CPM but it is executed independently. This is shown by the gap between the pre-process and the main process in Figure 3.1. The script is only required when the database is used as input data for the first time. The script creates a database where the above mentioned problems are corrected.

To ensure that the original database is available in an unchanged state the pre-processed database is named differently. After using the script the pre-processed database is ready to be used as input for the developed *Python*.

The main process starts by reading the input data. In the beginning the developed tool establishes a connection to the pre-processed *SQLite* database. When this is completed all data is gathered from the database and sorted into three packages of information.

Filtering information about the charging event and the shape of the modelled charging curve is the first step. Afterwards information of the chargers are obtained from the charging event data. Lastly the information about the dates when an charging event occurs are extracted from the event data as well.

The event data looks similar to the database entries 1, 3 and 4 in Table 3.1. The names of all charging points (Tab. 3.1 column 5) are extracted from the event data as information about the charger. The start times in column 2 of Table 3.1 are used to get a collection of all dates where charging events occurred.

3.2.2. Modelling of the charging profiles

When the second step of the main process is finished and all required data is collected, the modelling of the charging profiles begins. There are different options for format and time resolution which are shown in Table 3.2.

Three formats are possible with each of them having three of the most feasible

Format		Monthly			Weekly			Daily		
Time (24h)	Resolution	1 h	15 min	5 min	1 h	15 min	5 min	5 min	1 min	1 s

Table 3.2.: Possible output format and the time resolution of 24 hours

time resolutions of the measurement interval of 24 hours. The first row named "Format" describes how the database is structured. If the option "Monthly" is chosen the database has one table for one month. For "Weekly" every week is in a separate table in the data base and for "Daily" every day has its own table. In the last format the table consists of one column for the profile of each charger and one column in the end where all chargers are summed up.

The profile data of each charging event is described by start and end time. The data in each format is arranged in the 24 hours time interval. The correct time arrangement of the event data is always made with a resolution of $1s$. This ensures that the accuracy of the profile modelling is maximized.

When the chosen resolution differs from $1s$ and is for example $15min$ the mean over each $15min$ interval is calculated and the number of values is reduced from $60 \cdot 60 \cdot 24 = 86.400$ to $\frac{86.400}{60 \cdot 15} = 96$. The reduction of the resolution leads to a reduction of the number of values that are written into a database. Saving the database with less entries reduces the computation time so the overall execution time of the developed tool is shorter.

Before the resolution is reduced the first step is the modelling of the energy profile. The model is based on the energy value that is given in the charging event data and a base charging curve that was measured in another work [14]. This is shown in Figure 3.2.

It shows the time on the x-axis and the amount of energy respective the power factor in percent on the y-axis. In this figure the time interval is limited to $120s$ to show the ramp up of the profile. Each event is modelled as time interval with $duration = endtime - starttime$ number of seconds. That base profile determines the amount of energy used in each second during the charging event.

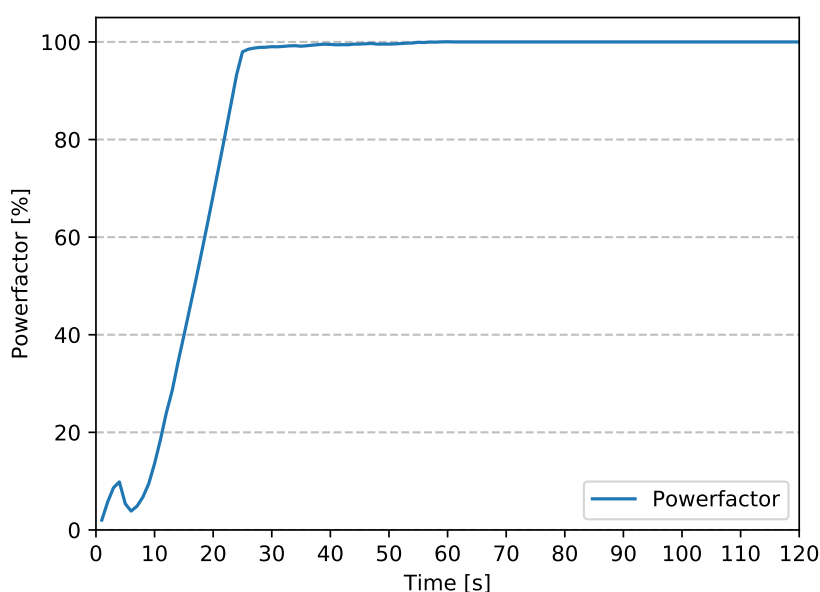


Figure 3.2.: Measured charging profile of a Tesla Model S for modelling charging profiles from energy data

The actual energy value is the limit of how much power can be charged per second. Because the charging profile is reaching 100% of the charging power after 60s the the EV is charged with the maximum power value (see Fig. 3.2).

The internal charging electronics of the EV allow a 100% power flow from the charging station into the car after those 60 s. This behaviour is modelled realistically. When the model curve reaches 100% the value remains until the cars charging time is over. This behaviour is assumed in the model but it is not realistic.

In reality many EV slow down the charging process after a specific SoC is reached. Mostly the limit for fast charging lies around a SoC of 80% [63][64]. This is neglected in the charging profile model, because the actual SoC is not obtainable from the given data (Tab. 3.1).

Those information are either not collected from the station or not provided by the EVs to the charger. When the charging power is reduced, depends on the charger type as well as on the maximum charging power the station can provide.

Once all charging events are modelled as charging profiles they are written into the output database. For each charger all charging profiles are collected and summed up depending on the start and end time of the charging event. For one charger it is illustrated by Table 3.3.

The first row contains the time that might have one resolution as explained in Table

Time	1	2	3	4	5	6	7	8	9	10	11	12	13	...
EV 1	-	-	x_1	x_2	x_3	x_4	x_5	-	-	-	-	-	-	...
EV 2	-	-	-	-	-	y_1	y_2	y_3	y_4	y_5	y_6	y_7	-	...
Charger 0	-	-	x_1	x_2	x_3	$x_4 + y_1$	$x_5 + y_2$	y_3	y_4	y_5	y_6	y_7	-	...

Table 3.3.: Example for the *SQLite* database regarding the merging of two charging events at one charging station

3.2. One charging event is shown in each row labelled with EV. Both EVs charge at the given charger "Charger 0". The charging events occur at different times. "EV 1" charges in time interval $[3, 7]$ and "EV 2" in $[6, 7]$. The values x_n and y_n signify the charging profile values at the time of the charging event.

The last row depicts how the charging profile values of the charger look like. It explains that charging parallel at one charger leads to a summation of the two above charging values in that time slot. A similar procedure (see Tab. 3.4) is carried out when the formats "Monthly" and "Weekly" are chosen for the output file. Additionally all chargers in one charging site are summed up. More charging events appear then because the charging profile of each charger contains every charging event of that charger.

Time	1	2	3	4	5	6	7	8	9	10	11	...
Charger 1	a_7	-	-	x_1	x_2	x_3	x_4	-	-	-	c_1	...
Charger 2	-	-	-	-	-	y_1	y_2	y_3	y_4	y_5	y_6	...
Charging Site	a_7	-	-	x_1	x_2	$x_3 + y_1$	$x_4 + y_2$	y_3	y_4	y_5	$c_1 + y_6$...

Table 3.4.: Example for the *SQLite* database regarding the merging of two charging stations at one charging site

3.2.3. Writing charging profiles to a database

After finishing the evaluation of the charging profiles depending on the format and the resolution, the data is finally ready to be written to the database. The data is written one table at a time. That is because of how *SQLite* databases are written. Table by table is the easiest way to do that.

All data that should be contained in one table is exported simultaneously with one command. Beforehand the table names are specified after the date, week or month of the event dates depending on the format. This finishes the main part of the whole tool process (see Fig. 3.1).

The last step of the process in the developed tool is the presentation of the charging

profiles. There are two possible ways. Either the developed tool plots the profile figures in the process directly after writing the output database or a special plotting script is used to plot the profile results from already existing output data.

3.3. Structure of the Charging Profile Modelling tool

In the following the structure of the CPM will be explained. As it is stated in Section 3.1 the developed tool implemented in *Python* makes use of several modules. The most important modules used within different parts of the tool will be mentioned as well as their task are exhibited this section.

The program structure of the main part of the modelling process (see Fig. 3.1) is briefly explained in this section. Figure 3.3 depicts the structure.

Python is object oriented so a program is usually based on objects that are instances of classes. Classes describe the behaviour of their objects. Each class contains properties created during the initialisation (`__init__()`).

Properties are variables that are made available to all class methods. During creation of an object it is possible to hand over parameters. Those parameters can be assigned to the properties. In this way they can be used in class methods. Class methods describe the actions an object is able to perform during runtime.

The classes used in this tool are *DBSQLite*, *BatteryElectricVehicle*, *DCCharger* and *ChargingStationBatteryElectricVehicle*. The last three classes have a special relationship to each other (see Fig. 3.3). *ChargingStationBatteryElectricVehicle* is a child class and inherits from the parent classes *BatteryElectricVehicle* and *DCCharger*. This means that the child class is able to use and overwrite methods from their parent classes. This has the advantage that methods that are already implemented in one of the parent classes do not need to be implemented again in the child class. This saves time and keeps the code more clear.

A disadvantage is that it is possible to overwrite the parent's methods in a child class. This overwriting can cause errors that arise unexpected and are hard to find. In this work the inheriting of classes is used but not the overwriting functionality to avoid unexpected behaviour during execution.

Main and *ChargingProcess* are scripts and in the top of the prom structure in Figure 3.3. A script is a file that contains a *Python* program. This is another way to develop in *Python* besides the object oriented programming.

Those two scripts in this thesis are used to start and head the charging process. All

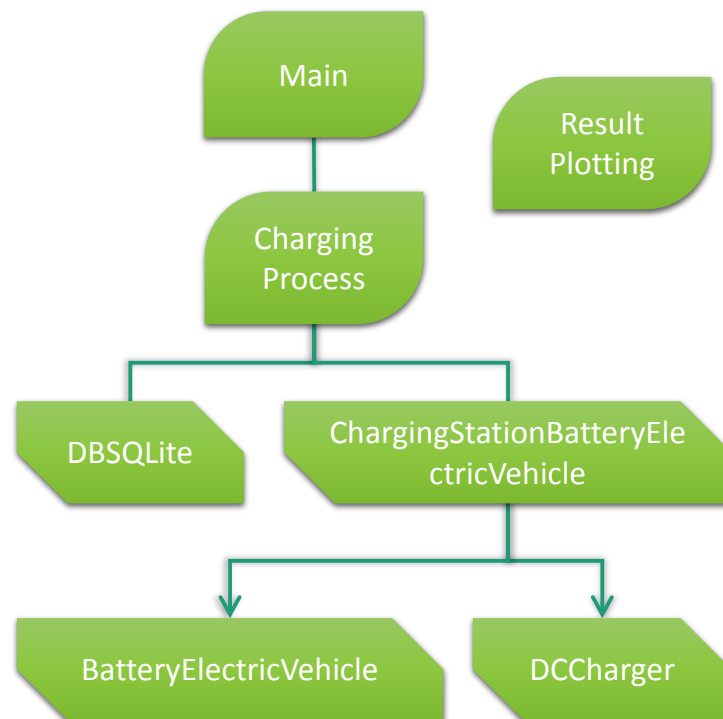


Figure 3.3.: Structure of the Charging Profile Modelling

the functionality from the classes are used to set up the main program process, to start the pre-processing of the received charging event data, to execute the modelling of the charging profiles, and to create the output database.

An additional script, *ResultPlotting* handles the plotting of the output charging profiles. In the scripts the implemented classes are used to connect the data with the functionality.

***BatteryElectricVehicle* and *DCCharger* classes** are the parent classes. They represent the basic objects used to model the charging profile. The properties of the classes are shown in Table 3.5.

The *BatteryElectricVehicle* class models the charging profile of a EV. It contains all properties and parameters needed for the charging profile. Every EV has a unique numeric identifier to simplify the relation between charging event and resulting EV. Depending on the charging event data every EV object has a maximum available power and maximum available energy. This limits the values for the charging profile. The date as well as the start and the end time of the charging event are also given by the event data. The date is in date stamp format. The start and end time are

Object	Properties and Parameter
EV	Unique numeric Identifier
	Maximum available power (kW)
	Maximal available energy (kWh)
	Charging date ($YYYY - MM - DD$)
	Charging start time (s)
	Charging end time (s)
	Base charging profile (array, 3.2)
	Charging values (array, charging duration)
	Charger name
DCCharger	Charger name
	Maximal available power supply (kW)
	Charging power at time X (kW)
	Charger occupied (boolean array, 24h interval)
	Energy charged (numeric array, 24h interval)

Table 3.5.: Properties of the parent classes *BatteryElectricVehicle* and *DCCharger*

calculated to seconds. It indicates how many seconds from midnight the EV starts charging. The base charging profile (see Fig. 3.2) is recorded in every EV object. The array of charging values contains a row with every second of the charging duration, a row with the values of the charging profile from start to end time as well as the energy calculated from the charging curve for every second. The name of the charger point is the identifier and marks where the EV charges.

The *DCCharger* class describes a DC charger. The charger name in this class is the same as in the *BatteryElectricVehicle* class. The maximum available power supply describes how much power the charger can possibly provide to a EV. The maximum available power of the EV object cannot exceed this value. The charging power at time X describes the value the charger provides to all EV.

If the charger is occupied at a given time (in s) this is noted in an array. This array contains every second of a 24h interval that represents one day. For each day an array is used that is initialized with zeroes. The array contains boolean values and has the value 0 if no EV charges in a time slot and 1 if the charger is occupied. The energy that is charged over the occupied time is stored in an array with the same size as the array that shows if and when the charger is occupied.

The methods in the *BatteryElectricVehicle* class calculates the charging duration from the charging times, the sum of the charged energy as well as creating the array for the charging values and calculate the content of this array. The methods in the *DCCharger* class check if the charger is free for charging at the requested time interval, set the charger occupied for the charging duration of one EV and calculate

the charged energy at each second.

Both parent classes use *Numpy* (see chap. 3.1.2) to handle and calculate the different arrays. Each EV charging values array is used to define how much energy each charger charged and at what time. One example is given in Table 3.3. The result is saved in the energy charged array.

ChargingStationBatteryElectricVehicle class depicts a charging station respectively a charging site with X chargers and Y EVs, which have to be charged. The properties and parameters are shown in Table 3.6.

The chargers contained in the charger list originate from the charging event data

Object	Properties and Parameter
ChargingStationBatteryElectricVehicle	List of <i>DCCharger</i> objects
	List of <i>BatteryElectricVehicle</i> objects
	Station power provided (<i>kW</i>)
	Any charger available (boolean)

Table 3.6.: Properties of the child class *ChargingStationBatteryElectricVehicle*

which is explained in 3.2. The EVs in the EV list correspond to the charging events. One EV object equals one charging event.

The provided station power is containing the power that each EV takes from the charging site. If any charger is available at the time a EV tries to charge at the station this is provided by the last property of the *ChargingStationBatteryElectricVehicle* class. The value is true if a charger is available and false if not. This parameter is especially useful if there is no real charging data but modelled random charging data is given. That kind of charging data may have many EVs charging at the same time.

If there are not enough free chargers available the surplus EVs are not supplied. Besides the parameters and properties in Table 3.6, the *ChargingStationBatteryElectricVehicle* class contains all properties and methods of their parent classes.

The methods in *ChargingStationBatteryElectricVehicle* depict adding a charger to the site, adding an EV to the site and to a charger, initialise the charger objects and their arrays, initialise the charging values array for each *BatteryElectricVehicle* object, charging the EV at a charger and changing the resolution of the calculated charging profiles.

The class uses the parent classes *BatteryElectricVehicle* and *DCCharger* as well as the *Numpy* package (see chap. 3.1.2) to handle the arrays used in the methods.

DBSQLite class contains the properties in Table 3.7 and methods to read a *SQLite* database in simple form with the *sqlite3* module (see sec. 3.1.5) or by using *pandas* (see sec. 3.1.3) for more advanced use-cases (chap. 3.1). The most important methods are the establishing of a connection with the database, getting table and column names, change the decimal format from “,” to “.” and writing a database. Those methods are used in the beginning and the end of the main process for reading the database and output the calculated results in a database as well (chap. 3.2).

Object	Properties and Parameter
DBSQLite	Path of database
	Read in data
	Database in <i>pandas</i> DataFrame format

Table 3.7.: Properties of the *DBSQLite* class including a *pandas* DataFrame (see sec. 3.1.3)

4. Extension of the Charging Profile

Modelling tool with a peak-shaving optimization of a BES and a PV system

The energy system has new challenges to go through due to the electrification of traffic by EVs. The charging of EVs needs a lot of power especially when it is thought about a future where all cars are electrified. It can be difficult to find the optimal place for a charging station where the grid assets are resilient enough to handle the additional load without overloading. One solution to provide a part of the additional energy is the integration of renewable sources and/or an energy storage system in the charging site.

In the following part of the thesis two combinations of a DC fast charging site are suggested as a solution. In the first suggestion, the charging site is connected to a BES system and in the second one a PV power plant is combined with the BES system. Both suggestions result in a fast charging site that relies less on the grid system. The aim of the peak-shaving optimization is to enable the user to find the best sizing of the BES system and the PV system out of a number of different configurations and to show the influence of the additional sources on the resulting charging profiles.

Firstly in this chapter the concept for each the added BES and the combination of BES and PV is explained briefly. The optimization problem with constraints and boundaries is explained for each configuration as well as the modelling of the PV power output is described. Finally the connection to the developed CPM (see chap. 3) is drawn and the used solving algorithm is explained. In Chapter 5 the results of the optimization are presented as well as the influence of the PV power plant on the system behaviour.

4.1. Optimization problem for using a BES system to supply a DC charging site

The proposed system is depicted in Figure 4.1. The charging site is connected to the power grid. The charging site contains the DC fast chargers as well as a BES system. For this optimization the precise BES and PV systems are not relevant. It is investigated how the extended charging site behaves with an integrated BES system of various capacity and output power as well as an PV system with various output power.

In the following the optimization problem is explained. It is formulated as

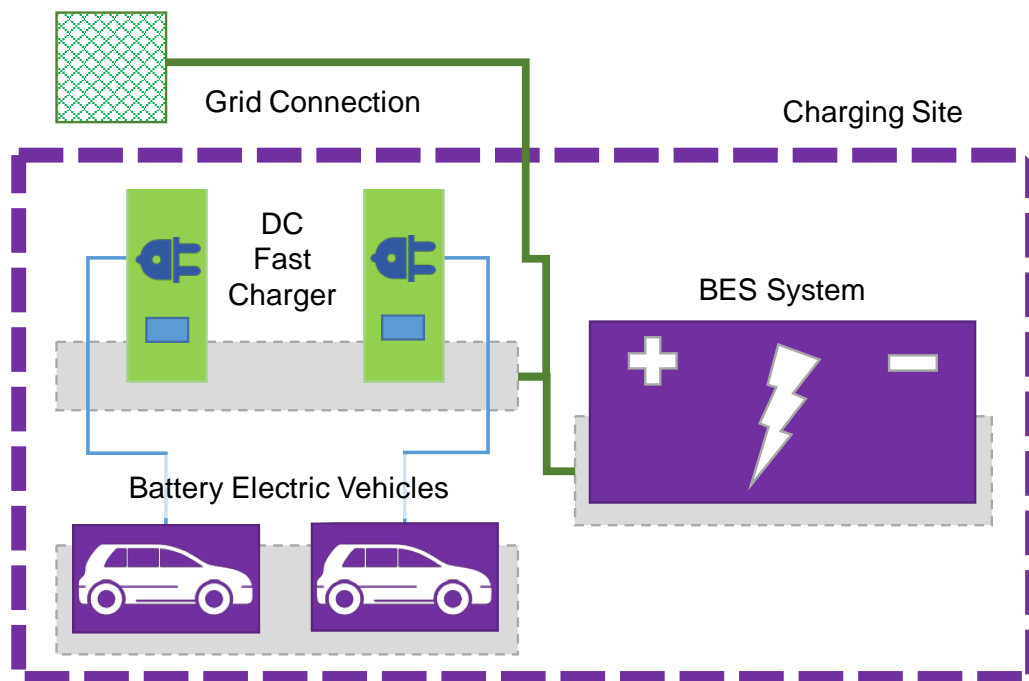


Figure 4.1.: Setup of a charging site containing several chargers, several EVs, a grid connection, and a battery energy storage (BES) system

Quadratic Programming problem. As explained in Section 2.3 the objective function is quadratic and the constraints and boundaries are linear. The aim of the optimization is to minimize the peak load of the EVs charging. With the optimization the behaviour of the charging and discharging is modelled so the high peak-load is shifted to times with lower load within the charging site. This minimizes the impact on the grid but also has an economical advantage for the owner. As explained in Section 2.1 the price during off-peak times is expected to be lower than during high peak-load. Furthermore the use of a BES is expected to reduce the peak-load. The

need of upgrading the grid infrastructure because of the high peak-load should be reduced by the BES system added to the charging site. The BES system needs to have enough capacity and output power to satisfy the peak-load. To show the impact of the BES system and the comparison of different sizes, the peak-shaving optimization is done.

4.1.1. Objective function

As explained before the aim is to shave the peak of the load profile. The design parameter x is equal to the charging and discharging power of the BES system P_{BESS} . The objective function in Equation 4.1 is quadratic. Quadratic functions have the advantage that they weight variations like extrema more than linear functions do. This is important because the peaks of a EV fast charging site are strong variations from the average that need to be flatten.

P_{EVload} is the modelled EV data from the CPM in Chapter 3 that presents the charging profile of EV in an $24h$ interval. The output of the optimization is the charging or discharging power of the BES for every time step i . Where $N = \frac{24h}{\tau}$ with τ as resolution of the simulated time.

$$\begin{aligned} f(x) &= \sum_{i=1}^N (x(i) + P_{EVload}(i))^2, \forall i \in [1, N], \\ x(i) &= P_{BESS}(i), \\ P_{EVload}(i) &= P_{modelled}(i) \end{aligned} \quad (4.1)$$

4.1.2. Constraints and boundaries

The constrains are linear. The inequality constraint is presented in Equation 4.2. The SoC after charging or discharging cannot exceed the maximum or the minimum SoC of the BES system.

Q_{BESS} is the capacity of the BES system. The output power of the BES system is given by $P_{BESS}(i)$ at time step i . The initial SoC is $SoC_{BESS,init}(i)$ and it varies with every time step i .

$$\begin{aligned} SoC_{BESS,max} &\geq SoC_{BESS,init}(i) + \tau \cdot \frac{\sum_{i=1}^N P_{BESS}(i)}{Q_{BESS}} \\ SoC_{BESS,min} &\leq SoC_{BESS,init}(i) + \tau \cdot \frac{\sum_{i=1}^N P_{BESS}(i)}{Q_{BESS}} \end{aligned} \quad (4.2)$$

The equality constraint is shown in 4.3. It says that the SoC from the beginning of the time interval must be the same as at the end of interval. This predefined SoC is a capacity reserve that ensures that the BES is already able to react to a load-peak at the beginning of the time interval. This ensures that the BES can operate all the time. The full potential of the BES is used because the system has to inject the exceeding power to the grid at the end of the time interval to satisfy the constraint.

$$SoC_{BESS,d}(n) = SoC_{BESS,d+1}(1) \quad (4.3)$$

The boundaries in Equation 4.4 limit the power that can be provided by or charged to the BES at time i .

$$\begin{aligned} x(i) &\leq P_{BESS,max} \\ x(i) &\geq P_{BESS,min} \end{aligned} \quad (4.4)$$

4.2. Optimization problem for using a PV and BES system to supply a DC charging site

In Figure 4.2 it is depicted how the PV system is connected to the proposed charging site. The figure is very similar to Figure 4.1.

The solar system can be pictured as panels on the roof of the house of the BES or on a carport's roof that shelters the EV from rain, snow and sunlight. This additional benefit of the site makes it more attractive to the user.

If it snows in the winter and the EV is parked for a full fast charging time of about an hour without a roof, snow and ice would cover the EV. This is a disadvantage for the user because the car needs to be scraped again.

In summer times when a EV is standing therefore the same period of time in the full sun, not only the passenger cabin but also the battery and the motor is heating up. The EV battery is already stressed by the charging process.

A roof has not only the possibility to carry a PV system but also has a purpose for convenience. This makes it useful in the winter time even when the sun radiation is lower.

Firstly in this section is optimization described with the objective function as well as the constrains and boundaries. Finally the model of the power output of the PV system is described.

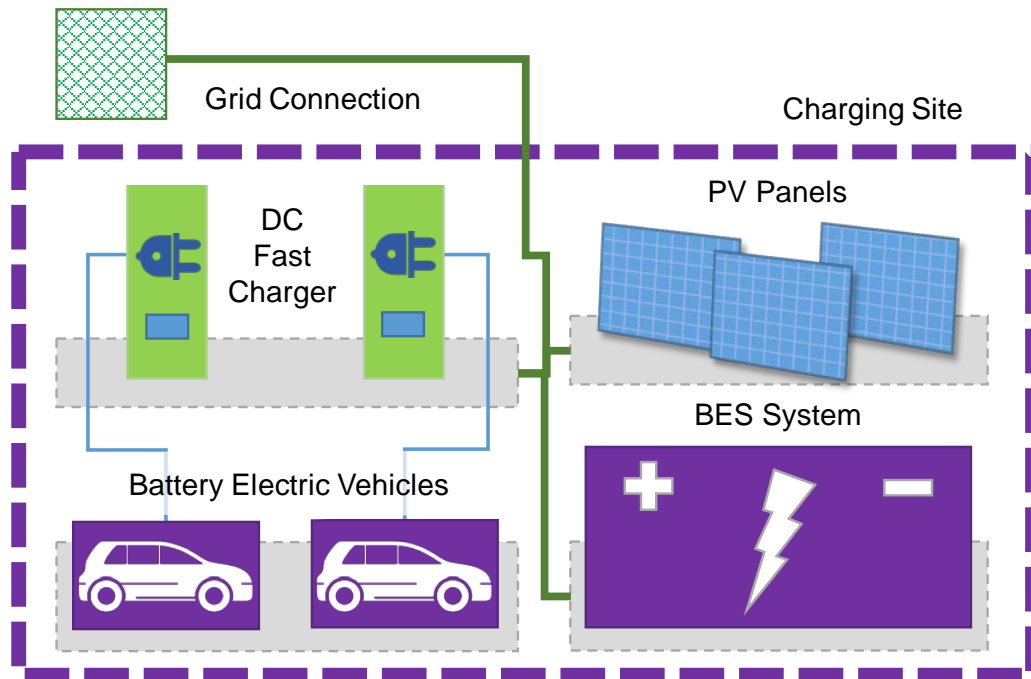


Figure 4.2.: Setup of a charging site containing several chargers, EV, a grid connection, a BES system, and photovoltaic (PV) panels

4.2.1. Objective function

The objective function needs a modification to consider the PV power additionally to the BES system. The modelled power generated from the PV panels is set by the irradiance and is no design parameter. The only design parameter stays the power stored in the BES. As it is shown in Equation 4.5 the PV power generation is added in the quadratic term.

$$\begin{aligned}
 f(x) &= \sum_{i=1}^N (x(i) + P_{EVload}(i) + P_{PVgen}(i))^2, \forall i \in [1, N], \\
 x(i) &= P_{BESS}(i), \\
 P_{EVload}(i) &= P_{modelled}(i), \\
 P_{PVgen}(i) &= P_{irragianceModel}(i)
 \end{aligned} \tag{4.5}$$

4.2.2. Boundaries and constraints

The first inequality function is the same as in 4.2 but instead of the equality function 4.3 there is another inequality function added. The second inequality function enables that the maximum potential from the PV system is used but still a minimum reserve remains in the BES. It makes the capacity reserve flexible within 20% and

80% of the maximum capacity the BES has.

$$\begin{aligned}
 SoC_{BESS,max} &\geq SoC_{BESS,init}(i) + \tau \cdot \frac{\sum_{i=1}^N P_{BESS}(i)}{Q_{BESS}}, \\
 SoC_{BESS,min} &\leq SoC_{BESS,init}(i) + \tau \cdot \frac{\sum_{i=1}^N P_{BESS}(i)}{Q_{BESS}}, \\
 SoC_{BESS,d}(N) &\leq Q_{BESS,max} * 0.8, \\
 SoC_{BESS,d}(N) &\geq Q_{BESS,max} * 0.2
 \end{aligned} \tag{4.6}$$

4.2.3. Modelling of the solar power output

The used model is ideal which means only direct irradiance is modelled so no clouds, reflections or other disturbances are considered. The basis is a Gaussian distribution (see eq. 4.7). The distribution is over time and has the highest point around noon, that is depicted by the mean μ . It is calculated by the sunset and the sunrise of the interval. The times of sunset and sunrise are based on the data from Oslo, Norway in 2018 ¹. Four cases are evaluated depicting the four seasons of a year. They are represented by the dates of the spring and autumn equinox (20. March, 23. September) as well as the summer and winter solstices (21. June, 21. December) for the year 2018.

$$\begin{aligned}
 f(x) &= \frac{p}{\sigma\sqrt{2\pi}} e^{-\frac{1}{2}\left(\frac{x-\mu}{\sigma}\right)^2} \\
 \text{with } \mu &= t_{sunraise} + \frac{t_{sunset} - t_{sunraise}}{2}
 \end{aligned} \tag{4.7}$$

The factor p is added to the Equation 4.7 because the irradiance on the earth's surface is not the same around the year due to the earth's axial tilt. The factor is based on the average solar insolation for Oslo, Norway (see Tab. 4.1). The maximum insolation is in summer. This depicts a factor of 1. The other factors are the insolation values referred to the maximum insolation.

The resulting Gaussian distributions are presented in Figure 4.3. The x-axis shows the time interval of $24h$ and the y-axis the factor p . It can be seen that the time of the highest point varies around noon. The start and end time of the radiation is controlled by the choice of σ , the variance. The given variances are chosen by trying out.

The irradiance in the summer is shown in green, and blue in the winter. The irradi-

¹<https://www.timeanddate.com/sun/norway/oslo?month=6&year=2018>

Season	Average Solar insolation in kWh/m ² /day ^a	Factor p	Variance σ
Spring (medium 1)	3.7	0.67	7
Summer (high)	5.5	1	10
Autumn (medium 2)	4.1	0.75	7
Winter (low)	1.4	0.25	4.3

Table 4.1.: Calculation of Factor p to model the solar irradiance seasonally

ance in autumn and spring is shown in red and orange. It is noticeable that maximum point of irradiance varies in the time for the four seasons.

To get the assumed power output from the PV system at each time the irradiance

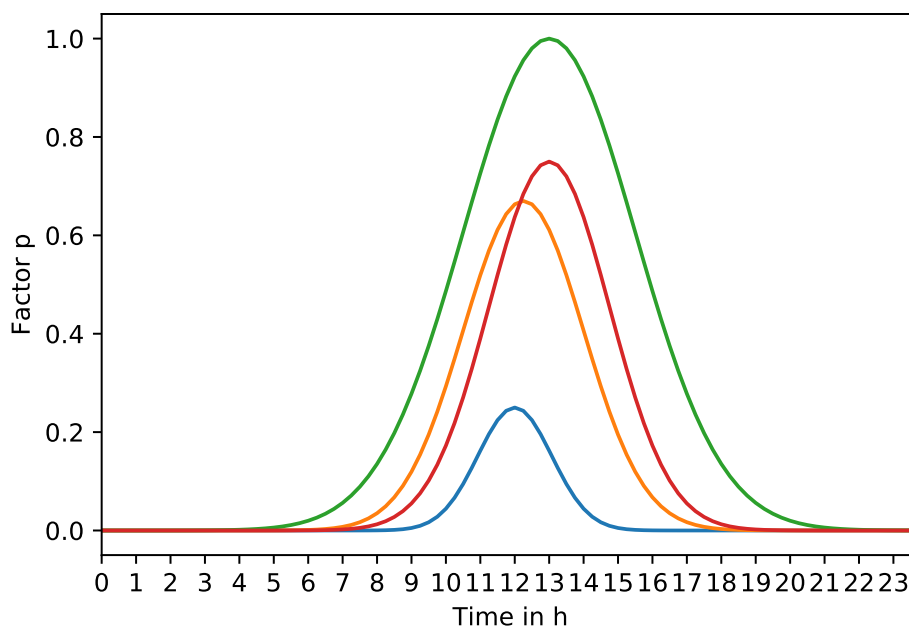


Figure 4.3.: Parameter for the solar irradiance model

model is multiplied with the maximum power output of the system. This is either at 20kW for a small-sized or 40kW for a larger sized PV panel. All cases examined in the peak-decrease optimization are shown in Table A.1 in the appendix.

4.3. Developed optimization for peak-shaving and the used algorithm in *Python*

The purposed optimization is based on a function developed in *Matlab* for the project *ideal grid for all²*, a 3-year demonstration project funded by European Commission [65]. In the project they used the solver *fmincon*. It optimizes the constraint objective function by minimizing it.

The aim is to extend the developed CPM with an optimization that is following the output of the CPM is generated (see Fig. 4.4). This expands the CPM process (Fig. 3.1) conveniently with the modelling of a charging site with integrated, and optimized BES and PV systems as a peak-shaving application. As explained in Section 3.1.4,

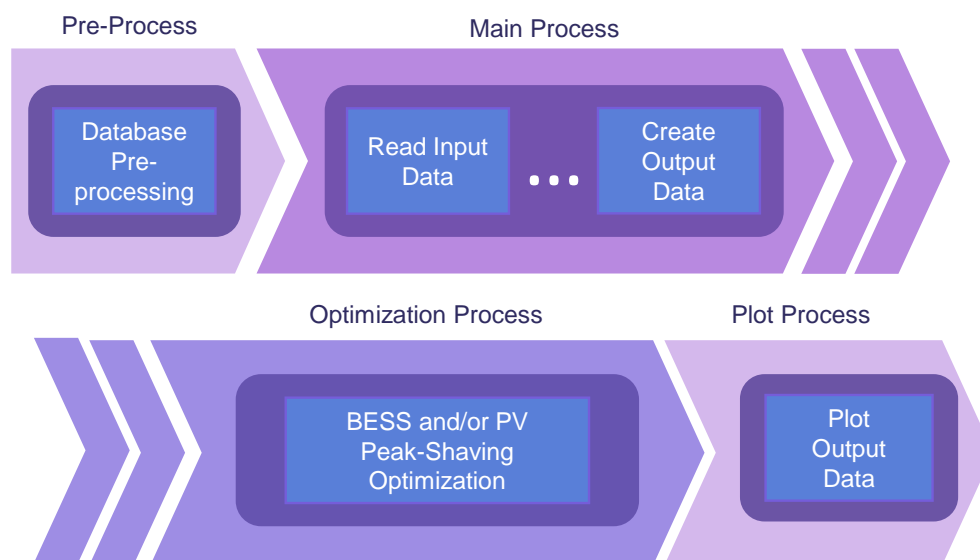


Figure 4.4.: Program process extended with the Optimization of PV and/or BES system as well as plotting the output

Python has a module named *SciPy* which is specialized for scientific programming and optimization problems. Because of the compatibility of all *Python* modules, there is no problem to combine the CPM tool and the optimization.

The general optimization process can be started in the main script like the plotting of the output (see Fig. 3.3). The optimization can be used as own script as well.

Each optimization which is presented in the sections 4.1 and 4.2, has an own *Python*

²<http://ide4l.eu/>

function. They have a similar program flow (see Fig. 4.5) but they differ in boundaries, constraints, and the objective function.

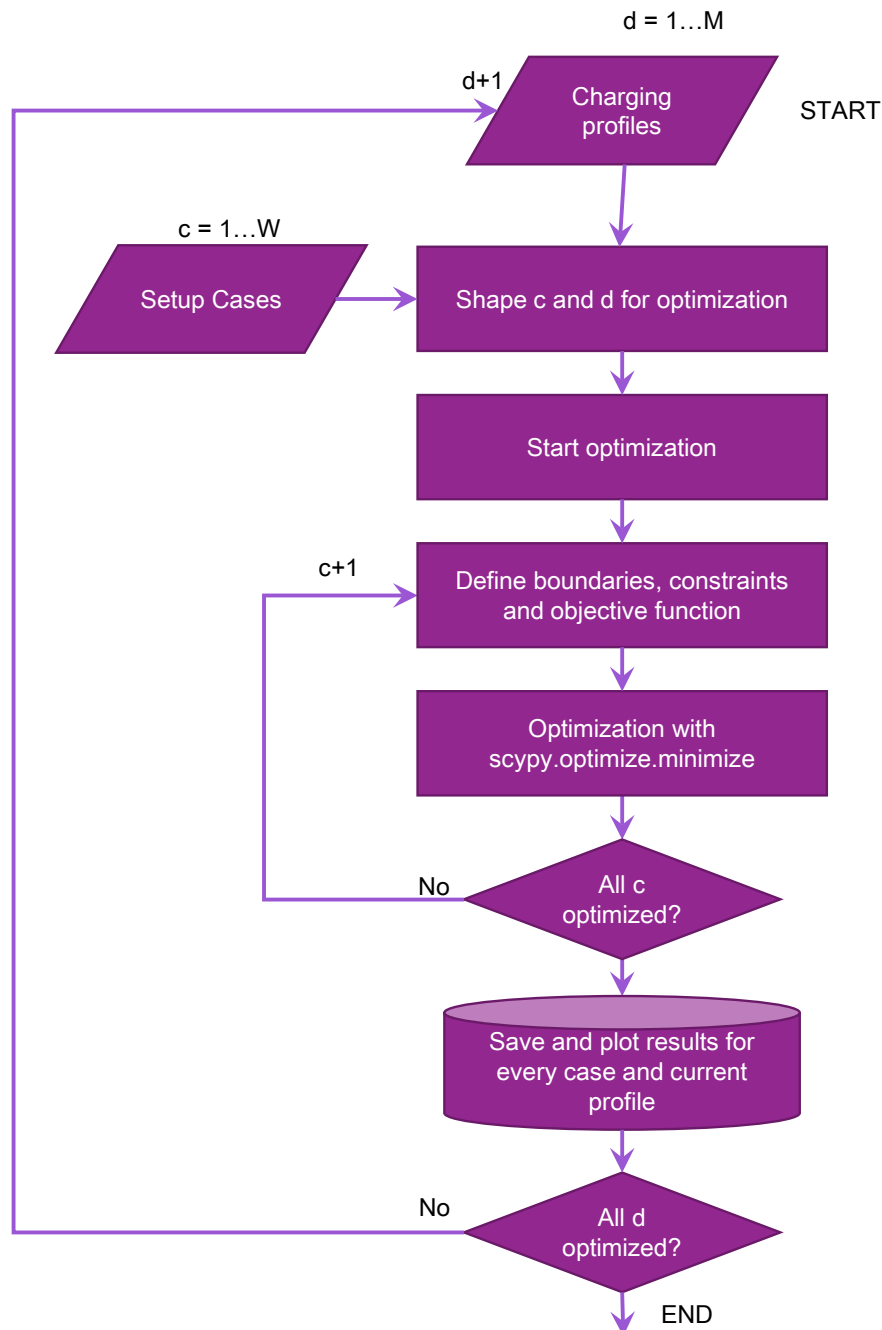


Figure 4.5.: Optimization flow diagram with the charging profiles as input database

Both optimization approaches have a similar input and output. The *SQLite* databases contain the charging profiles. Those are one of the inputs for the optimization. The setup cases are the second input. The PV and BES optimization has

many setup cases because not only the different capacity sizes and output powers of the BES have to be considered but also different radiation cases that depict different weather and season conditions and therefore have different power outputs. Figure 4.5 shows the general flow diagram of the optimization process. There are two for-loops in this optimization. The outer loop goes over every charging profile in the input database. The inner loop runs through every setup case that is considered. The setup cases are chosen configurations for the BES system capacity and maximum output power as well as the maximum output power of the PV system. The inputs are arrays. Every d has the size $k \times 1$ (*rows* \times *columns*) where $k = \frac{24}{\text{stepsize}}$ is the number of time steps in the 24h interval that is used to create the charging profiles. M is the number of charging profiles that are about to be optimized. c has the shape $1 \times W$ where $W = p \cdot q$ with p as number of different power outputs and q as number of capacity sizes. Before the optimization starts a 2-dim array filled with zeroes of the shape $k \times W$ is created. After the optimization the 2-dim array contains the optimization results for one d . This result is stored into a *SQLite* database table. Then the process continues until all charging profiles are optimized.

The actual optimization with the *Python* module *SciPy* (see chap. 3.1.4) takes place in the inner loop. There the boundaries, constraints and objective function are defined. The boundaries and constraints need to have vector and matrix shapes. This is done by using the *Numpy* n-dim arrays (see chap. 3.1.2). The boundaries, constraints, and the objective function, that are used in the optimizations are explained in sections 4.1 and 4.2. Boundaries, constraints, and the objective function change for every c so they need to be set up in every loop again. From the module *SciPy* the method *scipy.optimize.minimize* is used with the *Sequential Least Squares Programming* solver. It is a constraint minimization method that wraps a part of the 'Software package for sequential Quadratic Programming'³ [66].

When all setup cases are optimized, the results are saved and plotted. It continues with the next charging profile. When all charging profiles are looped through the optimization method has reached its end and stops running. The user has the possibility to chose the best setup case for each charging profile. To do that visually plots can be created. The results from the gathered charging profiles which are based on real data are presented in Chapter 5.

³Kraft, D. A software package for sequential quadratic programming. 1988. Tech. Rep. DFVLR-FB 88-28, DLR German Aerospace Center - Institute for Flight Mechanics, Colone, Germany

5. Use Case: Evaluation of Charging Profile Modelling tool and three DC charging sites in Norway

In this chapter the evaluation and result presentation of the real charging data from Norway is presented. The original data set is kindly provided by *Fortum Charge & Drive*. In Section 3.2 the database structure is explained detailed as well as the filtering of charging events. The specifics of the provided data are presented in Table 5.1. Three charging sites with a different number of charging events and charging stations are evaluated. The charging sites are named *A*, *B*, and *C*. Each charging

Charging Site	Charging Site A	Charging Site B	Charging Site C
Number of Charging Events	1, 400	8, 500	30, 700
Number of Charging Stations	2	5	10
Observation Period	23.05. - 31.12.2018 (223 days)	22.05. - 31.12.2018 (224 days)	22.05. - 31.12.2018 (224 days)
Runtime of CPM (<i>sec</i>) (Weekly/Monthly)	~ 280/ ~ 320	~ 1, 550/ ~ 1, 600	~ 6, 200/ ~ 6, 300
Time per Charging Event (<i>sec</i>) $\frac{avg.Runtime(s)}{ChargingEvents}$	~ 0.21	~ 0.19	~ 0.20
Runtime of optimization (<i>sec</i>) (BES/BES&PV)	~ 580/ ~ 3, 800	~ 730/ ~ 4, 500	~ 2, 100/ ~ 12, 200
Time per optimization Case (<i>sec</i>) $\frac{avg.Runtime(s)}{ChargingEvents \cdot Case}$	~ 0.02	~ 0.022	~ 0.024

Table 5.1.: Key data of the analysed charging sites that are located in Norway

site has one databases of charging data. The databases are named each after the charging sites *a*, *b*, and *c*.

Each station has N chargers, where N is not given in the data. The number of charging events for site *C* is the highest as well as the number of charging stations. All sites have at least two of the DC chargers mentioned in Table 2.1 (exclude America).

The observation period differs in one day. It begins in the end of May and ends with the last day of December. The first month of the 2018 are no measured and are therefore not in the observable time period. The analysis will concentrate on the full month (June to December) so this does not have an effect on the results.

The runtime is measured by a built-in module *time* that provides a function to start and stop a counter. The time counter is started at the beginning of the main process in the CPM tool and stopped before the plotting process. For the CPM tool the runtime is given for each database for the monthly and the weekly format with *15min* resolution. There is a slight difference between the weekly and the monthly format. The runtime counter for the optimization is started before the optimization process begins and ends after the results are written to the database.

Significant is the increasing runtime for an increasing number of charging events. The time of execution per charging event is similar for all charging site. The runtime is not only dependent on the number of charging events but also on the performance the hardware¹.

In the following sections the *Python* and the gathered data is evaluated. First output of the charging profile modelling tool is examined. The charging energy is presented on weekly and monthly bases.

Afterwards the optimization including the BES and PV system is evaluated. Therefore the mean charging power of three month represent a low, a medium and a high demand scenario. They are studied in detail for the BES-only optimization. This enables a comparison of different challenges for each BES configuration case. The optimization of the combined PV and BES system is presented for the medium demand scenario and three different solar irradiance scenarios representing low, medium and high irradiance.

¹Device information: Windows 7 64bit. Intel i5-2410 CPU. 10GB Ram. PyCharm IDE 2019.1.3

5.1. Evaluation of the results of the Charging Profile

Modelling tool

In the following section the results from the CPM tool are presented. The results for charging site C from Table 5.1 are described in detail. The results for the charging sites A and B are in the appendix A.2.

Firstly the results are evaluated by weekdays in a $24h$ resolution. Afterwards the results are evaluated on a monthly basis with two different types of presentation. Type one is a monthly overview of the charging on each day. The second type is the $24h$ charging profile of each month. The months are evaluated in detail for both types to investigate possible seasonal changes and other influences to validate the developed CPM tool.

5.1.1. Evaluation of the results on each weekday

Figure 5.1 shows an overview of the weekdays from Monday to Friday. The time resolution is $15min$ in a $24h$ interval. The mean of all values of a $15min$ interval is calculated and plotted in a bar plot in dark green. The maximum values of the particular $15min$ interval from all observed weeks are given as well. The mean value between 02 : 00 and 06 : 00 is almost zero at every weekend. At those weekdays the charging stations are rarely used in those four hours. The highest mean value is marked in light green. It appears on Mondays to Wednesdays between 16 : 30 and 17 : 15 and on Thursdays and Fridays between 14 : 45 and 15 : 15. From 06 : 00 to the maximum value the energy is increasing in a slower rate than it decreases from the maximum value to 02 : 00, except on Fridays. On Fridays after 15 : 15 the charging energy stays around $10kWh$ until midnight.

In Figure 5.2 Saturdays and Sundays are examined in the same way as before. It is noticeable that shape of Saturdays and Sundays charging profile is similar. The maximum values have a sinus curve shape with a significant peak in the early afternoon. On Saturday there is also a peak around 22 : 30. Between 02 : 00 and 08 : 00 the demand at the charging site is very low. It increases fast up to 13 : 00 and is over $10kWh$ until 19 : 00. On Saturdays the highest value is at 19 : 00 on Sundays it is already at 17 : 00. Compared with the weekdays the demanded energy between 00 : 00 and 02 : 00 is higher on Saturdays and Sundays. Significant is that Sunday is the only day when there are neither in the mean nor in the maximum values is a gap of charging. A gap in the maximum value means that there is no charging

event in the whole database for this time interval and the minimum, the mean and the maximum value equal zero. It is noticeable that the maximum charging values by night are significantly lower than by day.

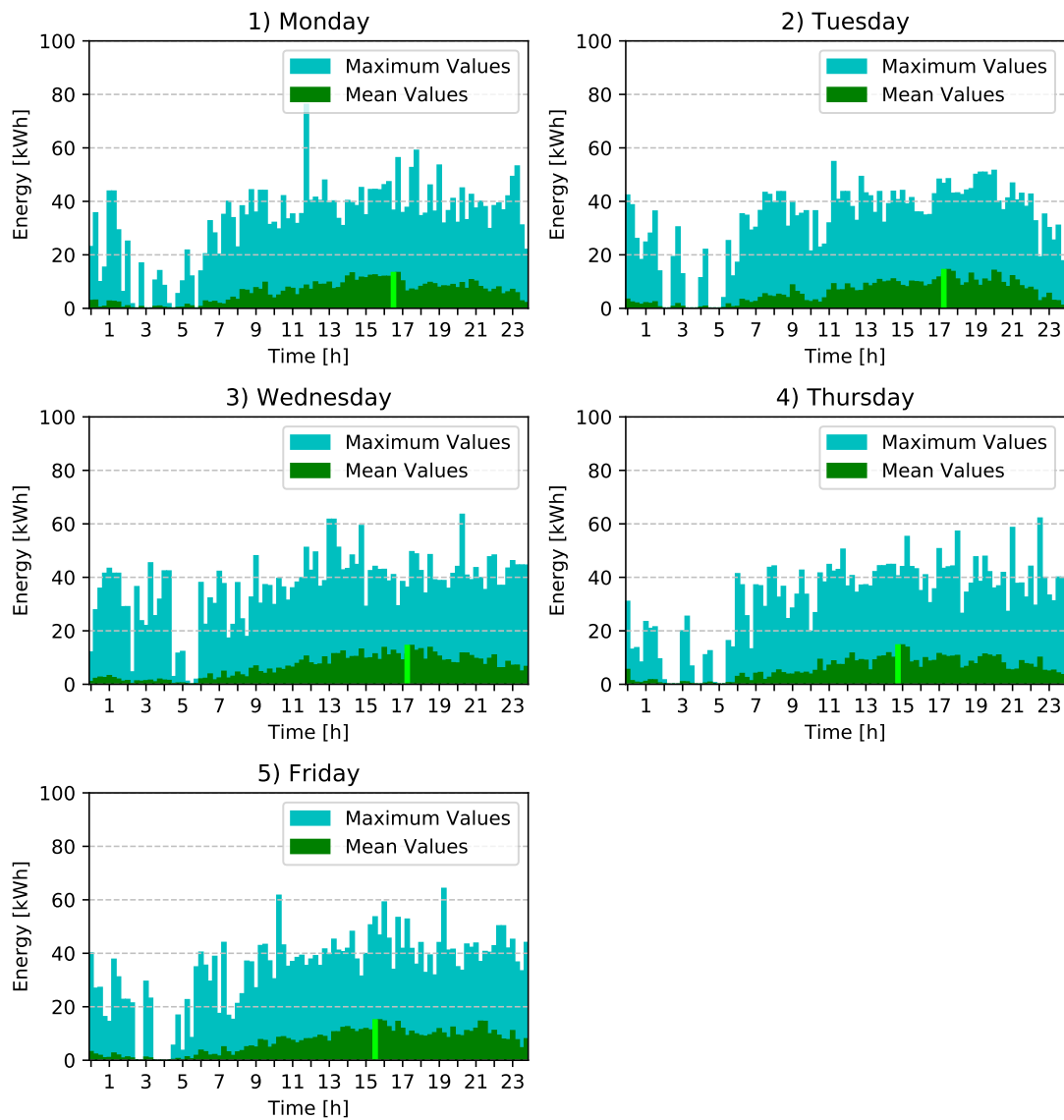


Figure 5.1.: Mean of all Mondays to Fridays in the observation period from charging site C

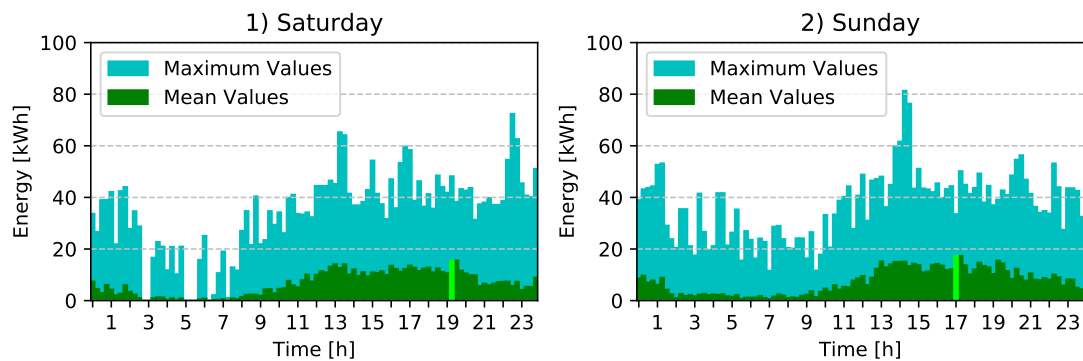


Figure 5.2.: Mean of all Saturdays and Sundays in the observation period from charging site C

Table 5.2 gives a summary of statistical values for the presented results in the figures 5.1 and 5.2. The calculated values are:

- the mean value
- the standard deviation from the mean value
- the minimum value
- the maximum value
- the 50% percentile also known as median

This means one half of the mean charging profile values are less than this and the other half is above this value. All values have the same unit as the data itself, kWh . For the analysis the mean values of each month is analysed. Most noticeable is that the minimum value on Sundays is not equal to zero like on the other days. This portends that in average the charging site is used around the clock on Sundays. Sunday also has the largest values for all other columns as well.

in kWh	Mean	Standard Deviation	Min. Value	50% Percentile	Max. Value
Monday	5.81	3.94	0	6.77	13.28
Tuesday	5.80	4.16	0	5.82	14.37
Wednesday	6.39	4.17	0	6.68	14.42
Thursday	5.62	3.93	0	5.24	14.61
Friday	6.69	4.46	0	7.68	15.02
Saturday	6.45	4.64	0	6.04	15.51
Sunday	7.29	4.89	0.56	7.76	17.32

Table 5.2.: Statistical analysis of the mean value of charging profiles per weekday, in kWh

5.1.2. Evaluation of the results on monthly basis

Figure 5.3 shows an overview of six full month of the observed period. This month include June, July, August, September, November and December. The month May and October are left out. In May only the last week was observed and in October was an construction nearby so the station was not accessible as usual. That leads to a significantly lower charging demand that is not representative. The measurement data is from charging site C. The plots show the mean charging energy and the maximum charging energy of each day. Every 7th day is marked, to make it easier to analyse the data. The marked day is Monday.

It can be seen that in July the charging energy is lower than in June or August. In the last week of September the charging energy decreases on a daily basis. In the first two weeks of November the charging energy increases. But it decreases again in the last week of November. A low charging energy per day is observable in December. In the last week the energy is again increasing per day.

Overall there is no significant pattern noticeable during the observed weeks. It is noticeable that the charging energy on Sundays is almost always equal or greater than the charging energy on Mondays.

Figure 5.4 shows the average daily charging energy per $24h$ in each month. The maximum value that is charged during one $15min$ interval is shown as well as the mean value. These charging profiles are similar to the ones discussed in Section 5.1.1. The mean energy is highest in August, September and November. The highest maximum value is charged in August. The time where in average almost no charging takes place are between 02 : 00 and 06 : 00 in the morning. December is different because the charging time is almost twice as long between 01 : 00 and 08 : 00.

The maximum values are showing, that in June, July, and September the charging stations are used also by night. Only half an hour long there took no charging place in all events of that month.

In August, November and December the amount of time where no charging at all took place equals the gaps in the maximum value of the day. It is more than an hour. Noticeable is that the normal charging decrease in November starts around 07 : 00 and in December around 08 : 00. That is a difference of 1 hour. In July the charging increases from 09 : 00 until the afternoon. After the night there is a peak between 06 : 00 and 07 : 00.

In Table 5.3 the statistical summary is also presented for the $24h$ charging profiles

in <i>kWh</i>	Mean	Standard Deviation	Min. Value	50% Percentile	Max. Value
June	7.29	4.52	0	7.22	15.64
July	5.39	3.62	0	5.55	13.72
August	8.14	5.41	0	7.46	19.19
September	9.69	6.18	0	9.24	22.61
November	8.8	6.23	0	9.5	21.18
December	4.58	3.52	0	4.12	12.21

Table 5.3.: Statistical analysis of the mean value of charging profiles per month, in *kWh*

in each month. The highest mean is in September as well as the highest maximum value. The median is highest for November that has the second highest maximum value and also the highest deviation from the mean. It is noticeable that the minimum value is zero for each month which means in every month is a at least one time step when no charging at all is done. This is confirmed by the plots in 5.4

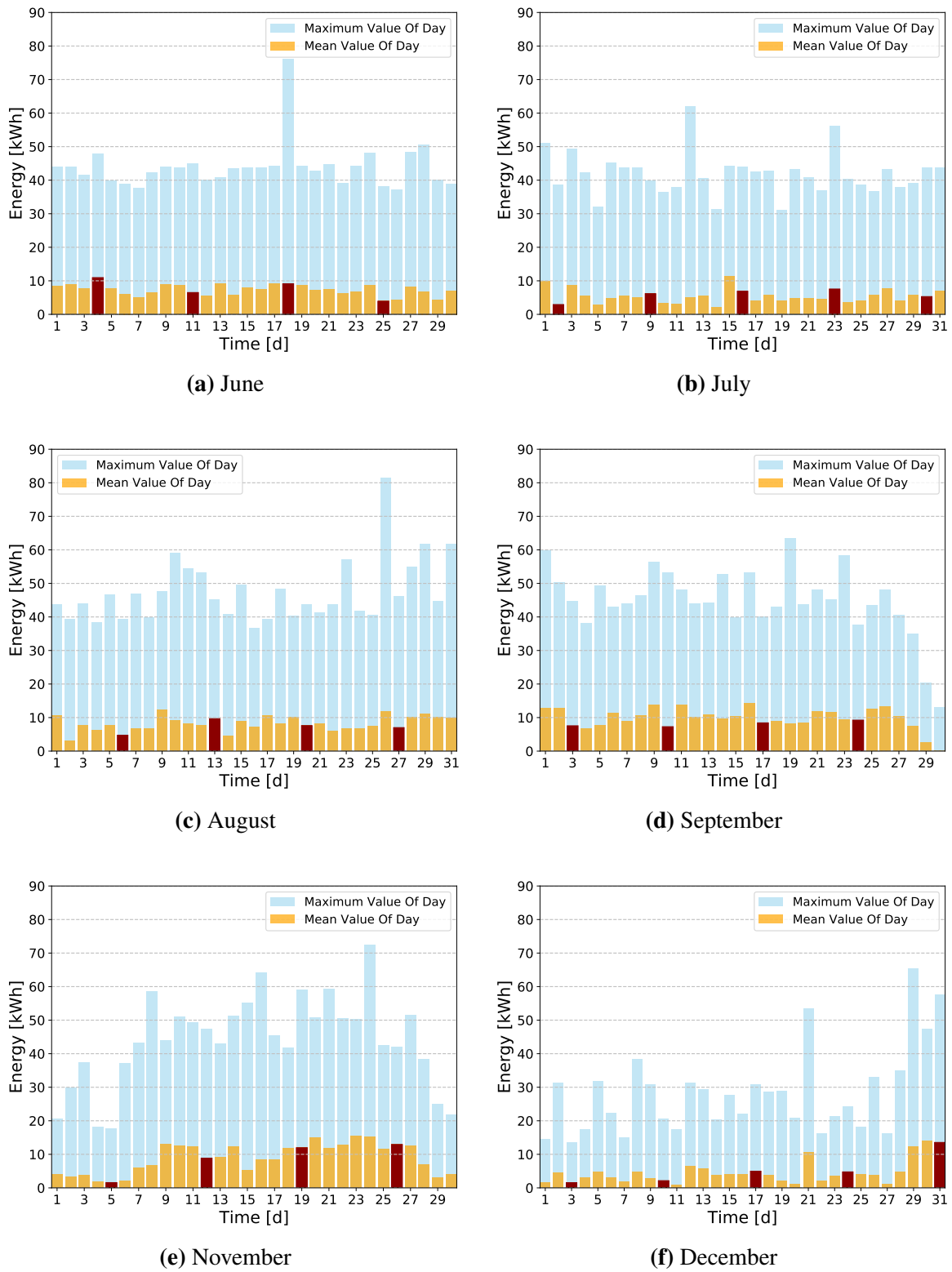


Figure 5.3.: Monthly evaluation of the charging profiles on a daily basis (Charging Site C)

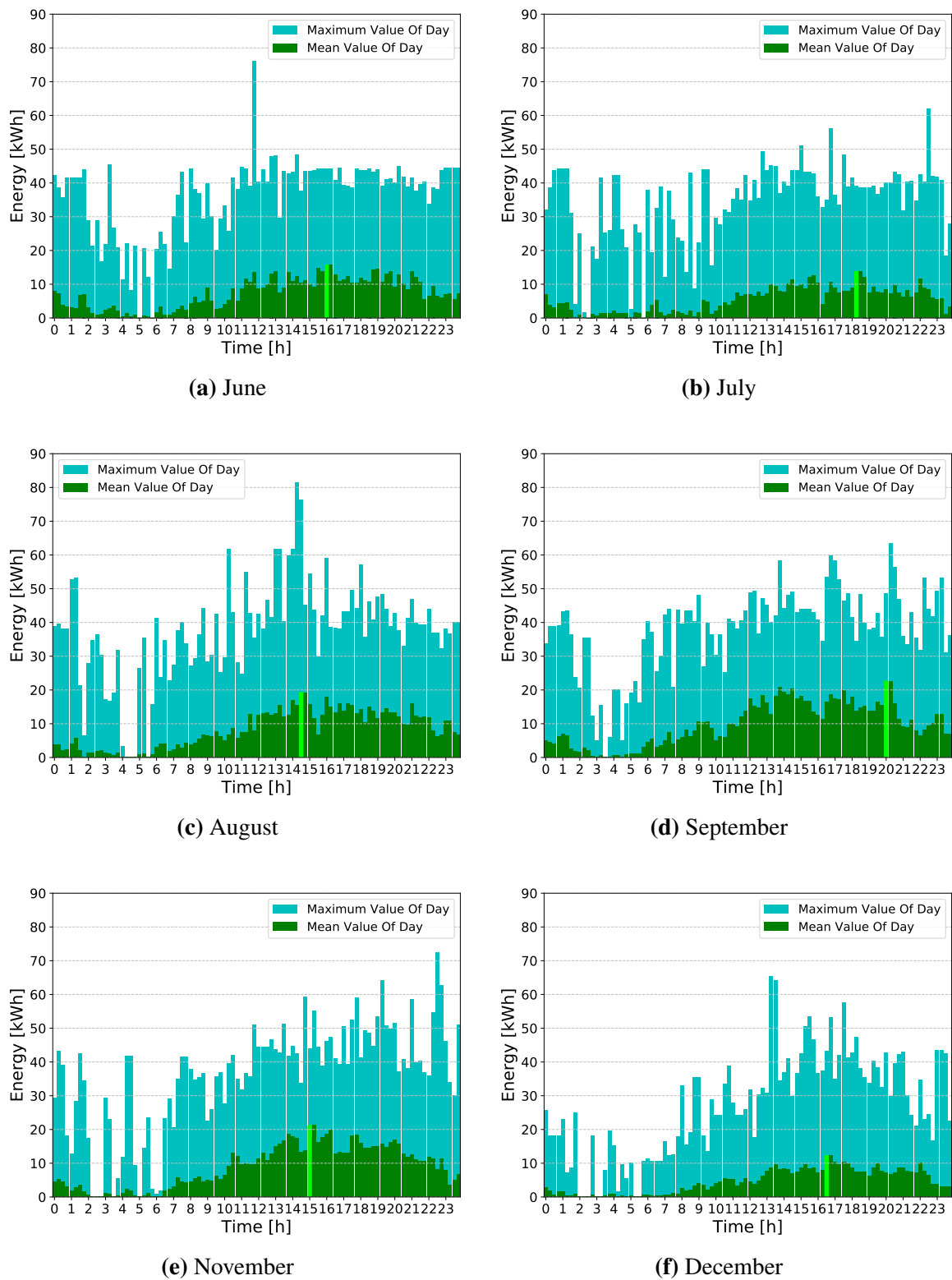


Figure 5.4.: Monthly evaluation of the charging profiles on a 24h basis (Charging Site C)

5.2. Evaluation of the results of the peak-shaving optimization

The developed optimization tool includes two possibilities for peak-shaving. The first one uses only a BES system and the second one uses a BES in combination with a PV system. In both methods the desired charging and discharging profile of the system is calculated by the optimization algorithm. In this section the results from the peak-shaving with help of the optimization are evaluated. The results for charging site C (see Tab. 5.1) are described in detail. The results for the charging sites A and B are in the appendix A.2.

Firstly the results of the BES system optimization are evaluated for three month. The basis are $24h$ charging profiles as they are presented in Figure 5.4. Three month are each evaluated to have three different charging demand scenarios which can be compared:

- low demand scenario: The maximum peak demand is less $50 kW$, the mean value is around $20 kW$.
- medium demand scenario: The maximum peak demand is around $75 kW$, the mean value is around $30 kW$.
- high demand scenario: The maximum peak demand is $90 kW$, the mean value is around $40 kW$.

Afterwards the optimization with the combined BES and PV system is applied for medium demand scenario. The used values for the BES power and capacity cases as well as the size and irradiance cases of the PV system are depicted in Table A.1.

5.2.1. Evaluation of the results of the BES-only system optimization for peak-shaving

In the following the results are presented for the peak-shaving with help of a BES. With the developed optimization tool the desired and optimised BES behaviour is calculated for each use case. The data is output to a database as well as the results are plotted for a $24h$ interval. The power output of the BES is presented and the resulting demand is calculated by adding the BES power to the requested charging power to achieve a resulting charging profile.

Those profiles are evaluated in this section. The original and the resulting charging profiles are compared regarding the peak-decrease. This gives a hint on the impact

that a BES can have on the grid consumption of the charging station. By comparing different BES system sizes in mean of capacity and power it is evaluated which size might have the biggest influence. It is also beneficial to know what BES system size is preferable for different charging demands.

In general the aim of peak-shaving is to reduce the maximum peak occurring in a time interval. This is done by shifting the load from the peak with help of the BES. The BES stores the energy in times of lower or off-peak phases. When the demand arises the power is released from the BES to reduce the peak. This can prevent over sizing grid assets if there is no further reason but the occurring high-peak during a short time of the day.

The examined charging profiles are displayed in the following figures:

- low demand scenario: 25 & 50 *kWh* in Figure 5.5 and 100 & 150 *kWh* in Figure 5.6
- medium demand scenario: 25 & 50 *kWh* in Figure 5.7 and 100 & 150 *kWh* in Figure 5.8
- high demand scenario: 25 & 50 *kWh* in Figure 5.9 and 100 & 150 *kWh* in Figure 5.10.

Firstly each charging scenario will be explained. Afterwards the three scenarios are compared with each other.

As it can be seen each figure contains two plots and two figures belong to each scenario. Each plot handles one of the chosen capacities for the BES. The order of plots is ascending of the capacity for all the three scenarios. The y-axis describes the power that is charged at each moment of time, which is on the x-axis.

The resolution to create the charging profile is 15 *min* and the time steps in the plot are from 00 : 00 to 23 : 45. The original charging demand which is created by the CPM is plotted in green. The storage power is plotted for each charging power variation in a different shade of violet. The resulting charging profiles are orange.

Low demand scenario

In Figure 5.5 a) the peak decrease is about 37%. This means the maximum value of the resulting profile is 63% of the peak without any BES support. It is also visible that the charging profile with the peak-shaving is narrower.

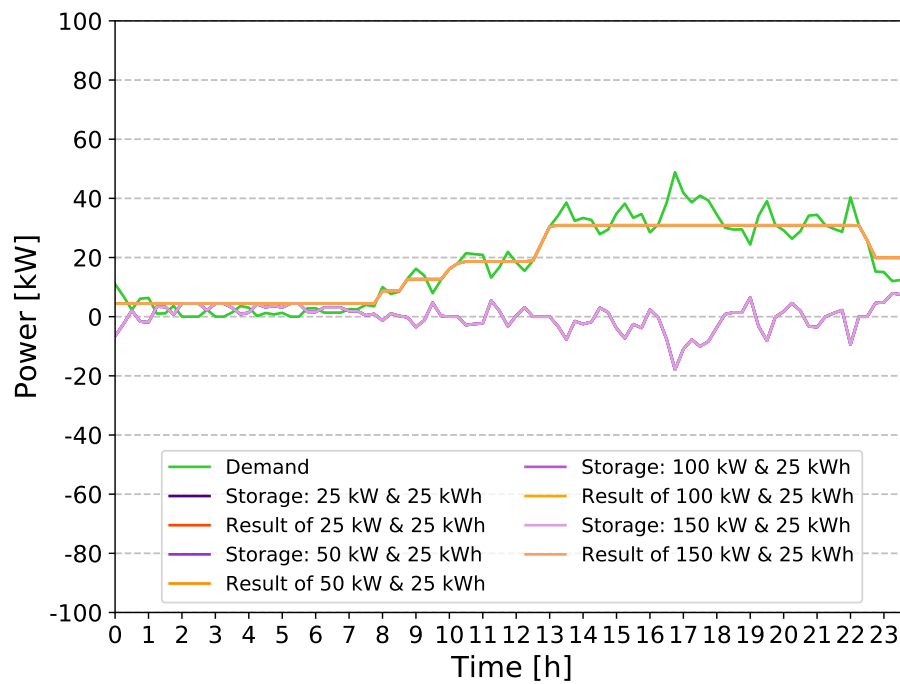
When the BES power is lesser than zero this means the discharging starts. When the power is above zero, the BES charges. At zero the BES system is neither providing nor charging energy. It is noticeable that all BES and resulting profiles are

congruent. The variance of the BES power has no effect on the result when the BES capacity is at 25 kWh .

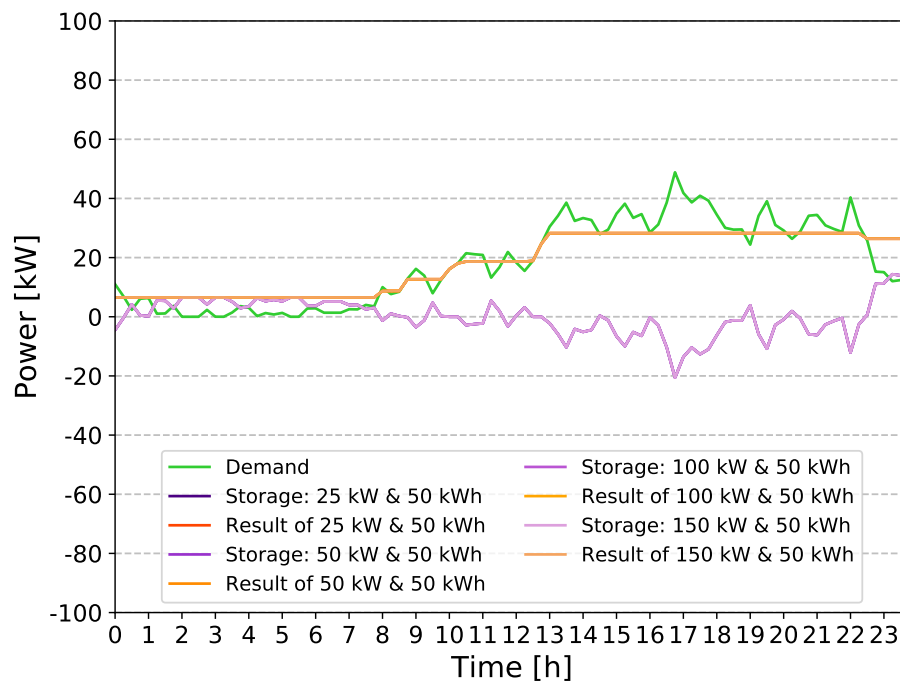
A similar congruent behaviour can be seen in Figure 5.5 b), and in Figure 5.6 a), b) as well. In Figure 5.6 b) there is a spike for the first case at the time of the high-peak value. It seems that the charging profile flattens with increasing battery capacity. It can be seen that the load is shifted from the peak time to times with almost no peak. For Figure 5.6 b) this means that the BES system charges from midnight to 09 : 00 in the morning. From 13 : 00 to 23 : 30 it is discharging.

A summary of the peak-decreases is given in Table 5.4. The peak decreases are 42 %, in Figure 5.5 b), Figure 5.6 a) 49 %, and in Figure 5.6 b) over 51 %.

The peak-decrease seems to increase with the BES capacity. The values over the different power cases for the same capacity are equal except for the highest capacity case. There is a difference of three percentage points between 25 kW and greater or equal 50 kW BES power.

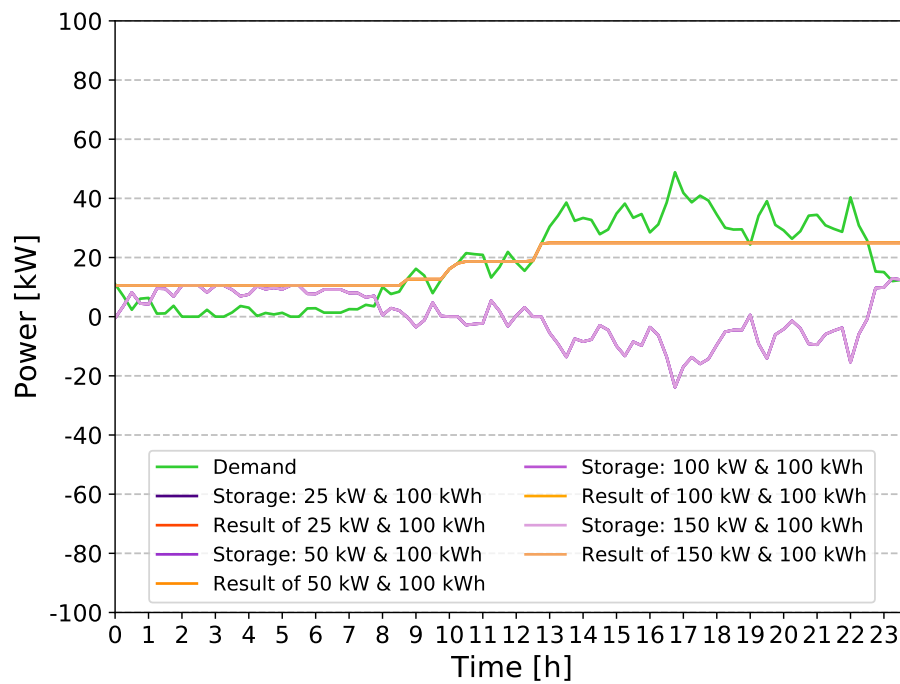


(a) Capacity: 25 kWh

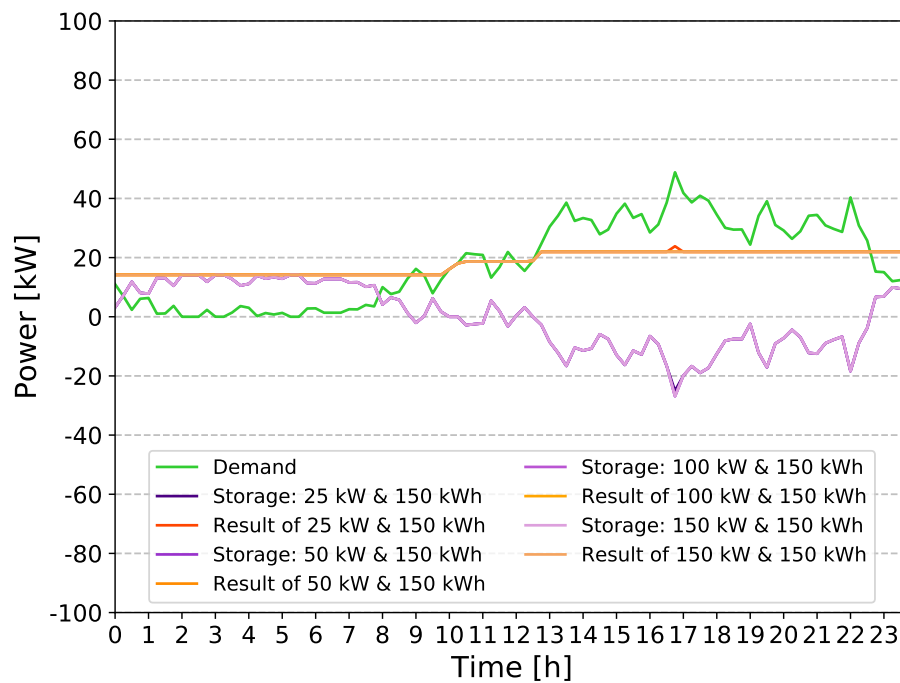


(b) Capacity: 50 kWh

Figure 5.5.: Evaluation of the peak-shaving optimization with the BES system in a low demand scenario (Charging Site C; 25 & 50 kWh)



(a) Capacity: 100 kWh

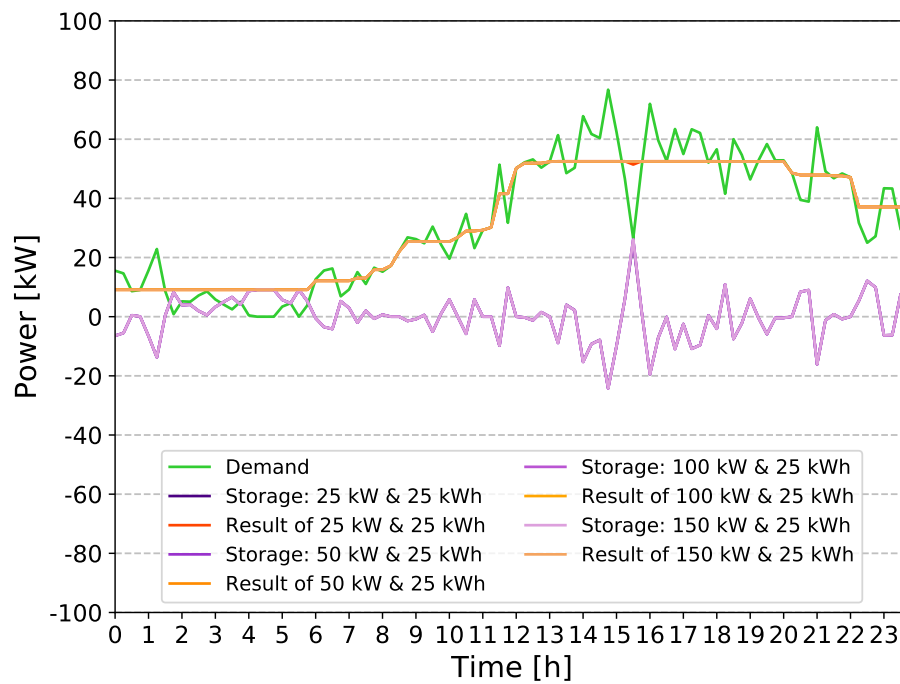


(b) Capacity: 150 kWh

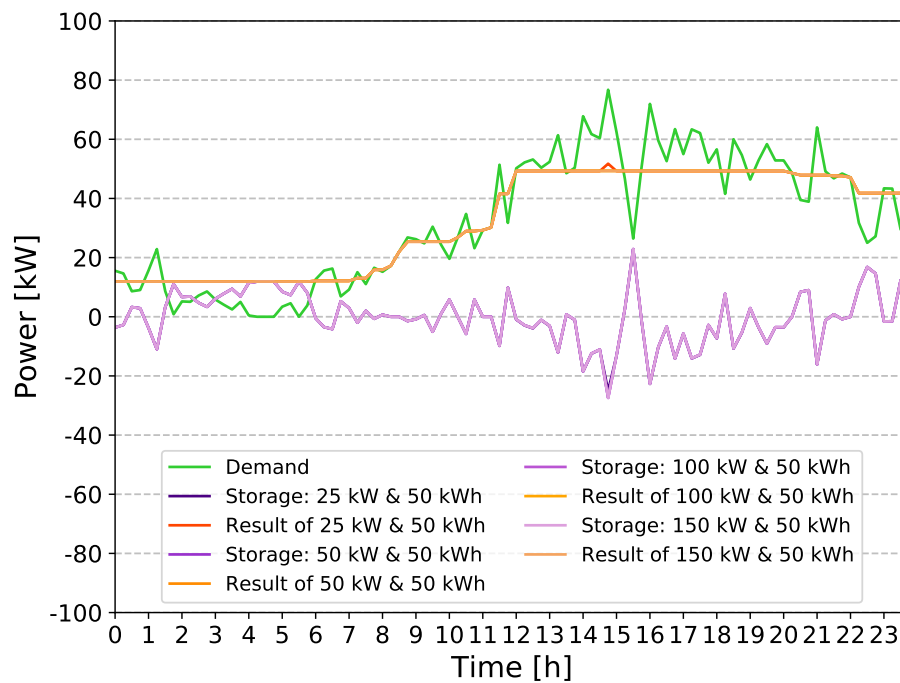
Figure 5.6.: Evaluation of the peak-shaving optimization with the BES system in a low demand scenario (Charging Site C; 100 & 150 kWh)

Medium demand scenario

The figures 5.7 and 5.8 show the medium charging demand scenario. The maximum peak is around 15 : 00 with a value of 76 kW. The different BES power case profiles in Figure 5.7 a) are almost congruent, except for the first case, the 25 kW. There is a spike at the low-peak directly next to the maximum value. The charging and discharging times are very intermittent so there is no time when the BES is mainly charged or discharged. The peak-decrease is at 32%. Case 5.7 b) is similar to 5.7 a) in having congruent resulting charging profiles. There again a spike appears in the first case, but it is now at the high peak time. The peak-decrease is between 33% – 36%. In 5.8 a) there are again spikes. This time it is more visible at the time of the maximum peak and at time of the second highest peak. The amplitude is the same as before. It is visible that the spikes correlate with a small divergence in the amplitude of the power of the BES. The time of charging the BES is again mainly in the early morning and stops at 09 : 00. The discharging is between 12 : 00 and 22 : 00 with short intermittences. The peak-decrease is between 33% – 41%. For 150 kWh the peak-decrease lies between 33% – 44%. Considering only the higher value the peak-decrease decreases with the battery capacity. The lower value is caused in all cases by the peak that arises in the resulting power. The amplitude of this spike is the same for all cases. Although the capacity is greater than Figure in 5.7 b) the peak-decrease for case one is the same for the figures 5.8 a) and 5.8 b) too. With a BES power of greater or equal 50 kW the peak decrease is higher.

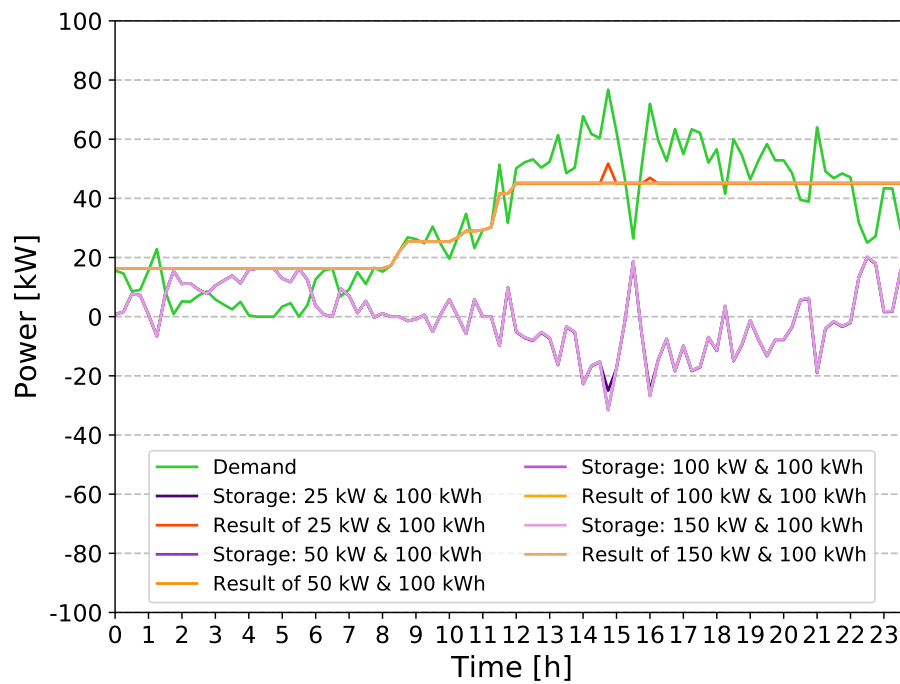


(a) Capacity: 25 kWh

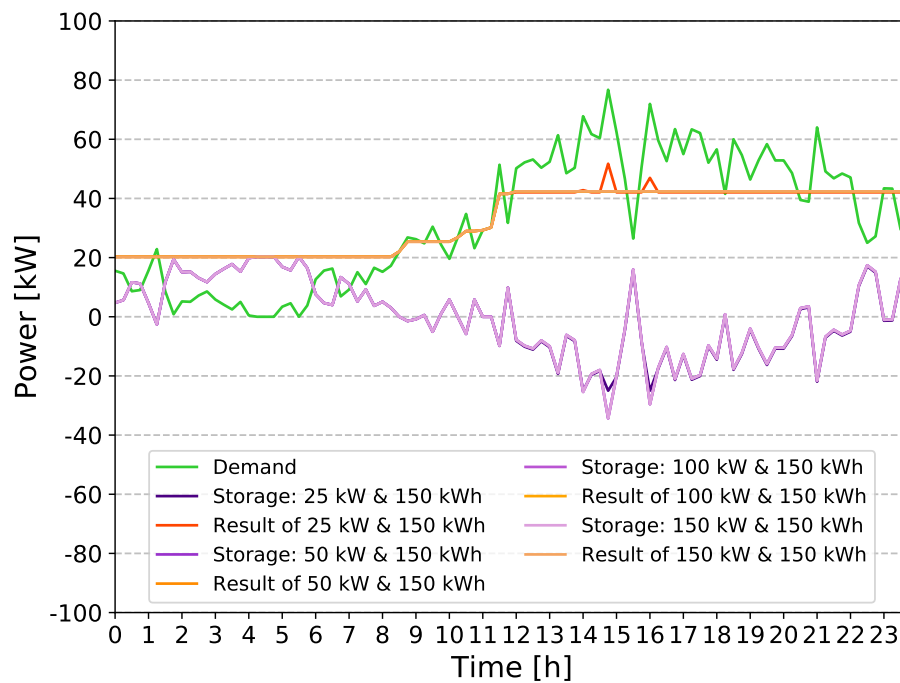


(b) Capacity: 50 kWh

Figure 5.7.: Evaluation of the peak-shaving optimization with the BES system in a medium demand scenario (Charging Site C; 25 & 50 kWh)



(a) Capacity: 100 kWh

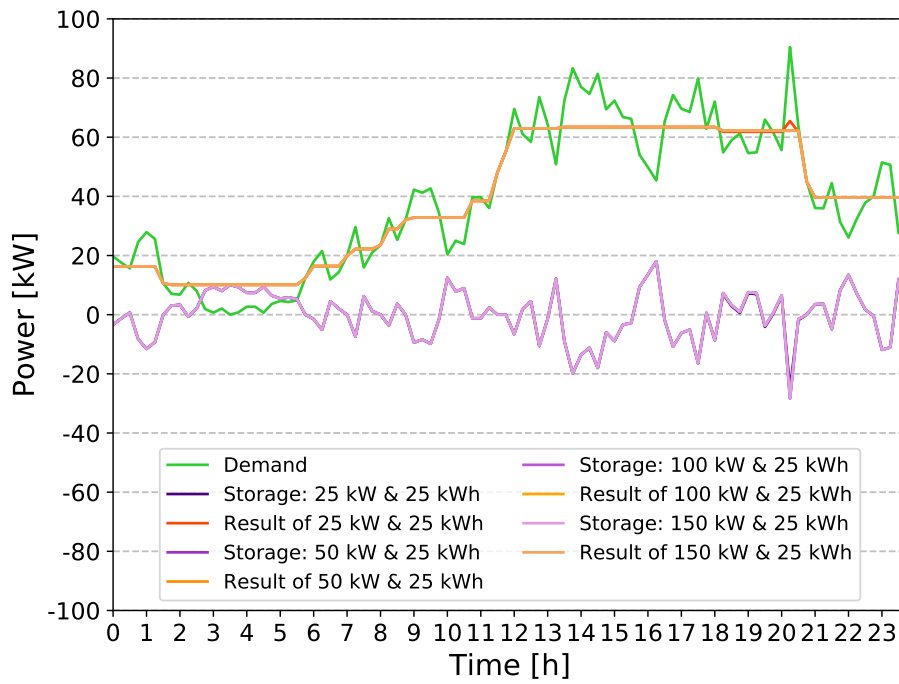


(b) Capacity: 150 kWh

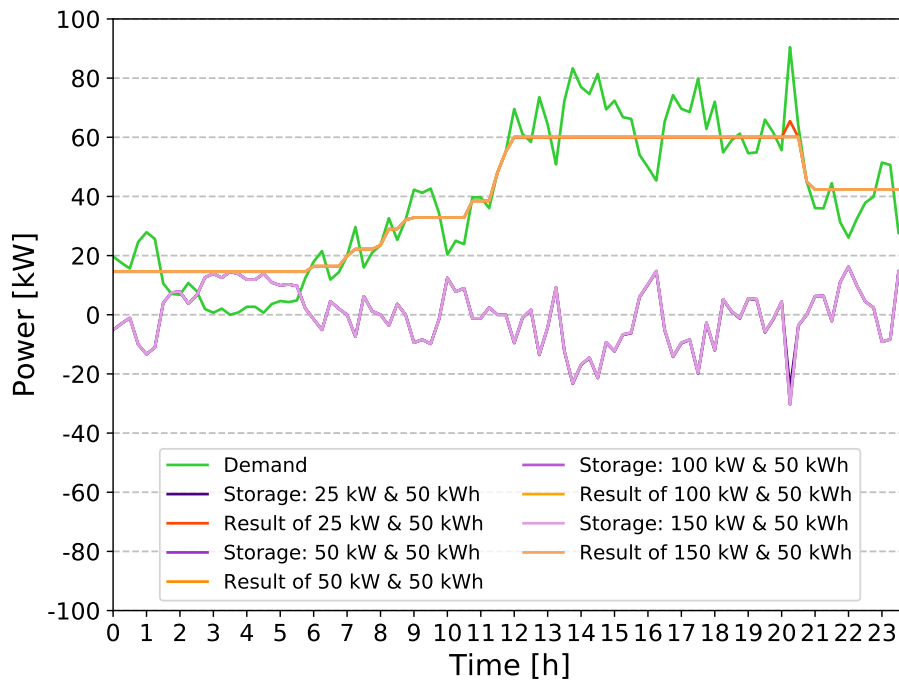
Figure 5.8.: Evaluation of the peak-shaving optimization with the BES system in a medium demand scenario (Charging Site C; 100&150 kWh)

High demand scenario

The high demand scenario is depicted in the figures 5.9 and 5.10. The maximum power of 90 kW occurs around 20 : 00 in the evening. In the first capacity case 5.9 a) the resulting charging profile has still noticeable steps, but the peaks are smoothed. At time of the peak occurs again a spike for case one as described before for the medium demand scenario. The peak-decrease is around 28 % – 30 %. For case 5.9 b) the resulting profile is similar to 5.9 a). The peak-decrease is between 28 % – 34 %. Case 5.10 a) is significantly different to the cases before. The resulting charging profile is significantly lifted in the first half of the day and decreased in the second half compared to the cases before. There are spikes in the resulting power at the times of the highest peaks again for case one. The peak-decrease is between 28 % – 40 %. For the first case it is again limited because the desired discharging power exceeds the power that can be provided by the BES of 25 kW size. In 5.10 b) more spikes occur at the time of the highest peaks for case one. The increased capacity of the BES makes it possible that more energy can be charged and discharged. The main charging time is again in the first half of the day between 00 : 00 and 07 : 00. There is also a comparable long period of 2 h in the late evening. Discharging mainly takes place between 12 : 00 and 21 : 00. In this case the peak-shifting is highly noticeable. The resulting charging profile in case 5.9 a) has a difference between maximum value and minimal value of almost 50 kW . This difference is half in case 5.10 b). The peak decrease is between 28 % – 45 %. Compared with the first case of 25 kWh the peak is a third more decreased with a 150 kWh BES capacity and a power greater or equal to 50 kW .

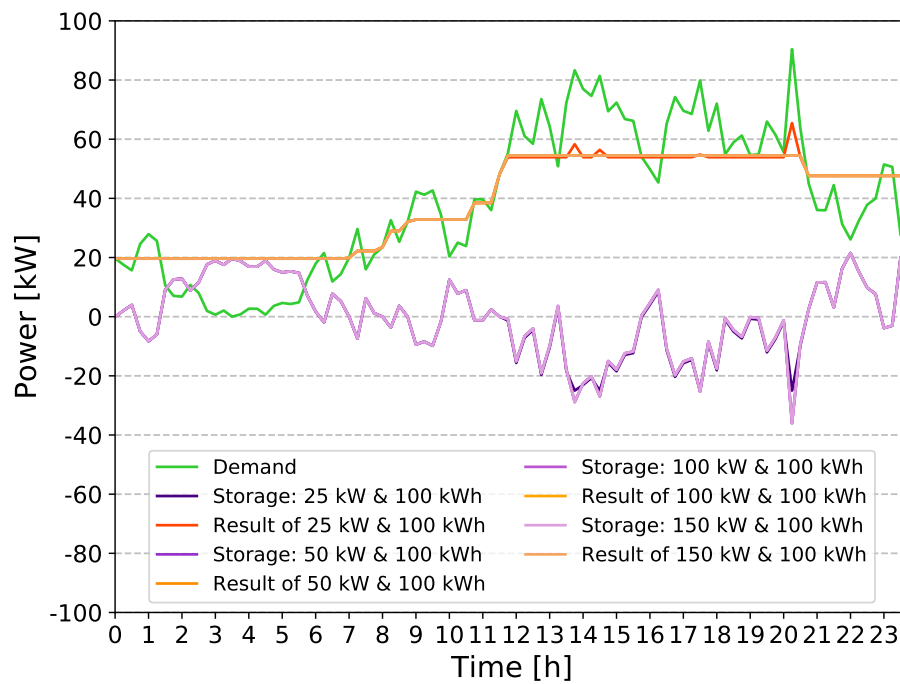


(a) Capacity: 25 kWh

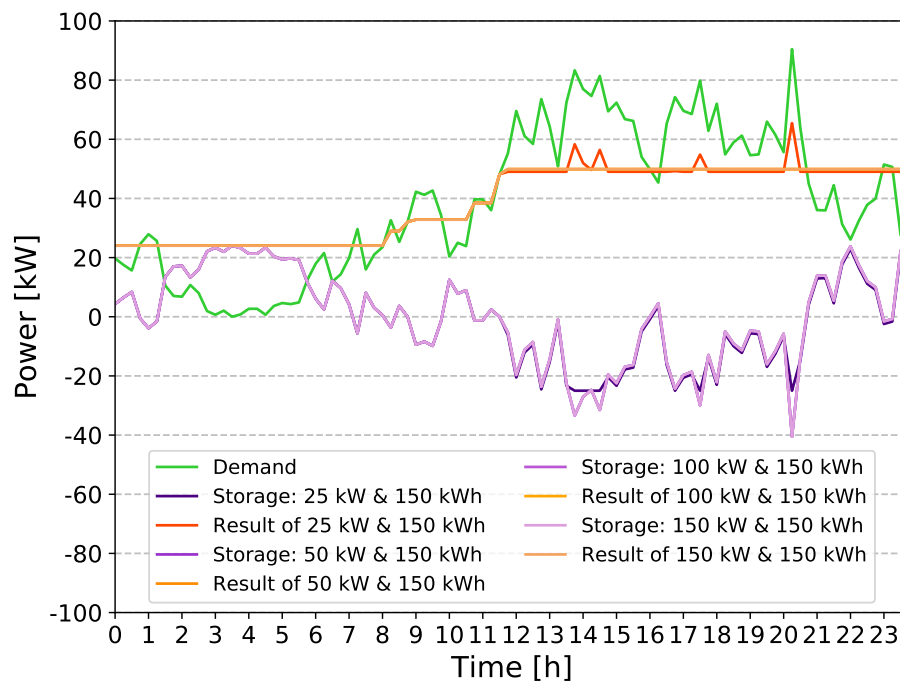


(b) Capacity: 50 kWh

Figure 5.9.: Evaluation of the peak-shaving optimization with the BES system in a high demand scenario (Charging Site C; 25 & 50 kWh)



(a) Capacity: 100 kWh



(b) Capacity: 150 kWh

Figure 5.10.: Evaluation of the peak-shaving optimization with the BES system in a high demand scenario (Charging Site C; 100 & 150 kWh)

Comparison of all scenarios

In all cases the capacity of the BES has a significant impact on the peak-decrease. Besides in the first case with 25 kW power of the BES all other power cases have produced a peak-decrease between 44 % – 55 %. Where as the capacity of 150 kWh may be oversized for the low demand case it has also shown great performance for the high demand case. In Table 5.4 it is visible that the peak-decreases for the low demand scenario are the greatest of all scenarios. The peak-decreases are similar when the medium and high demand scenarios are compared. It is most noticeable that the peak-decrease for the 25 kW BES power only increases during the low demand scenario.

in %	low demand			
	25 kW	50 kW	100 kW	150 kW
25 kWh	37	37	37	37
50 kWh	42	42	42	42
100 kWh	49	49	49	49
150 kWh	51	55	55	55
	medium demand			
25 kWh	32	32	32	32
50 kWh	33	36	36	36
100 kWh	33	41	41	41
150 kWh	33	45	45	45
	high demand			
25 kWh	28	30	30	30
50 kWh	28	34	34	34
100 kWh	28	40	40	40
150 kWh	28	45	45	45

Table 5.4.: Peak-decrease with the BES system in different sizes of Capacity and power for each demand scenario (Charging site C)

5.2.2. Evaluation of the results of the combined BES and PV system optimization for peak-shaving

Here the results of the peak-shaving with help of the developed optimization tool is presented in the following sections. This sections deal with the results for the peak-shaving with a combined system of a BES and a PV system. Those systems are topics in the actual research. The developed optimization tool uses a highly ideal

model for the solar power output based on a Gaussian distribution. The model parameters and the modelled power profile is shown in Section 4.2.3.

With the developed optimization tool the desired and optimised BES behaviour is calculated for each use scenario and case. The data is output to a database as well as the results are plotted for a $24h$ interval. The power output of the BES is presented and the resulting demand is calculated by adding the BES and the PV output power to the requested charging power to achieve a resulting power profile.

Those profiles are presented in this section. The original and the resulting charging profiles are compared based on the peak decrease. This gives an idea how big is the impact of the BES and the PV system on the grid consumption of the charging station.

To simulate different seasons the PV output power varies in shape and amplitude. To evaluate if a larger or a smaller PV panel is more desirable the output power is scaled with two different sizes, $20 kW$ and $40 kW$. The maximum output power is given for the summertime and is therefore the high power case.

By comparing different BES system sizes additionally in mean of capacity and power it is evaluated which size has the biggest influence. It is also beneficial to know what BES system size is preferable to handle different charging demands and PV power outputs.

In general the aim of the peak-shaving is to reduce the maximum peak value occurring in a time interval. This is done by shifting the load from the high peak time with help of the BES to the low peak time. A negative power peak can be added By the PV system, if the PV power excesses the demanded charging power and creates a power peak by feeding the surplus power to the charging site. In this case the BES is additionally charging that energy to minimize the grid injection of the PV power. This can prevent over-sizing grid assets and makes the handling of the PV system easier for the grid because there is as least grid injection as possible and the power flow is still most of the time in the usual direction.

The examined charging profiles are based on the medium demand case from Section 5.2.1. The irradiance scenarios are displayed in the following figures:

- low irradiance scenario: BES: $25 kWh$ and PV: $20 kW$ & $40 kWh$ in Figure 5.11, BES: $150 kWh$ and PV: $20 kW$ & $40 kWh$ in Figure 5.12
- medium irradiance scenario: BES: $25 kWh$ and PV: $20 kW$ & $40 kWh$ in Figure 5.13, BES: $150 kWh$ and PV: $20 kW$ & $40 kWh$ in Figure 5.14
- high irradiance scenario: BES: $25 kWh$ and PV: $20 kW$ & $40 kWh$ in Figure

5.15, BES: 150 *kWh* and PV: 20 *kW* & 40 *kWh* in Figure 5.16.

Firstly each irradiance scenario will be explained. Afterwards the three scenarios are compared with each other. As there are 128 cases for the irradiance only the most significant cases are described in the following sections.

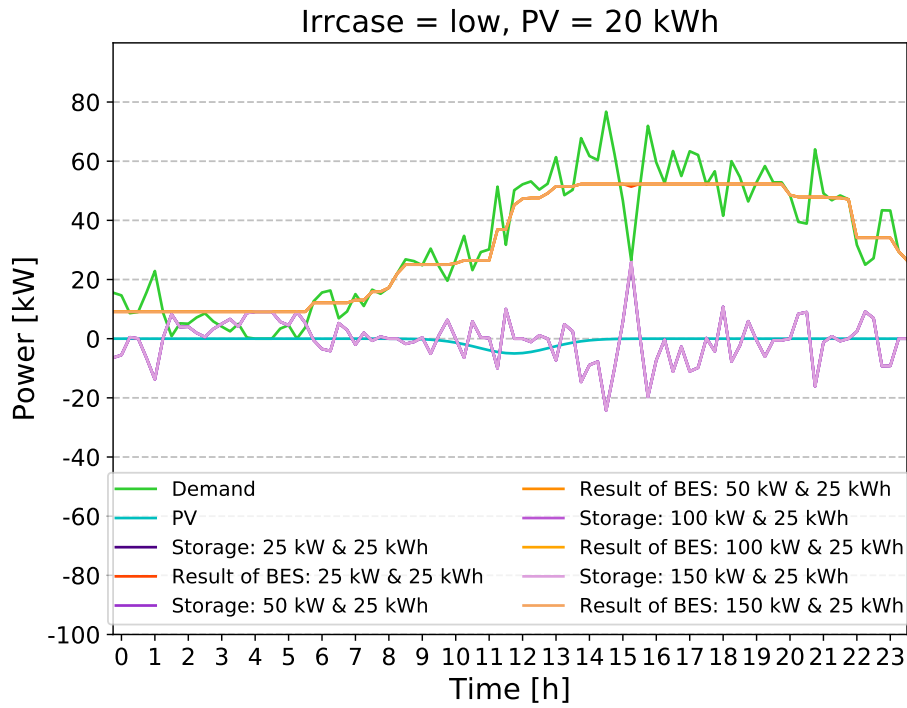
As it can be seen in the figures 5.11 and 5.12 they are divided into two plots a) and b). Each plot handles one of the chosen capacities for the BES. The order is the same for all the three scenarios. The y-axis describes the power that is charged at each moment of time, which is on the x-axis. The resolution used to create the charging profile is 15 *min* and the time steps in the plot are from 00 : 00 to 23 : 45. The original charging demand which is created by the CPM is plotted in green. The PV output is blue. The storage power is plotted for each charging power variation in a different shade of violet. The resulting charging profiles have different shades of orange. Only two different BES capacity cases are examined in detail: the 25 *kWh* and the 150 *kWh*.

Low irradiance scenario

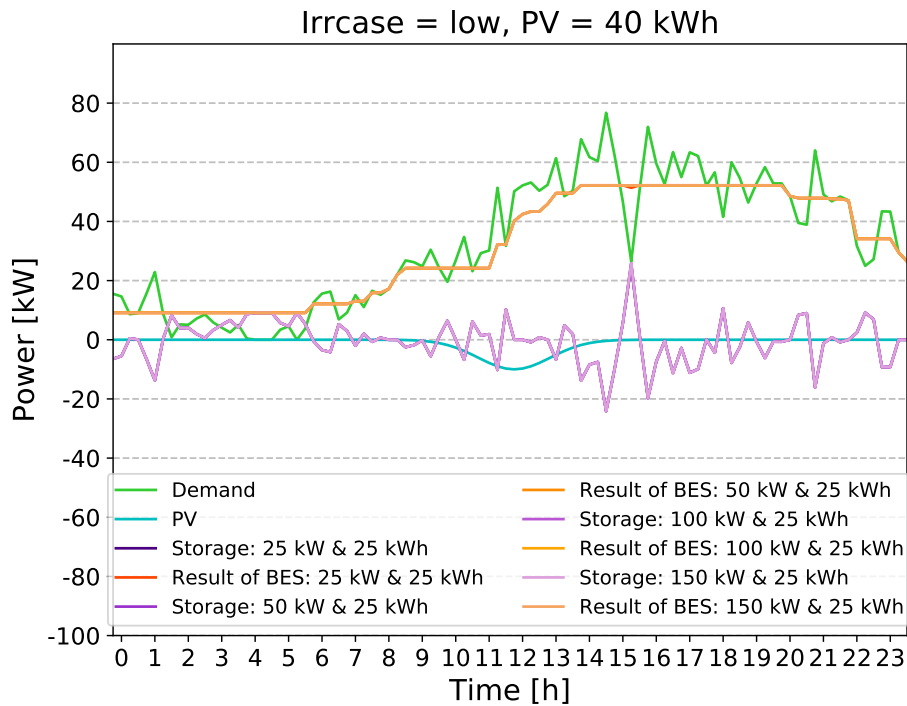
In the figures 5.11 and 5.12 the low PV irradiance scenario is examined with a factor of 0.25 on the output PV power. This means only a quarter of the installed PV output power is reached. In Figure 5.11 the BES system with a 25 *kWh* capacity is shown with different the PV power values 20 *kW* and 40 *kW*. Figure 5.12 shows the system with a BES capacity of 150 *kWh*.

It is noticeable that the maximum value of the PV power occurs on an earlier time than the charging peak. It is about three hours earlier. The time of the power injection to the charging site by the PV system is four hours long. The additional power from the PV system is barely noticeable in the power cases. The peak-decrease is around 32 %.

In Figure 5.11 b) in comparison the impact on the charging of the BES can be seen mostly during the PV peak time. This does not effect the peak-decrease, it is still 32 %. With the BES higher capacity in Figure 5.12 a) the peak decrease is between 33 % – 50 %. Here the peak-decrease is with 50 % around five percentage points higher in comparison to the same BES configuration in the medium demand scenario without PV. The peak-decrease is at 51 % when the PV power is doubled in Figure 5.12 b). The difference of the peak-decrease is not significant between the different power injections in the low irradiance scenario. Only the 25 *kWh* BES power cases is an exception again.

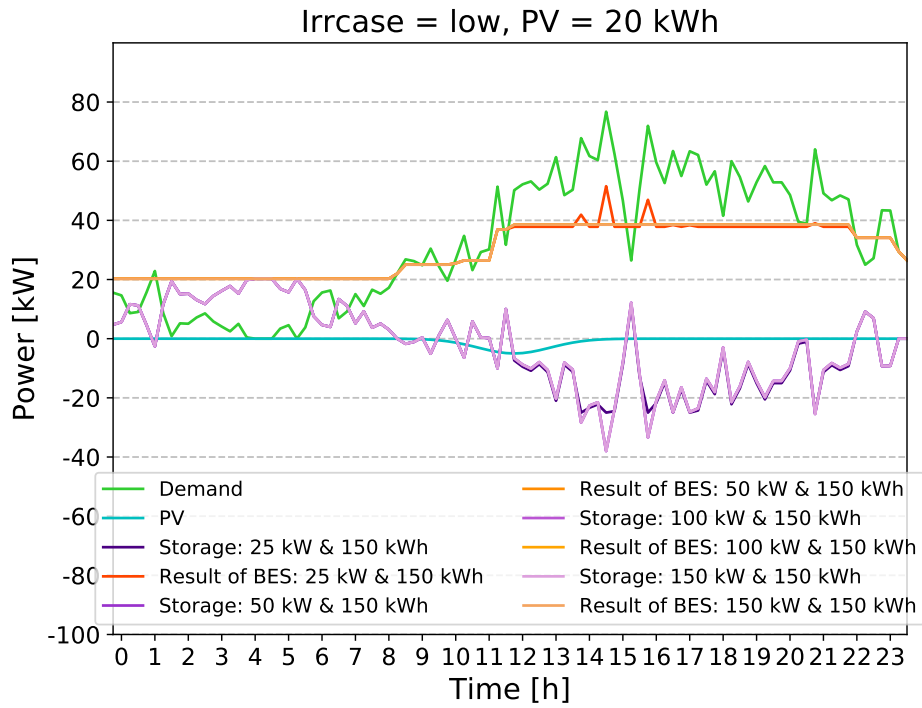


(a) BES Capacity: 25 kWh, PV Power: 20 kW

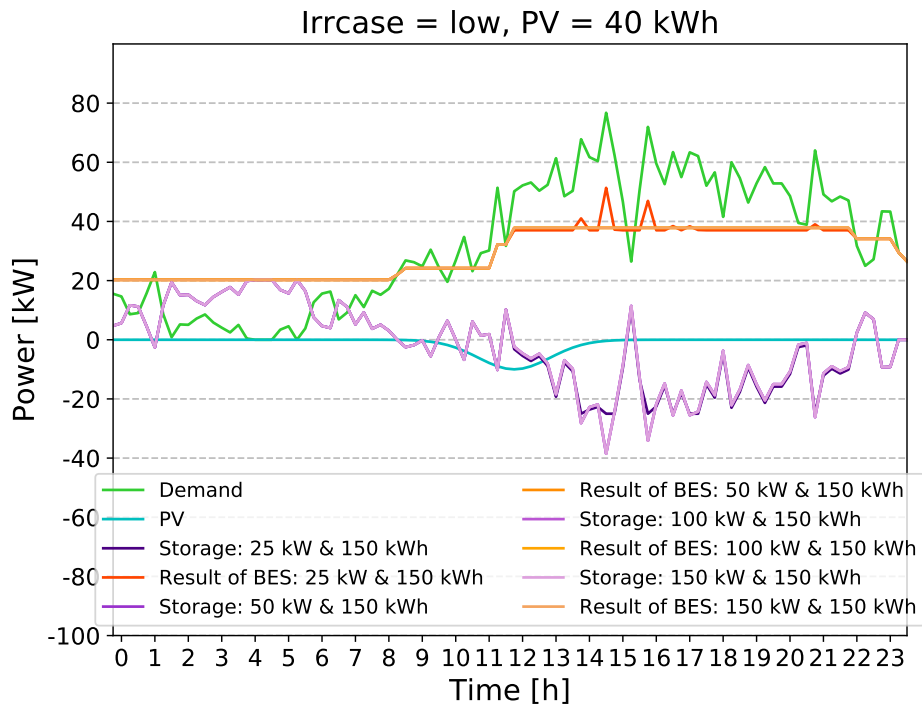


(b) BES Capacity: 25 kWh, PV Power: 40 kW

Figure 5.11.: Evaluation of the peak-shaving optimization with the BES combined with a PV system in a low irradiance scenario (Charging Site C; 25 kWh, 20 & 40 kW)



(a) BES Capacity: 150 kWh, PV Power: 20 kW



(b) BES Capacity: 150 kWh, PV Power: 40 kW

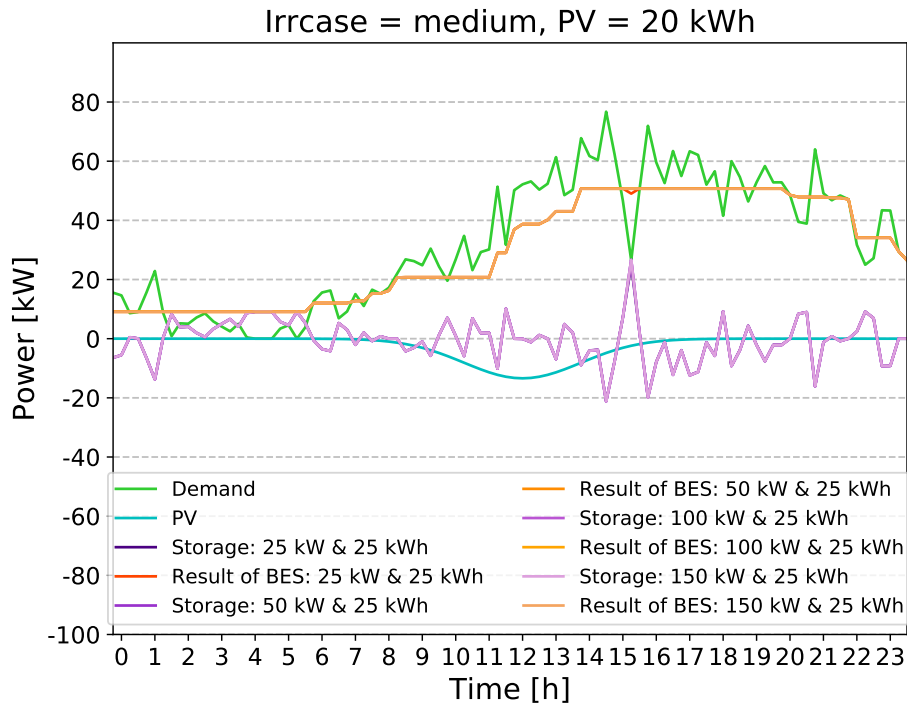
Figure 5.12.: Evaluation of the peak-shaving optimization with the BES combined with a PV system in a low irradiance scenario (Charging Site C; 150 kWh, 20 & 40 kW)

Medium irradiance scenario

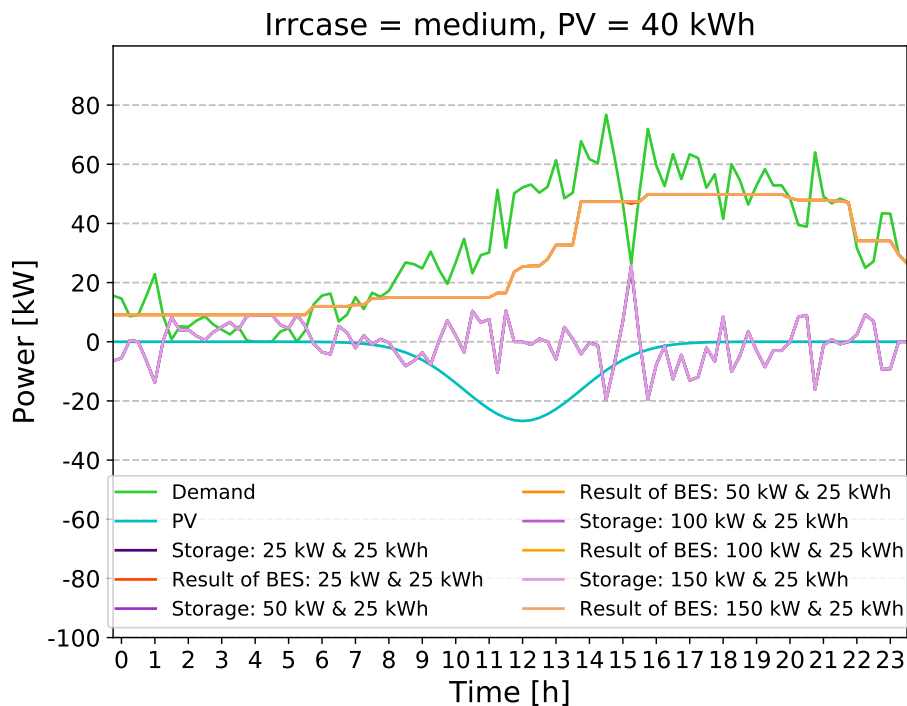
In the figures 5.13 and 5.14 the factor that limits the PV power is 0.67. The PV injects power between 08 : 00 and 16 : 00. There is a PV injection during the charging demand peak time.

The peak-decrease is 34 %. It is noticeable that the BES discharges less during the PV power injection. The opposite occurs and the BES charges more in the time of the peak than in the low irradiance scenario. This happens not the whole time in Figure 5.13 b) because around 09 : 00 the BES discharges more than in Figure 5.13 a). The peak-decrease is around 35 %. In Figure 5.14 a) the peak-decrease is between 39 % – 53 %. This is significantly higher than in Figure 5.13 b) but not compared with in the same case in the low irradiance scenario. The peak in the first case is reduced about five percentage points. This is more than in the low irradiance scenario. The discharging power is higher than in the figures 5.13 a) and 5.13 b).

In case 5.14 b) the peak-decrease is between 42 % – 56 %. The charging of the BES during the PV injection is now about the same as the discharging during that period. In the resulting charging profile is a step visible of 10 kW difference. Compared to the BES-only the PV has a positive impact of ten percentage points on the peak-decrease.

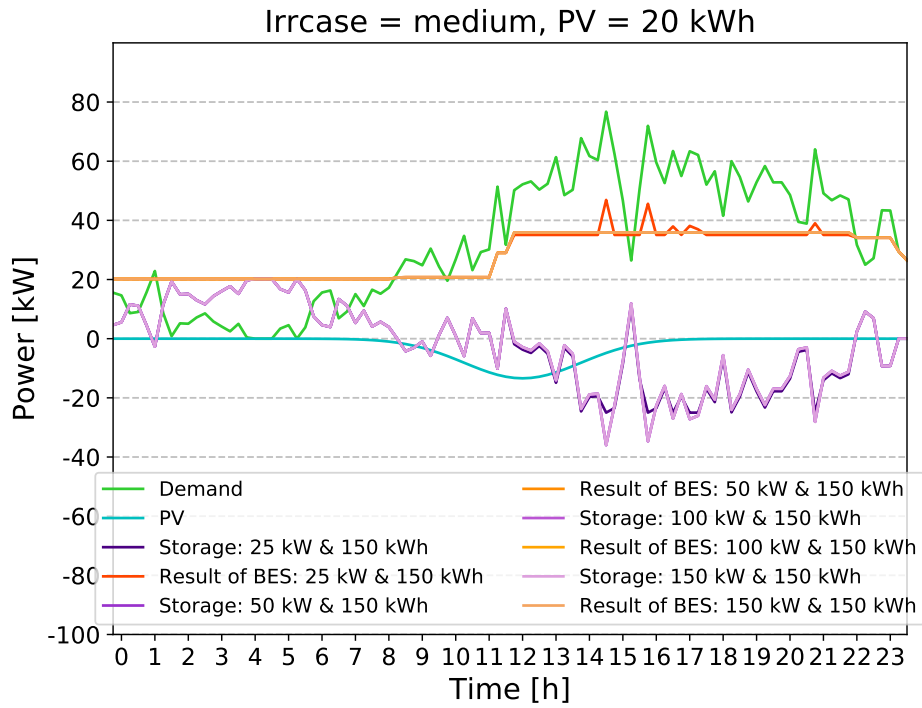


(a) BES Capacity: 25 kWh, PV Power: 20 kW

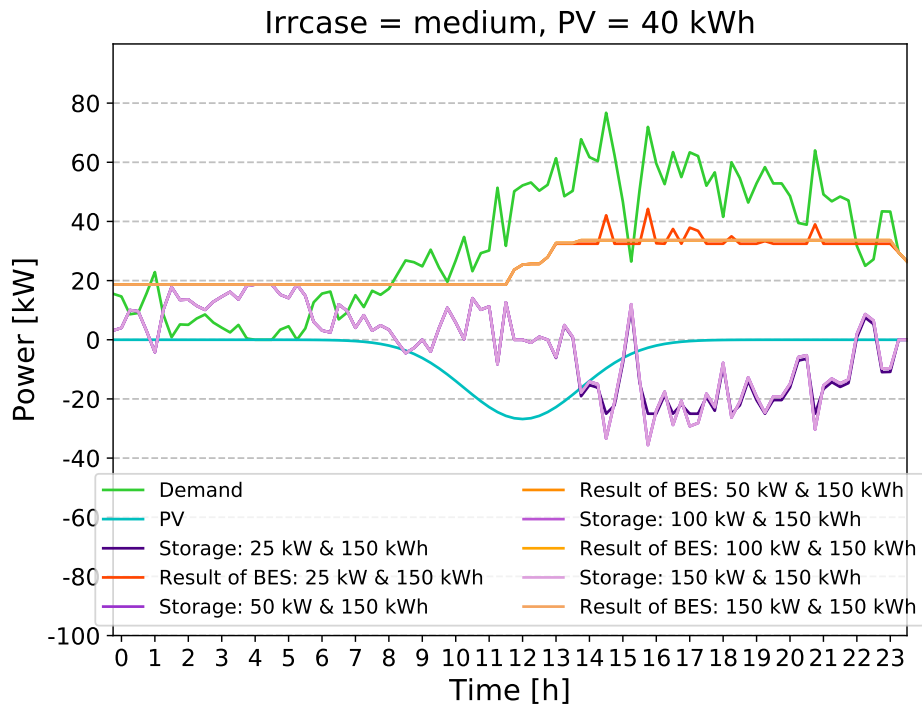


(b) BES Capacity: 25 kWh, PV Power: 40 kW

Figure 5.13.: Evaluation of the peak-shaving optimization with the BES combined with a PV system in a medium irradiance scenario (Charging Site C; 25 kWh, 20 & 40 kW)



(a) BES Capacity: 150 kWh, PV Power: 20 kW



(b) BES Capacity: 150 kWh, PV Power: 40 kW

Figure 5.14.: Evaluation of the peak-shaving optimization with the BES combined with a PV system in a medium irradiance scenario (Charging Site C; 150 kWh, 20 & 40 kW)

High irradiance scenario

In the figures 5.15 and 5.15 the high irradiance scenario causes the highest possible output power of the PV system. It reaches the given values of 20 kW respectively 40 kW because the factor is 1 (see Sec. 4.2.3). The power injection is between 07 : 00 and 16 : 00. The highest output power is shortly past noon. In this scenario is also a power injection during the highest charging demand. In between the highest injection peaks and the highest demand peak are still two hours difference.

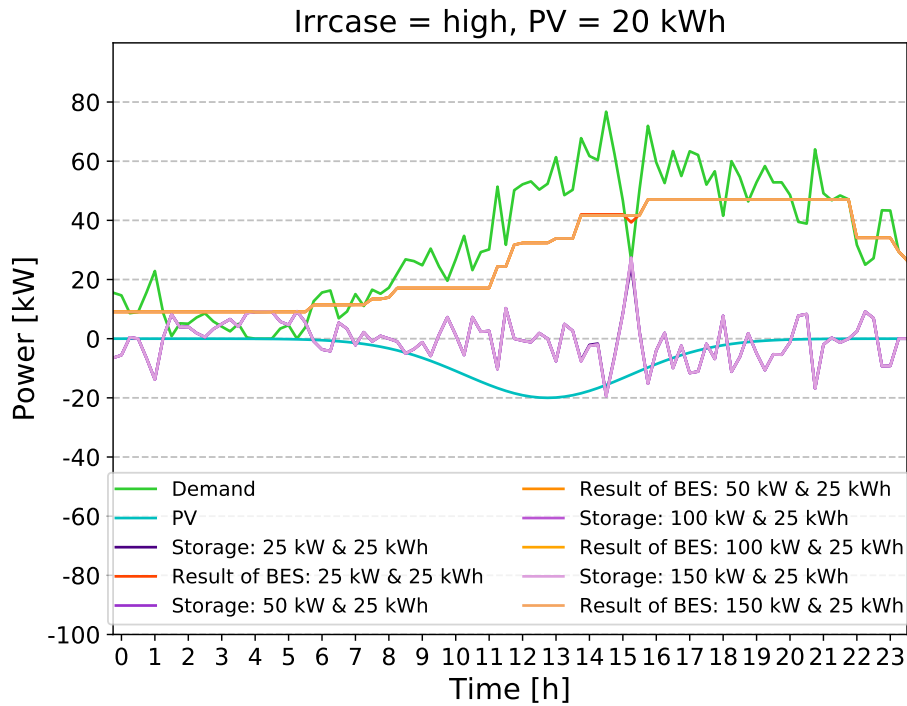
In Figure 5.15 a) the peak decrease is at 39%. Noticeable is that the highest resulting power is neither during the highest demanding power nor during the highest PV power injection. In the same time the charging and discharging power of the BES is equal in absolute value. There is a great difference between the resulting charging profiles in comparison to the medium high irradiance case of almost 10 kW during the charging peak time. And this even with the 25 kWh BES configuration.

The peak-decrease is 42% in Figure 5.15 b). This is a huge difference to case 5.15 a) in comparison to the difference between the PV power cases in the other two scenarios. The resulting power during the PV power injection is in Figure 5.15 b) different compared with Figure 5.15 a) and also the other scenarios. There is more charging of the BES, but about the same amount of discharging compared to Figure 5.15 a).

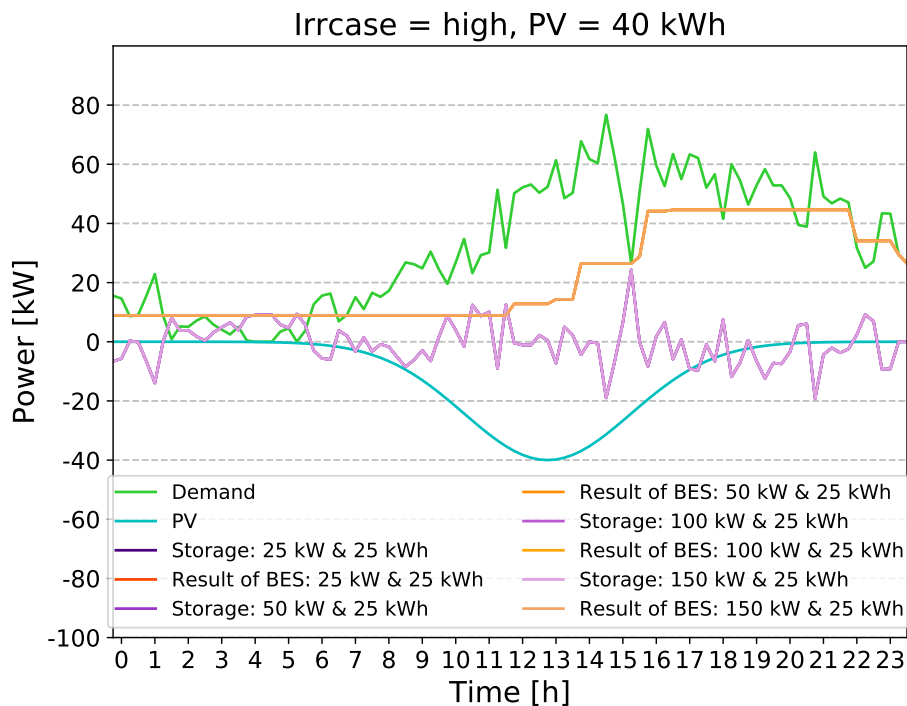
In Figure 5.16 a) the peak-decrease is between 49% – 59%. Around 11 : 00 there is an almost linear increase of resulting power from 20 kW to 30 kW . It is noticeable that more spikes in the lowest BES power case occur. In this case the BES discharges much more between 16 : 00 and 22 : 00 in comparison to case 5.15 a) and b).

In Figure 5.16 b) this effect is even more noticeable. Compared with Figure 5.16 a) the BES discharges less during the maximum charging demand peak time. The charging of the BES is more visible between 09 : 00 and 12 : 00 even more than in the medium irradiance case. The peak decrease is between 49% – 66%. The overall resulting power decreases except for the 25 kWh BES configuration. As before there are more spikes in the resulting charging profile. The amplitude of the peaks shifted. It is less during the time of the PV power injection in the figure 5.16 d) but higher after the injection. The spikes there have the same amplitude as in a), but seem higher in comparison to the average resulting power in this time period. The step between the two visible power level is around 13 : 00 and is seems to happen in between two 15 min time steps, so the increase is almost like a step. In Figure 5.16

a) this increase is more like a ramp.

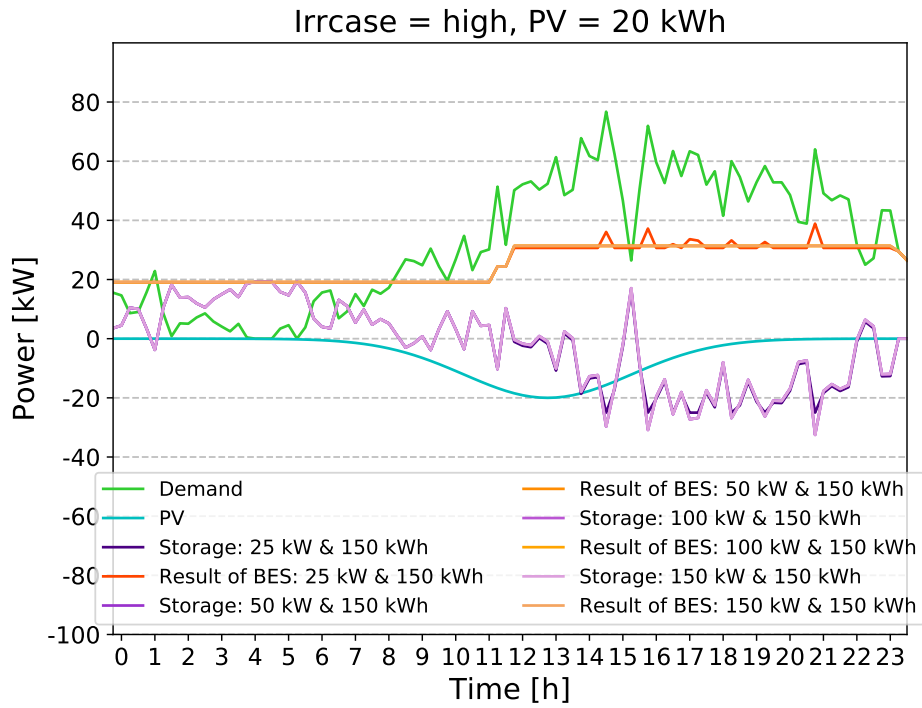


(a) BES Capacity: 25 kWh, PV Power: 20 kW

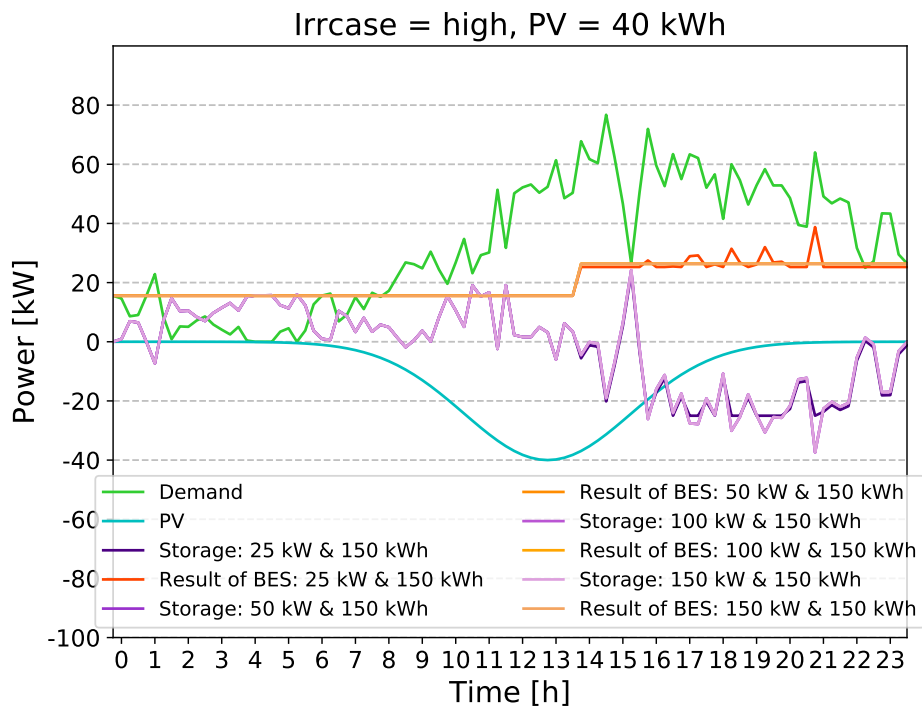


(b) BES Capacity: 25 kWh, PV Power: 40 kW

Figure 5.15.: Evaluation of the peak-shaving optimization with the BES combined with a PV system in a high irradiance scenario (Charging Site C; 25 kWh, 20 & 40 kW)



(a) BES Capacity: 150 kWh, PV Power: 20 kW



(b) BES Capacity: 150 kWh, PV Power: 40 kW

Figure 5.16.: Evaluation of the peak-shaving optimization with the BES combined with a PV system in a high irradiance scenario (Charging Site C; 150 kWh, 20 & 40 kW)

Comparison of all irradiance scenarios

The shape of all resulting charging profiles in comparison differs much. The maximum value of the resulting charging profile shifts the time depending on the irradiance case.

It is noticeable in Table 5.5 that the differences between the PV power cases regarding the peak-decreases are increasing with the irradiance scenarios. In the low irradiance scenario the difference is maximum one percentage point. In the medium irradiance it is from one to three percentage points and in the highest irradiance scenario it is from three to six percentage points.

Peak-decrease in %				
Irradiance	Low			
BES capacity	25kWh		150kWh	
PV power	20kW	40kW	20kW	40kW
25kW	32	32	33	33
50kW	32	32	50	51
100kW	32	32	50	51
150kW	32	32	50	51
Irradiance	Medium			
BES capacity	25kWh		150kWh	
PV power	20kW	40kW	20kW	40kW
25kW	34	35	39	42
50kW	34	35	53	56
100kW	34	35	53	56
150kW	34	35	53	56
Irradiance	High			
BES capacity	25kWh		150kWh	
PV power	20kW	40kW	20kW	40kW
25kW	39	42	49	49
50kW	39	42	59	66
100kW	39	42	59	66
150kW	39	42	59	66

Table 5.5.: Peak-decrease with BES and PV system over the examined scenarios

6. Discussion

The first goal of the thesis is to develop a accurate modelling tool in *Python* for charging profiles that are based on real measurement data. Furthermore these modelled charging profiles are used to show used and impact of peak-shaving. The used assets to get the peak-shaving are firstly a BES only-system and secondly a BES combined with a PV system. In Chapter 5 the output data of the CPM tool and the peak-shaving are presented.

In this chapter these results are discussed. Firstly the results from the CPM tool are discussed on a weekly and a monthly basis. Afterwards the results of the peak-shaving optimization are talked over.

6.1. Discussion of the results of the Charging Profile

Modelling tool

The following section discusses the findings from Section 5.1.2 and 5.1.1. Firstly the weekly results are discusses, followed by the monthly results. Finally the findings are summarized.

6.1.1. Discussion of the results on each weekday

On Fridays (see Fig. 5.1) the charging energy has a level of around $10 kWh$ from the afternoon until midnight. This is unusual compared to the other days. This implies that the EVs are charged more on Friday evenings. This can mean that more EVs are charged so more EV owners drive and charge their cars. Or each EV charges more energy which implies the same amount of EV owners as usual travel more during Friday evenings and each EV has a higher demand.

It is also noticeable that the charging energy during the night is significantly smaller than by day. This can be interpreted as low demand by night so either less people charge their EV or each EV is charged for a shorter time period.

The result of the statistical comparison of all weekdays (see Tab. 5.2) show that on Sundays are the largest values in all categories. At that weekday is no charging gap either (see Fig. 5.2). This implies that the charging on Sundays is in average more utilized by the users compared to other days. The assumptions are that the users have more time on Sundays and they have more need of charging at the end of the week to prepare their car for the next week.

6.1.2. Discussion of the results on monthly basis

To explain the monthly results a consideration of the public holidays can be useful. The school holidays in 2018 were from the mid of June to the mid of August in Norway. It is likely that many people are on vacation in this period and are therefore not at home. It can be seen that in July the charging energy is lower than in June or August. It is assumed that the vacation season and the lower charging energy are correlating.

A not certainly explainable behaviour is seen in December. The charging energy is very low in this month except for the last week. It is possible that less people use electric cars during the winter time. It is also possible that the station was not accessible as usual during this time due to constructions, similar to October. This is the most likely explanation because in the last week of November there is a decrease of energy from Monday to Sunday. An increase takes place in the last week of December. A similar pattern can be observed end of September and in the beginning of November. The increase at the end of December can also result from a higher traffic after the Christmas Days and before New Years Eve.

Another assumption is that the length of daylight correlates with the charging behaviour of the EV owners. It is based on the findings that in November and December the number of hours with no charging during the night is higher than in June, July and September. From May to August there is daylight from 14 to maximum 19 hours a day. During September the time of daylight decreases from 14 hours to 11.5 hours. From November to December the day length decreases from 8.75 hours to 6 hours. This would also explain why it seems that the charging in December (see Fig. 5.4) mainly begins around 08 : 00 one hour later than in the other month except July. In December the sun rises between 08 : 50 and 09 : 20. It seems that also the sunrise in Winter has an influence on the charging behaviour.

The impact of the summer holidays in July is visible because the charging increases from 09 : 00 until the afternoon. This indicates that most people start charging later

as usual probably related to the lack of duty to be at work early. Between 06 : 00 and 07 : 00 is a peak which indicates that there are still people charging as regular. The majority seems to start charging after 09 : 00.

6.2. Discussion of the peak-shaving optimization

In the following section the findings from Section 5.2.1 are discussed. Firstly the peak-shaving with the BES system is discussed. Afterwards the findings of the combined BES and PV system are discussed. It is closed with a summary of the findings.

6.2.1. Discussion of the results of the BES system optimization for peak-shaving

In all scenarios it is noticeable that the peak-decrease is higher when the BES system has a higher capacity. These findings imply that there is a correlation between the capacity of the BES system and the peak-decrease.

Another finding is that the peak-decrease for the 25 kW BES case is not above 33% for the medium and the high demand scenario. This limitation results in the limited output power of the BES that is at 25 kW. This power limit is reached at the time of the highest load peaks. This is noticeable because the storage profile stops at a discharging power of 25 kW for this first case. The charging profiles of the BES for the other cases in 5.8 and 5.10 reach beyond that value because their limit is at 50 kW and higher. This provides evidence that the peak-decrease also depends on the power of the BES. This occurs when the requested charging power at one time is higher than the power that can be supplied at once by the BES to reach the desired peak-decrease.

Which power size is preferable seems to highly depend on the maximum amplitudes of the charging profile. The capacity size of the BES seems to depend on the average power of the original charging profile. The higher the mean of the charging profile the higher is the needed of more capacity to reach the same peak-decrease. The mean of the low demand scenario is about the half of the mean of the high demand scenario. The difference in the mean between medium and high demand scenario is around 10%. The medium and high demand scenarios gain a similar peak-decrease. The low demand scenario has a peak-decrease that is five percent-

age points higher in every case (see Tab. 5.4).

6.2.2. Discussion of the results of the combined BES and PV system optimization for peak-shaving

In the combined peak-shaving the additional power of the PV system influences the charging behaviour of the BES. In the 25 kWh capacity case the peak decrease is between $32\% - 42\%$. The higher the irradiance scenario the higher is the peak decrease.

This leads to the conclusion that the 25 kWh capacity size of the BES is highly supported by the PV system in the desired manner. The additional power output of the PV system extends the limited power output of the BES so a higher peak-decrease is possible even for the maximum peak and the smallest BES capacity. This implies that the additional PV is compared to a PV with a higher output power. The peak-decrease for the 150 kWh BES capacity is as well increasing with the irradiance. The additional power of the PV system has a positive impact on the system. If the irradiance case is low the combined system behaves similar to the BES-only system. This means worst case of the peak-decrease is the same behaviour as without the PV system. In the selection of the size of the BES this finding should be considered. This selection depends also on the charging behaviour during low irradiance.

The lowest value of peak-decrease for the first case in each scenario results from the limitation of the BES power to 25 kW like described in the section before. The charging behaviour of the BES during the PV injection is different compared to the BES-only system.

It can be seen that the BES is charging the surplus power and keeps the resulting power as much as possible on the same level without peaks. To keep this power level, the BES is discharging at time of the demanded power peaks. The surplus charging and controlled discharging of this energy implies that an additional PV system extends the utilization and usefulness of a BES system.

In the highest irradiance scenario more spikes occur in the resulting profile of the 25 kW and 150 kWh BES configuration. This makes very visible that the BES reaches the power limits more often in that case. One reason is the high amount of charged surplus power, that needs to be discharged until the end of the day to meet the optimization constraints. In that case the BES discharges as much energy as possible to loose more energy over time. The BES reaches more often the power limit.

In the other power cases this is not a problem. Compared to the BES-only optimization the constraints allow the BES to hold minimum of 20 % and a maximum of 60 % of its maximum capacity at the end of the day. This broader constraints enable the BES to discharge the surplus energy until the end of the day if needed. In the 25 kW case the power limit is reached because the optimization keeps the resulting power on one level as long as possible. This can result in a problem regarding the spikes and the noticeable, quick increases of the power in the resulting profile.

In both cases the area of sudden power increase should be evaluated in a smaller time resolution like 1min. This could clarify if the gradient is critical over time. Critical would be if the gradient is still that high for a 1min resolution. If this is the case an evaluation with 1s should be considered. The problem with sudden increases in a power system is that these can cause harmonics because suddenly increasing power means that the voltage and/or the current are increasing suddenly too.

6.3. Summary of the discussion

In summary the results for modelling the charging profiles seem realistic, based on possible user behaviour. On weekdays people have a more structured and timed daily routine for example they commute to work and home afterwards. This is reflected in the results from Monday to Friday. The similarities are for example the time interval with very low charging. It is plausible that there is almost no charging at this time because most people are home at night. Therefore EV charging is unlikely. This is supported by the significantly lower charging energy by night in Figure 5.1.

On the weekend people have another daily routine. Most people leave the house later because they do not have to commute to work for example. That results in charging profiles that start increasing later than on weekdays.

The monthly results support this impression. They are explainable and seem to correlate with the circumstances of the real world for example holidays.

Therefore the CPM tool is fully validated. The results already show noticeable patterns although not a full year is observed and the number of charging events is around 30.000. This speaks for the quality of the modelling and the modelling tool.

Although the results are promising it is unfortunate that no more charging data could be provided. With more charging data and events the statistic reliability increases and the analysis regarding the charging behaviour would be more accurate. This would have also a positive impact on planning the business for the charging site

operators. It would already be helpful to have a full year to observe so more conclusions could be drawn regarding seasonal variation.

The needed execution time of $0.2s$ per event is also a positive outcome. It seems possible to process $N_{events,th} = \frac{(16 \cdot 60 \cdot 60)s}{0.2s} = 288,000$ charging events in a feasible overnight simulation between 16 : 00 and 08 : 00 theoretically. This means a database of almost 10 times the size of the used one can be modelled over night.

The CPM is neither optimized for databases with more events nor runtime optimised. That makes it possible that the tool cannot process so many charging events at once in its actual form. It is still desired to gain more charging event data so testing the tool with databases with much more entries is possible. In this way it is possible to find out more about the charging behaviour of EV drivers, especially from January to the end of May

The peak-decrease with the lowest configuration in the BES-only scenarios is around 30%. The highest configuration has a peak-decrease around 50% depending on the demand scenario. The BES is extended by the PV in a desired manner. The maximum peak-decrease with the highest configuration is 66%. It needs to be considered that all conclusions are based on the average charging profile of a day. To find the best size for the BES capacity and power the mean charging power and the peak charging power should be known. It is also possible to investigate those influences further and create a tool that may calculate a feasible BES sizing based on a charging demand profile. In the current research the sizing is often also determined by several optimization algorithms but in most cases the economic aspects dominate the objective function.

Fast increases in the resulting charging profile are not desirable. Step-like increases are visible in almost all cases also in the BES-only peak-shaving. A high gradient in the resulting demand that is equal to a step can cause harmonics in the grid. This is not desired. A more detailed evaluation should be considered for all increases that are occurring during one 15 min time step. The first step could be a 1 min resolution of the demand charging profile. The gradient then can be analysed if the increase is critical.

7. Conclusion

From the results gathered in this thesis it can be seen that modelling of charging profiles is highly useful for the evaluation of the charging behaviour. The evaluation of the peak-shaving optimization shows the large potential that lies in integrated battery electric storage (BES) and photovoltaic (PV) systems. A considerable reduction of the peak power can be expected with a well chosen BES configuration. Despite of an increasing number of charging sites the operation in a combined system will be less dependent on the grid.

The further processing of the measured charging events enables a detailed view on the charging behaviour of the users and reveals more insights on charging patterns. The analysis of the peak-shaving optimization uncovers a large unused potential for peak reduction in the operation of charging sites. The power peak is reduced by over one third even with the smallest BES configuration. The flexibility can be increased with the increase of the BES capacity, especially regarding an additional PV system. In the best case the peak-decrease can be about 65% with the highest irradiance scenario.

When the BES-only system reduces the peak enough to stay within the performance limits there is no shortage of energy supply with the integrated PV even during low irradiance. In high irradiance scenarios this capacity can extend the flexibility and offers a higher degree of independence of the grid. The results imply that the combination of a charging site with a well controlled BES and PV system is a feasible solution to prevent a bottleneck in the supply of the charging stations.

8. Future Work

In this thesis a full tool to evaluate charging site data is developed and new findings are made. Further there are concepts and ideas that were not considered in this thesis.

8.1. Analysing more data

With more data to analyse the tool can be validated with a dataset with more charging events. Further statistical analysis can be started. The charging profiles can be clustered, which means profiles with similar properties are classified in a group together. This is done in many fields and is used statistical analysis tool. Clusters can be the basis for further applications in the field of machine learning. Machine learning is interesting for the generation of data models based on the measured charging data. If modelled charging profiles base on real data, realistic data can be generated artificially. This helps further research because real data is rare and not every company is open to share their measurement results with research groups. Researchers would not need to produce their own models based on assumptions, but can use models based on real data, which can lead to big results and obliterate wrong assumptions.

Machine learning is used for predictions so it is possible to have an predictive charging approach based on real data. Based on the trained real charging data the algorithm may predict how the charging profiles will look like in the next time period. Therefore the generation and storage units in station could be controlled in advance to satisfy those predicted charging demand.

8.2. Vary the peak-shaving optimization

Clustering can also improve the optimization model by using non-linear approaches the optimization result becomes more detailed. One possibility is to add non-linear

losses to the model so they can be taken into account. This does not work in a linear or quadratic optimization because only linear constraints, boundaries, and linear or quadratic objective functions are allowed.

Although those non-linear models and optimizations are used much in research they can be very complex. Most of the problems have to do with investment costs and minimizing them. In this thesis is no study of economic aspects. Also ecological impacts are neglected. Those two aspects can be combined with the findings from this thesis to have a holistic approach on the charging site model with combined BES and PV that is based on real data. The costs and profits (not only economical) can be evaluated then.

It would be interesting to study the behaviour of other energy sources but the PV during the peak-shaving. One possible source could be a fuel cell or another CHP system. The case of a PV system that has a larger scale is also possible. The modelling of the PV output power is improvable. It would be more realistic when there is appropriate modelling that considers clouds and reflections not only the direct normal irradiation.

8.3. Improving the Charging Profile Modelling

To improve the CPM it is one step to create a GUI so the tool is then not scripts that are executed but a application that can be handled also by persons with no programming experience. The GUI would have simple input dialogues where the user simply chooses the databases that need to be processed. Parameters as the format and the resolution need to be chosen as well. Also checkboxes to select which process shall be performed with the database. Of course the plotting is included as well. Some general plots are pre-selected for the user to serve their basic need for visualization of the data. The output is saved and the process should be continuable after saving the results at any point. There are two modules that can be used for a GUI implementation: *Tkinter* and *PyQt*

It is advised to optimize the tool to handle databases with more charging events. It is not proofed that there are no runtime or memory issues without a extended database. This needs to be checked.

8.4. Accuracy of the charging profiles

To improve the accuracy of the charging profiles the base charging profile needs to be improved. By analyse statistically which EV model has which type of charger an own charging profile by charger can be generated. By using different charging curves of different EV models with the same charger type a mean charging profile for each charger can be created. Therefore a more accurate and reliable information about the chargers is needed. Also how many chargers are at one station. This helps to detect, if the charging event is possible or if there is a doubled saved charging event in the database with the same charger type at the same charging station. Another draw back of the modelled charging curve is that after a short increase 100% of the maximum power is provided by the charger. Normally the charging power decreases when the charging EV reaches a certain SoC. The SoC of a EV is not measured by the charging station so in the gathered charging data there is no information what was the SoC at the beginning of the event. If there is a communication between EV and the charging station about the SoC and the power decreasing the modelling of this decrease should be done. If the charging power is limited internally in the BES by the charging electronics the charging station provides as much power as before so there would be no need to model the power decrease. As first approach the decreasing of the charging profile can be estimated depending on the charging time. It is assumed that the charging power decreases when the charging time is mostly over.

A. Appendix

A.1. Cases for the peak-shaving optimization

	PV Irradiance	PV Power [kW]	BESS Capacity [kWh]	BESS Power [kW]
1	Low	20	25	25
2				50
3				100
4				150
5			50	25
6				50
7				100
8				150
9			100	25
10				50
11				100
12				150
13			150	25
14				50
15				100
16				150
17			40	25
18				50
19				100
20				150
21			50	25
22				50
23				100
24				150
25				25

26			50
27			100
28			150
29			25
30		150	50
31			100
32			150
33			25
34		25	50
35			100
36			150
37			25
38		50	50
39			100
40			150
41		20	25
42			50
43		100	100
44			150
45			25
46		150	50
47			100
48			150
49	Medium 1		25
50		25	50
51			100
52			150
53			25
54		50	50
55			100
56			150
57		40	25
58			50
59		100	100
60			150
61			25

62				50
63				100
64				150
65	Medium 2	20		25
66			25	50
67				100
68				150
69				25
70			50	50
71				100
72				150
73				25
74			100	50
75			100	
76			150	
77			25	
78		150	50	
79			100	
80			150	
81		40		25
82			25	50
83				100
84				150
85			25	
86	50		50	
87			100	
88			150	
89			25	
90	100		50	
91		100		
92		150		
93		25		
94	150	50		
95		100		
96		150		
97			25	

98			50
99			100
100			150
101			25
102		50	50
103			100
104			150
105			25
106		100	50
107			100
108			150
109			25
110		150	50
111			100
112			150
113			25
114		25	50
115			100
116			150
117			25
118		50	50
119			100
120			150
121		40	25
122			50
123		100	100
124			150
125			25
126		150	50
127			100
128			150

Table A.1.: All cases for BESS and PV optimization of different PV irradiance, PV Power, BESS capacity and BESS power

A.2. Results of weekly evaluation of charging sites A&B

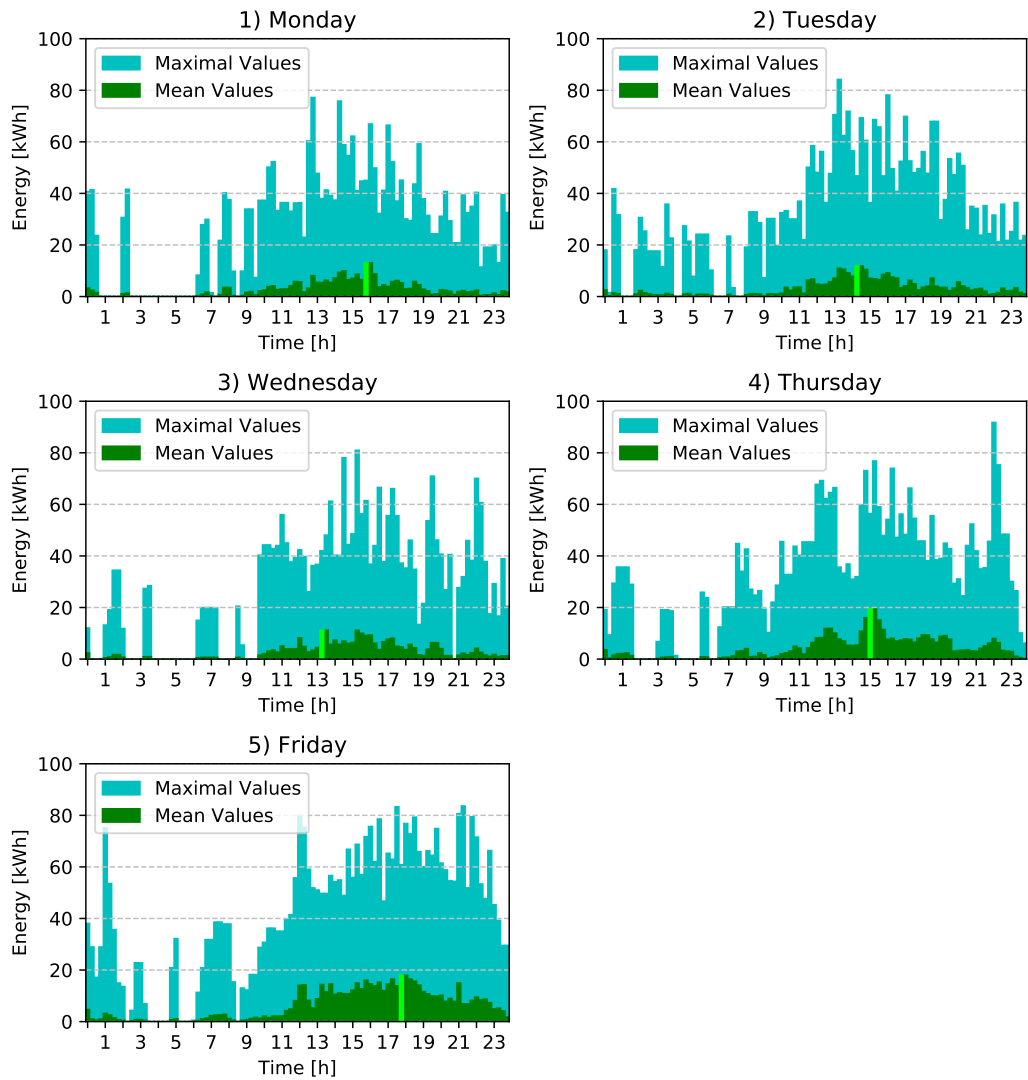


Figure A.1.: Mean of all Mondays to Fridays in the observation period from charging site A

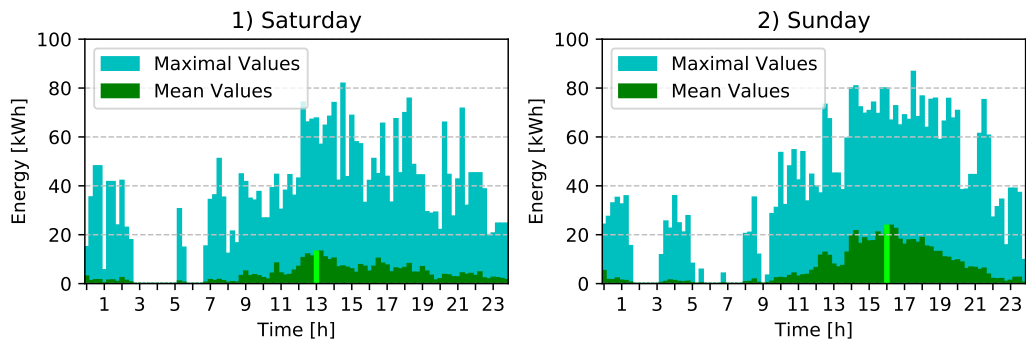


Figure A.2.: Mean of all Saturdays and Sundays in the observation period from charging site A

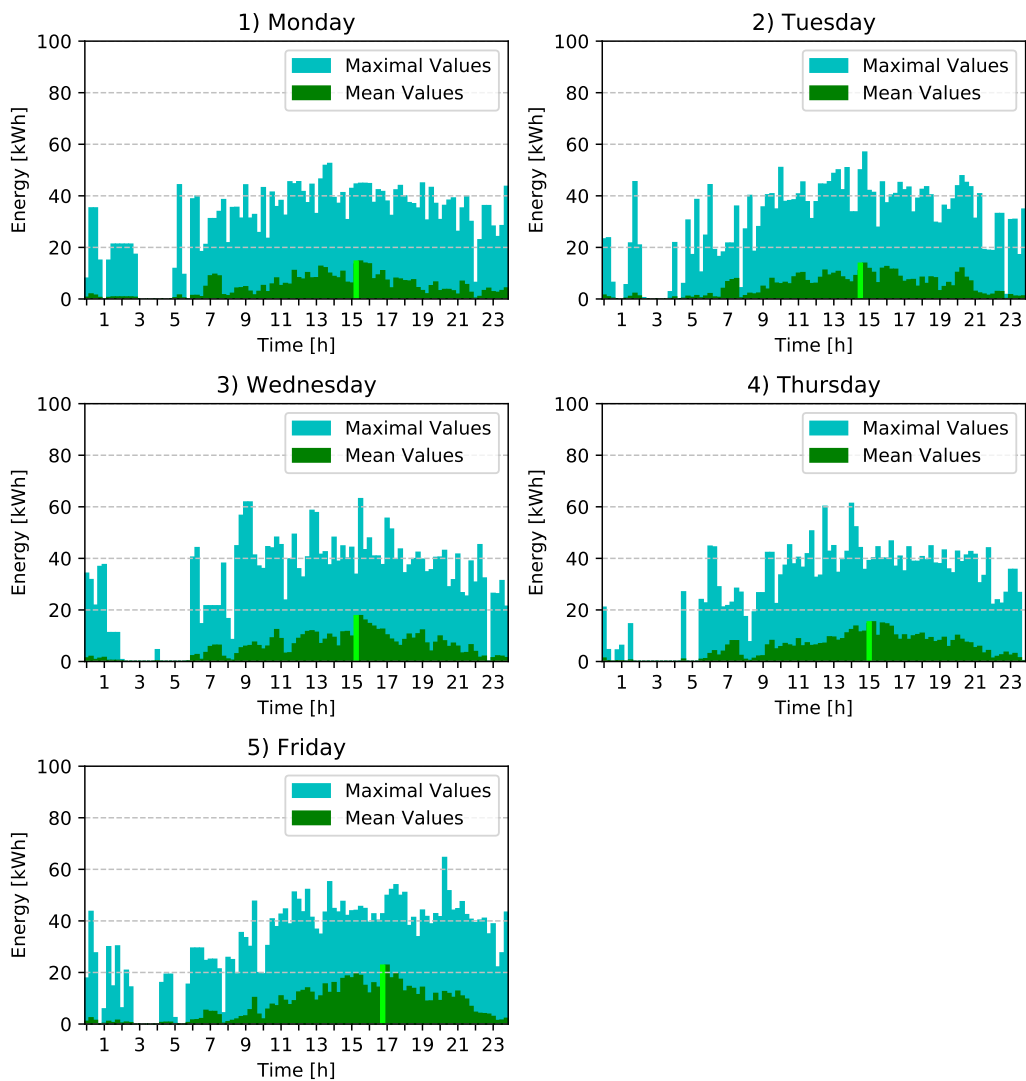


Figure A.3.: Mean of all Mondays to Fridays in the observation period from charging site B

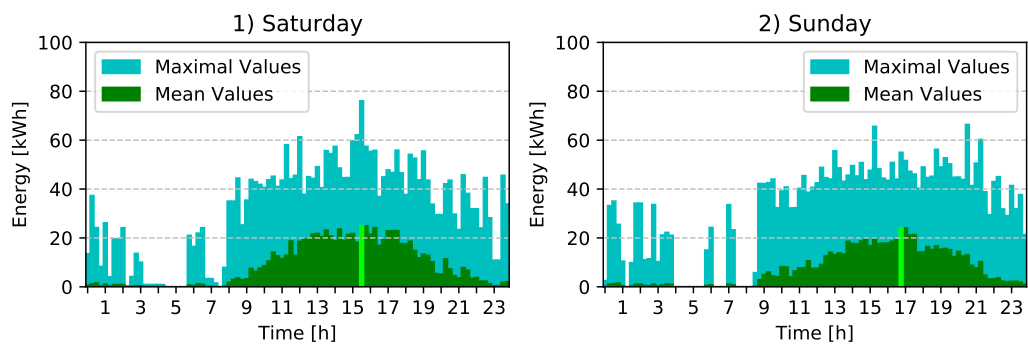


Figure A.4.: Mean of all Saturdays and Sundays in the observation period from charging site B

A.3. results of monthly evaluation of charging sites A&B

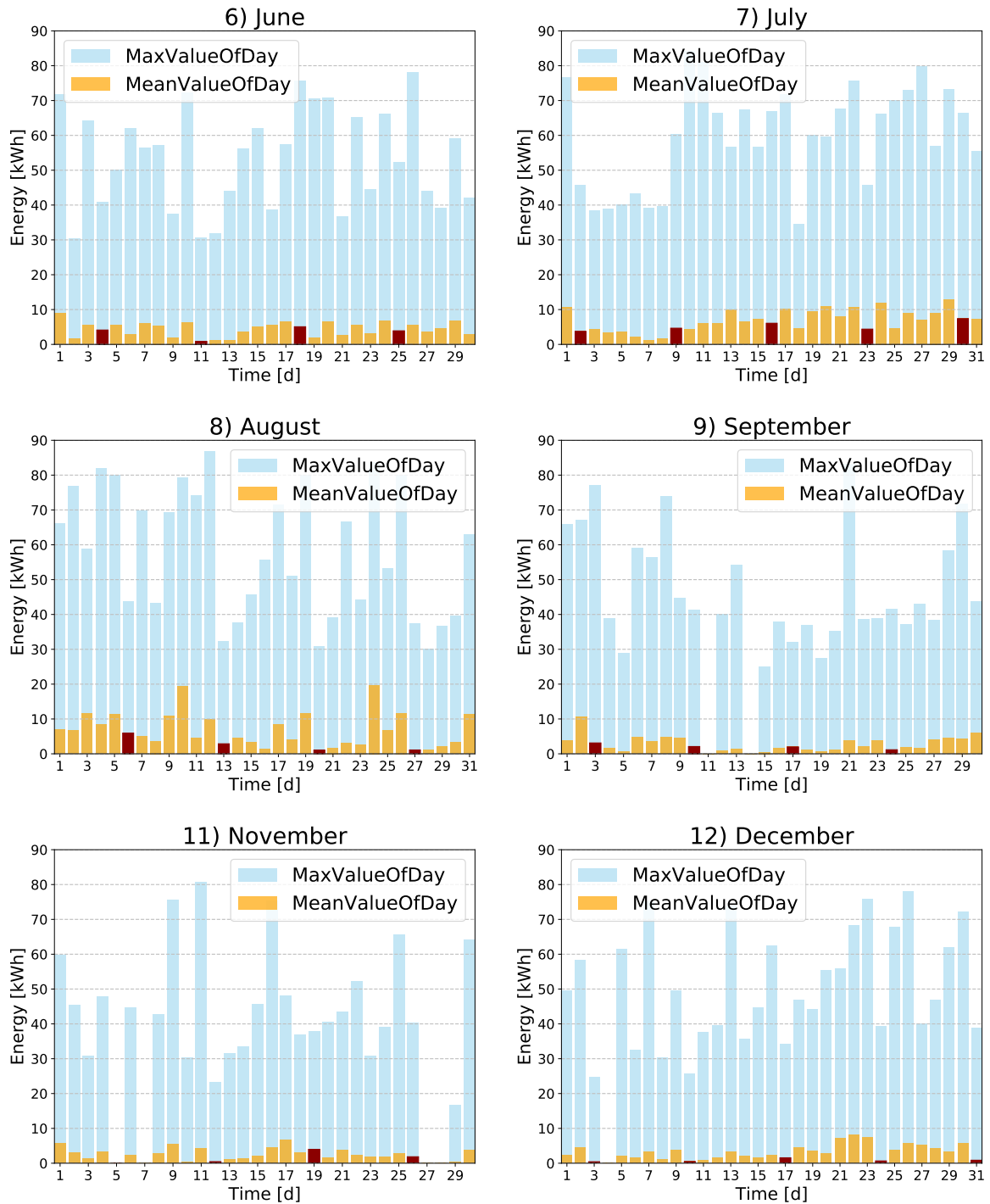


Figure A.5.: Monthly evaluation of the charging profiles on a daily basis (Charging Site A)

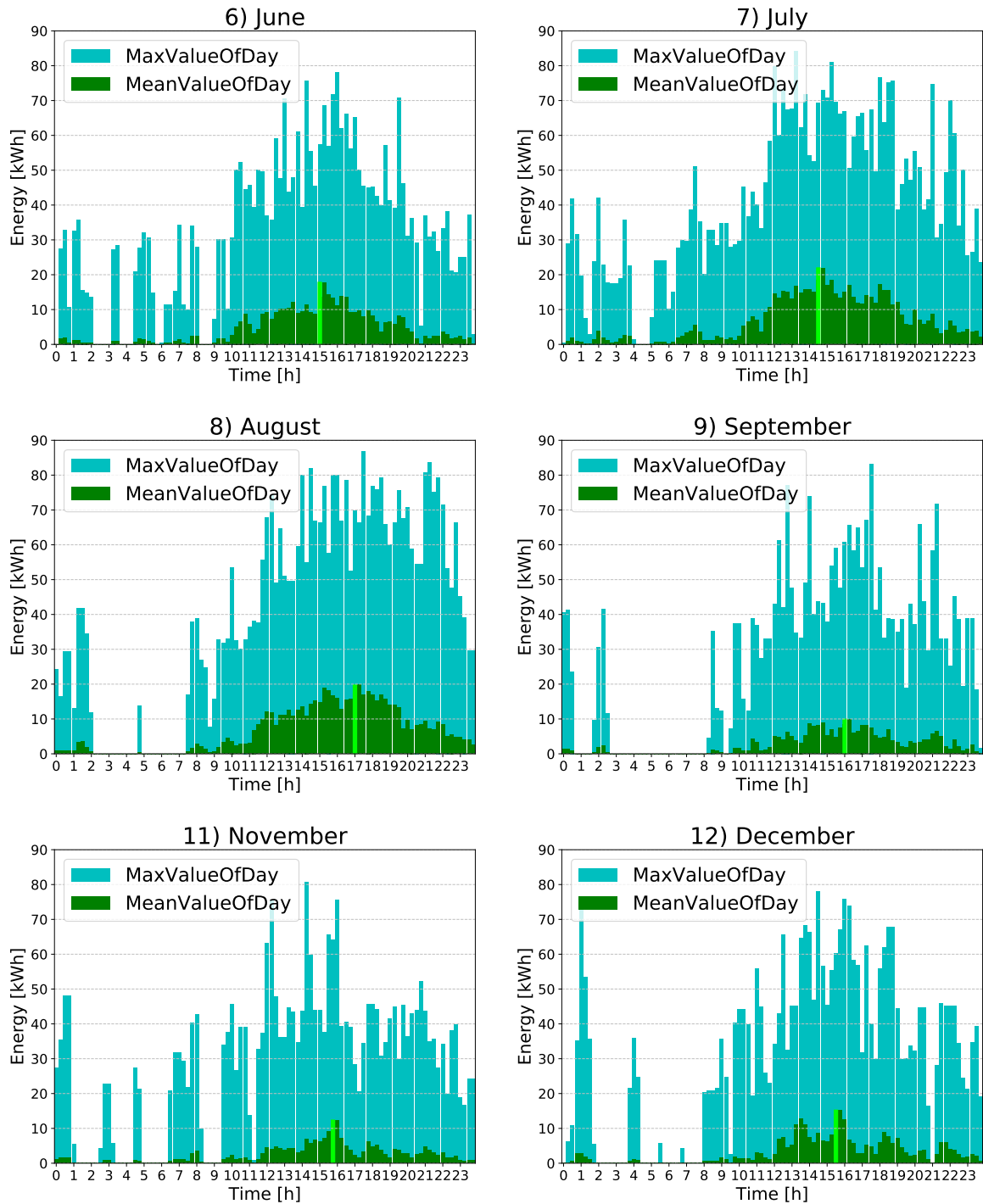


Figure A.6.: Monthly evaluation of the charging profiles on a 24h basis (Charging Site A)

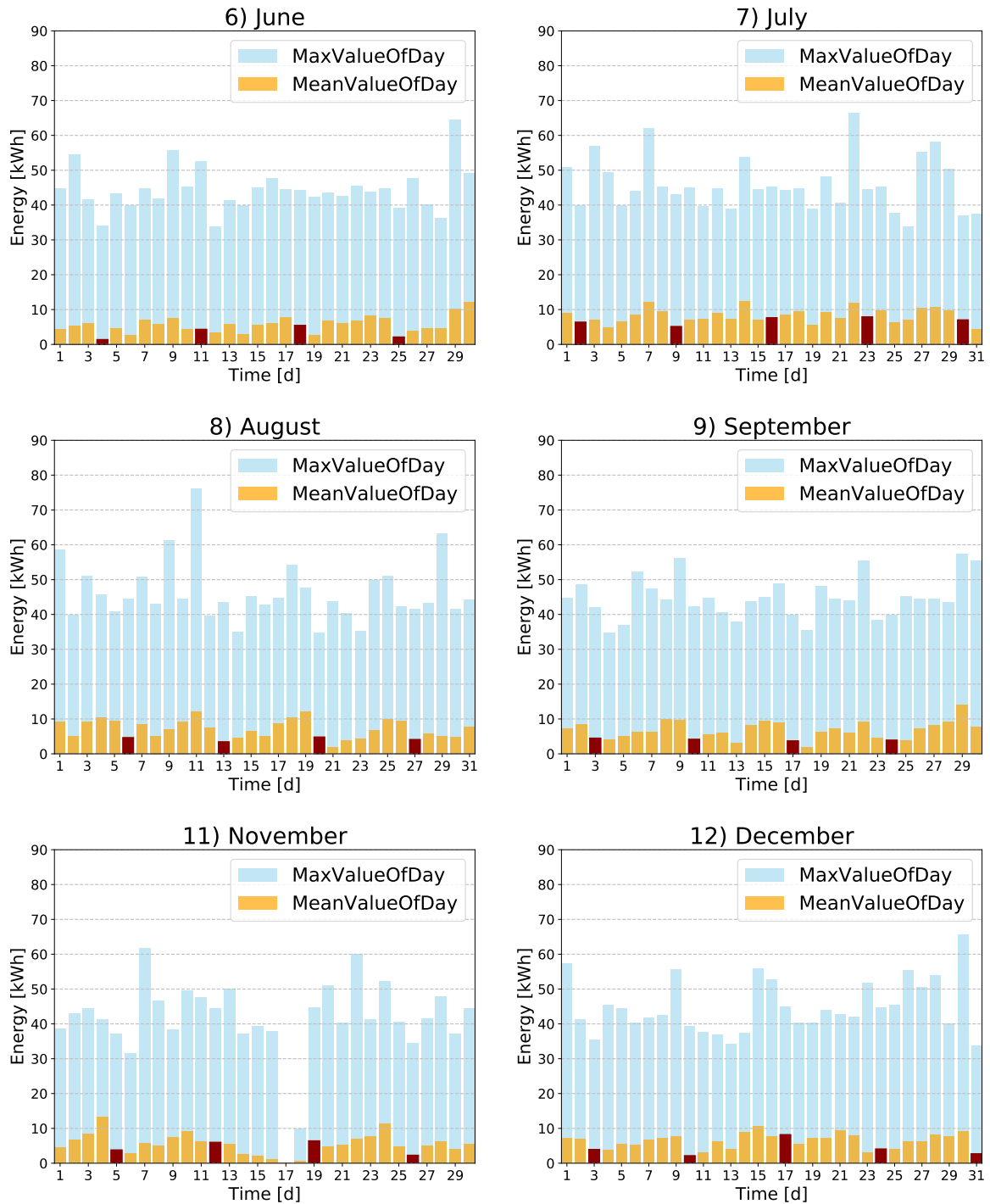


Figure A.7.: Monthly evaluation of the charging profiles on a daily basis (Charging Site B)

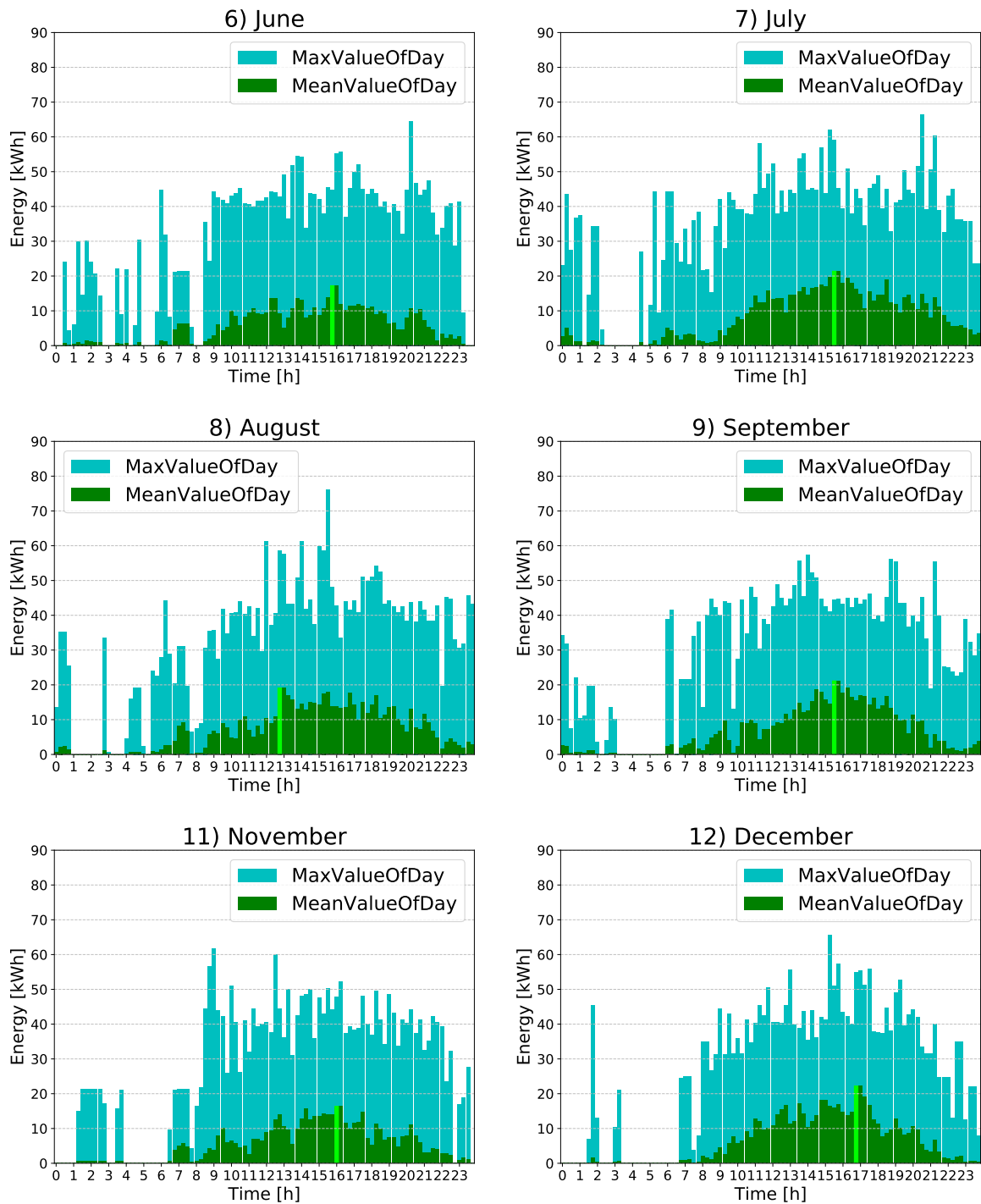


Figure A.8.: Monthly evaluation of the charging profiles on a 24h basis (Charging Site B)

A.4. Results of peak-shaving optimization with the BES for charging sites A & B

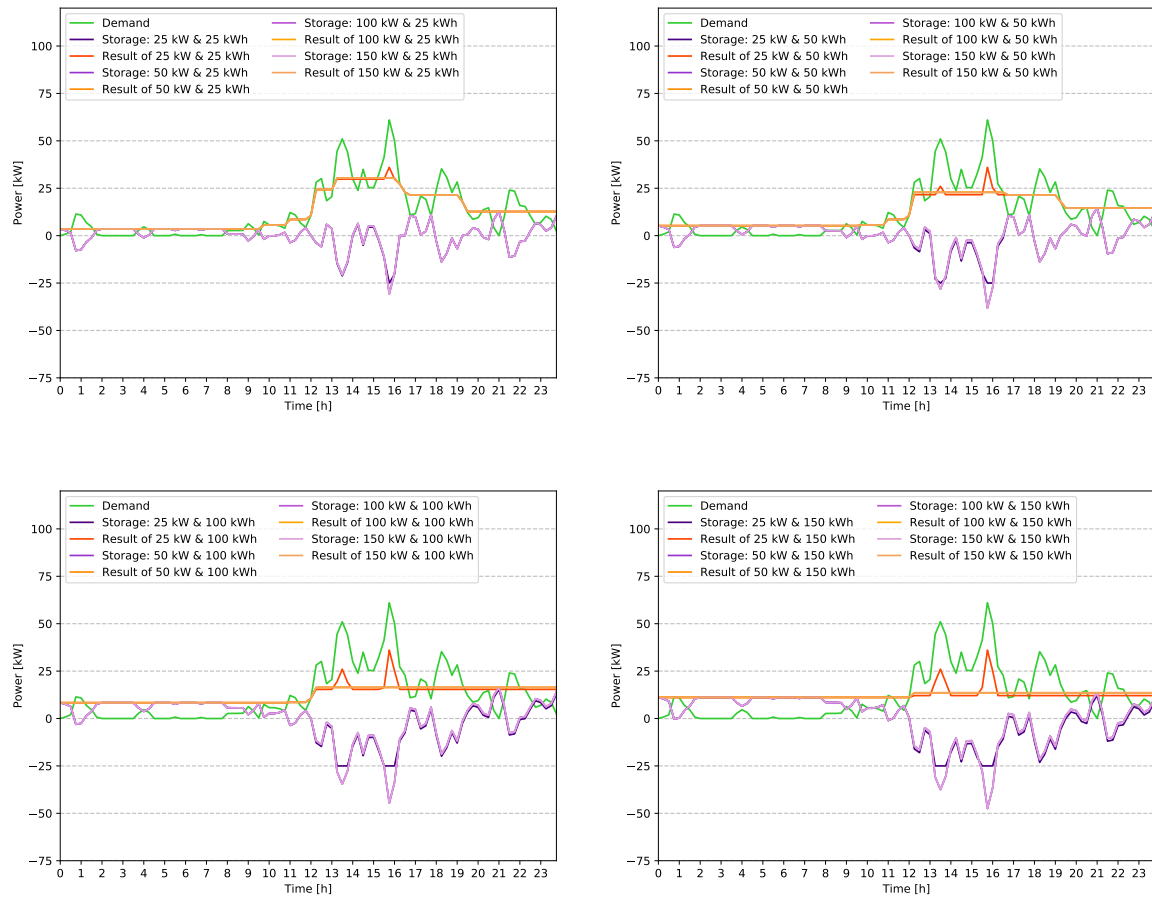


Figure A.9.: Monthly evaluation of the charging profiles with BES system on a 24h basis (Charging Site A, low demand)

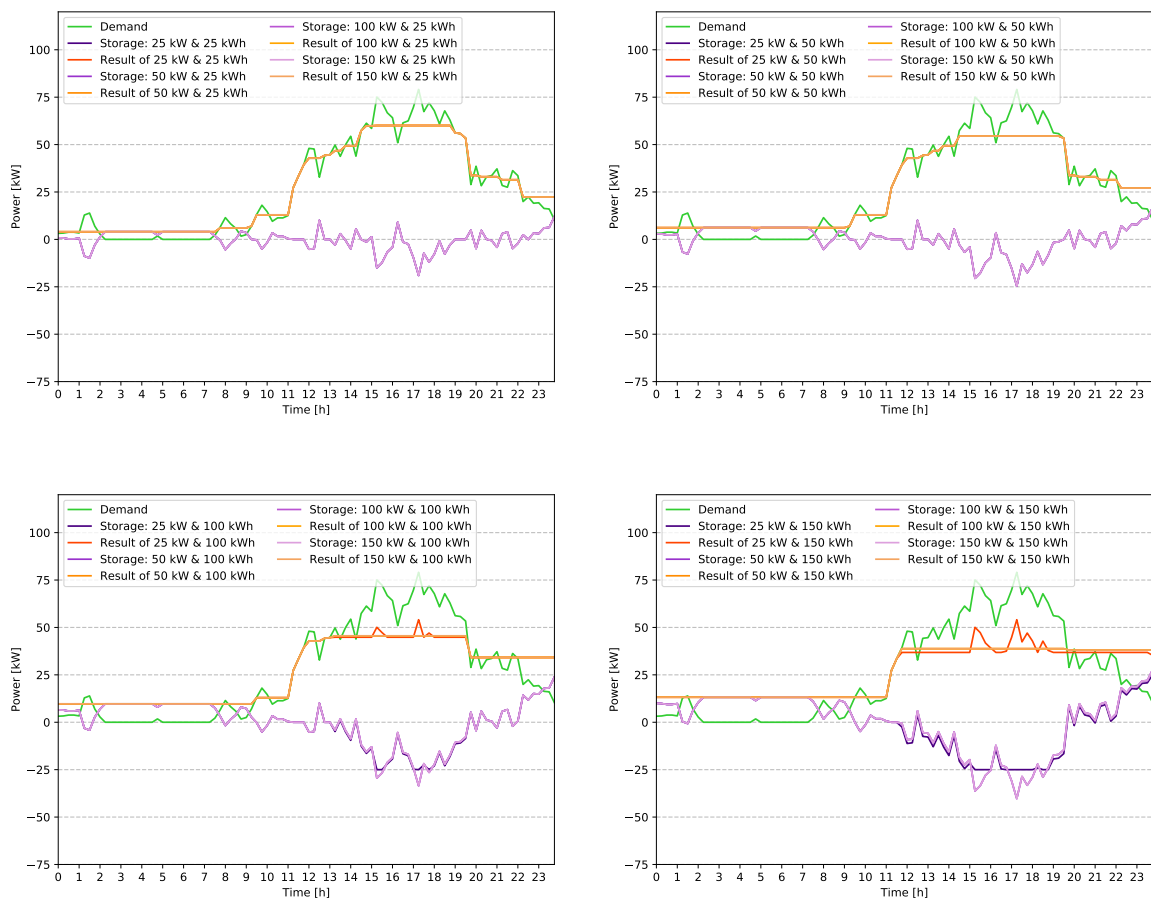


Figure A.10.: Monthly evaluation of the charging profiles with BES system on a 24h basis (Charging Site A, medium demand)

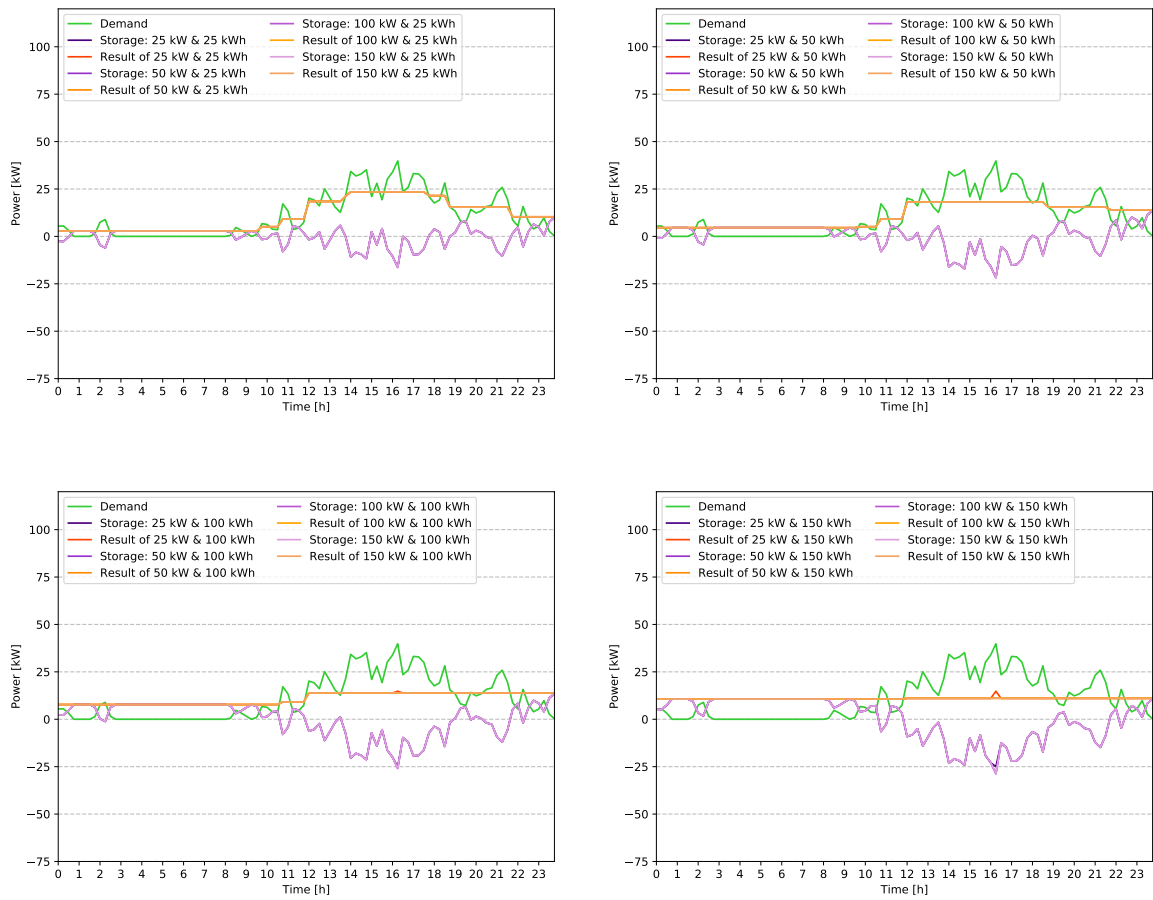


Figure A.11.: Monthly evaluation of the charging profiles with BES system on a 24h basis (Charging Site A, high demand)

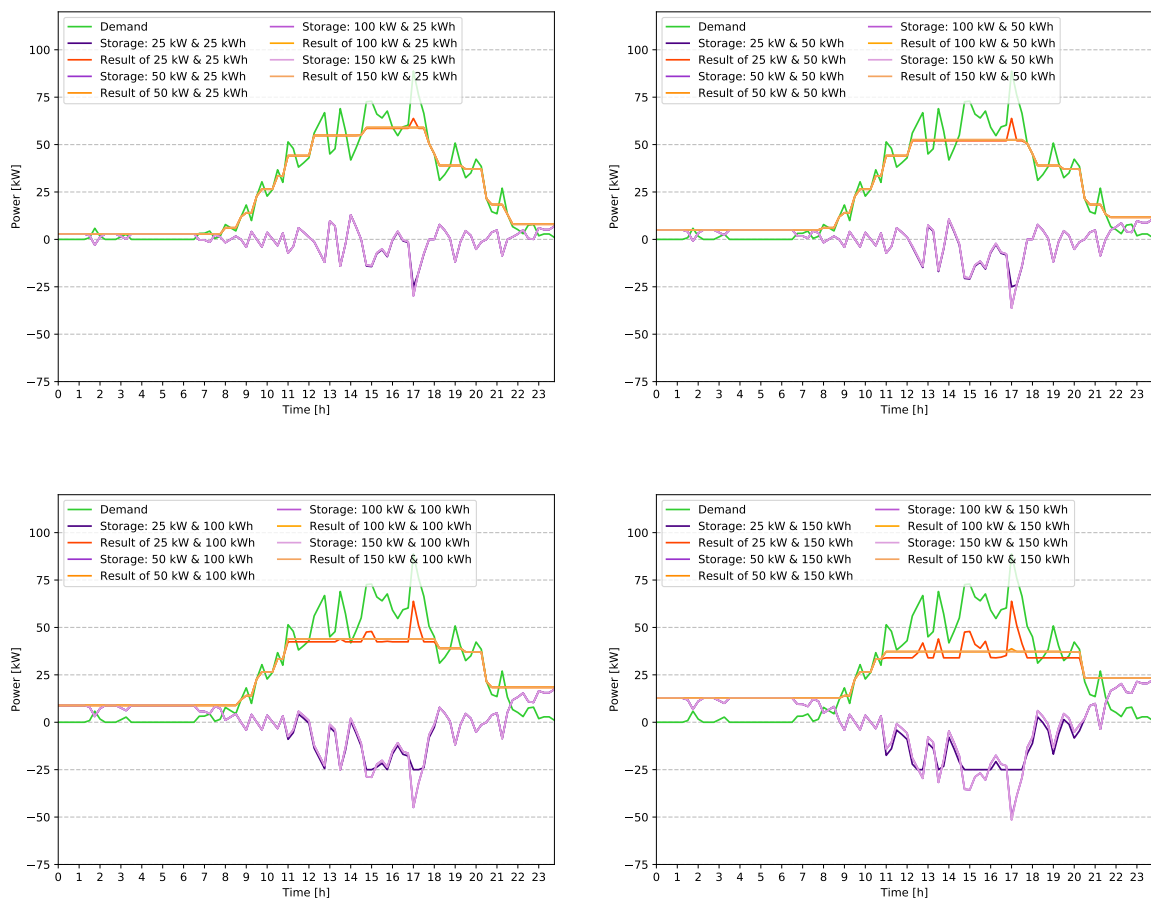


Figure A.12.: Monthly evaluation of the charging profiles with BES system on a 24h basis (Charging Site B, low demand)

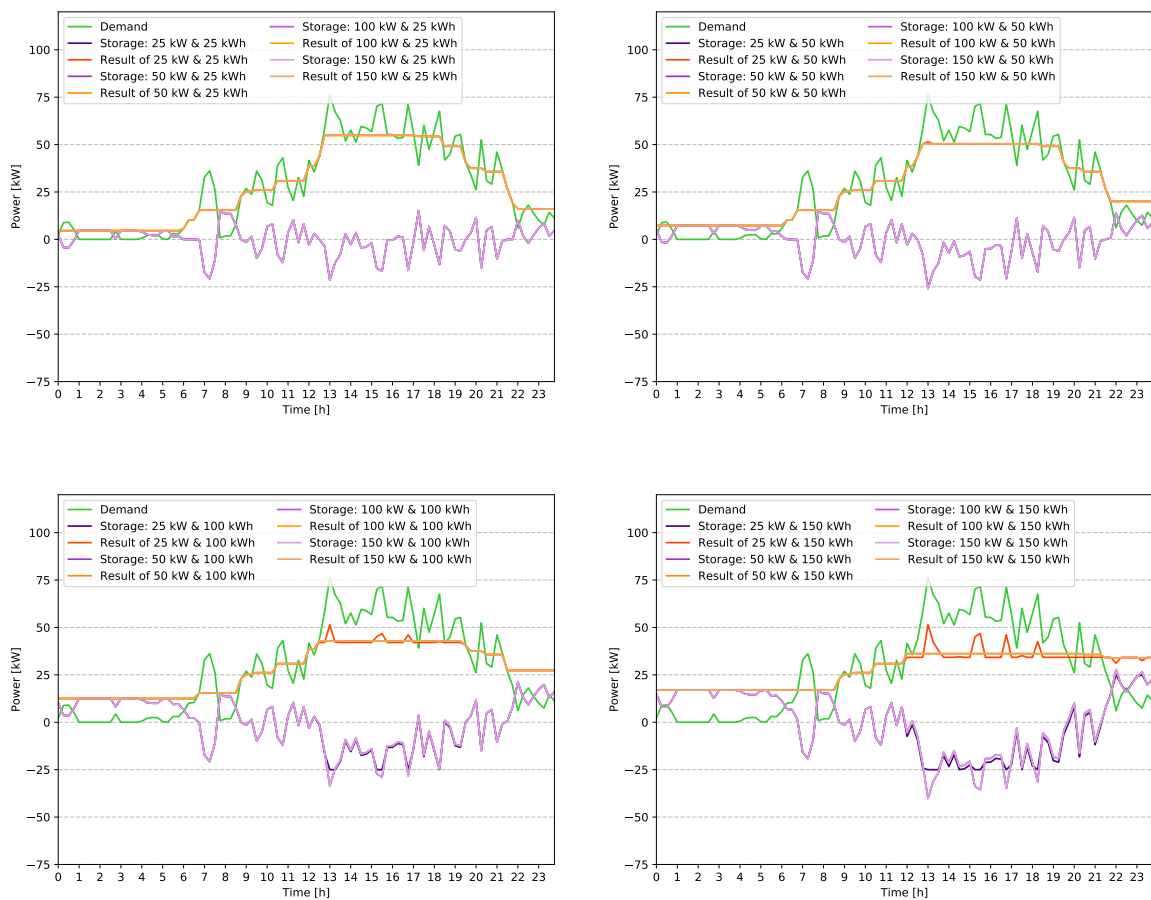


Figure A.13.: Monthly evaluation of the charging profiles with BES system on a 24h basis (Charging Site B, medium demand)

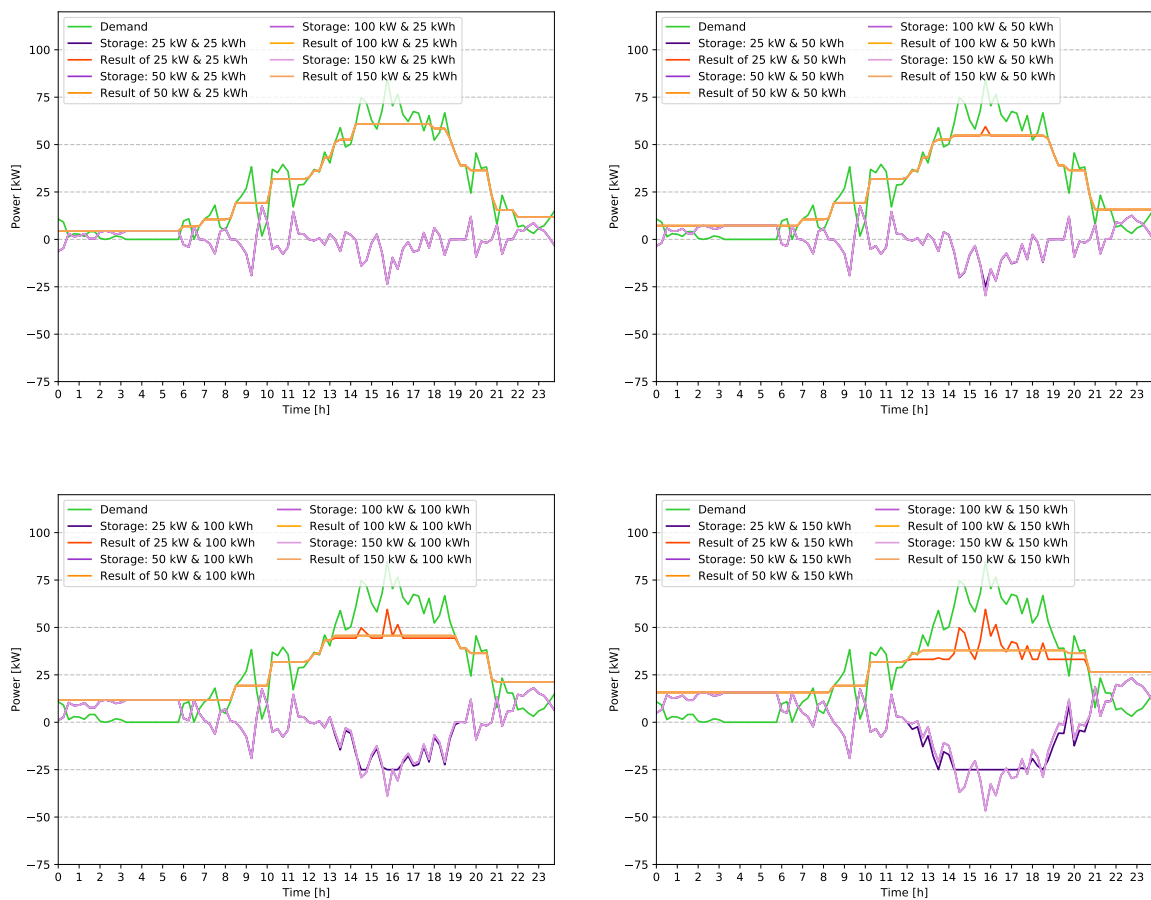


Figure A.14.: Monthly evaluation of the charging profiles with BES system on a 24h basis (Charging Site B, high demand)

A.5. Results of peak-shaving optimization with BES and PV system for charging sites A & B

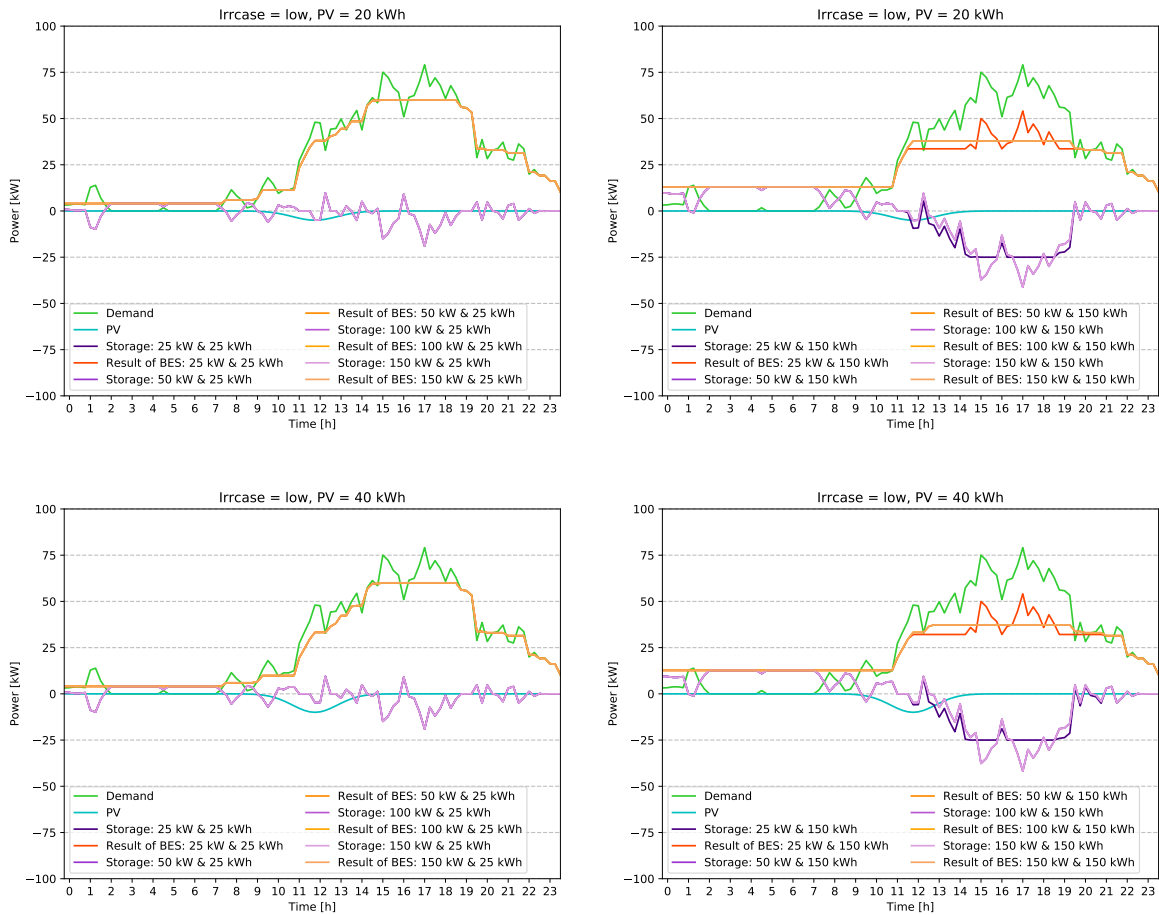


Figure A.15.: Monthly evaluation of the charging profiles with BES and PV system on a 24h basis (Charging Site B, low PV power)

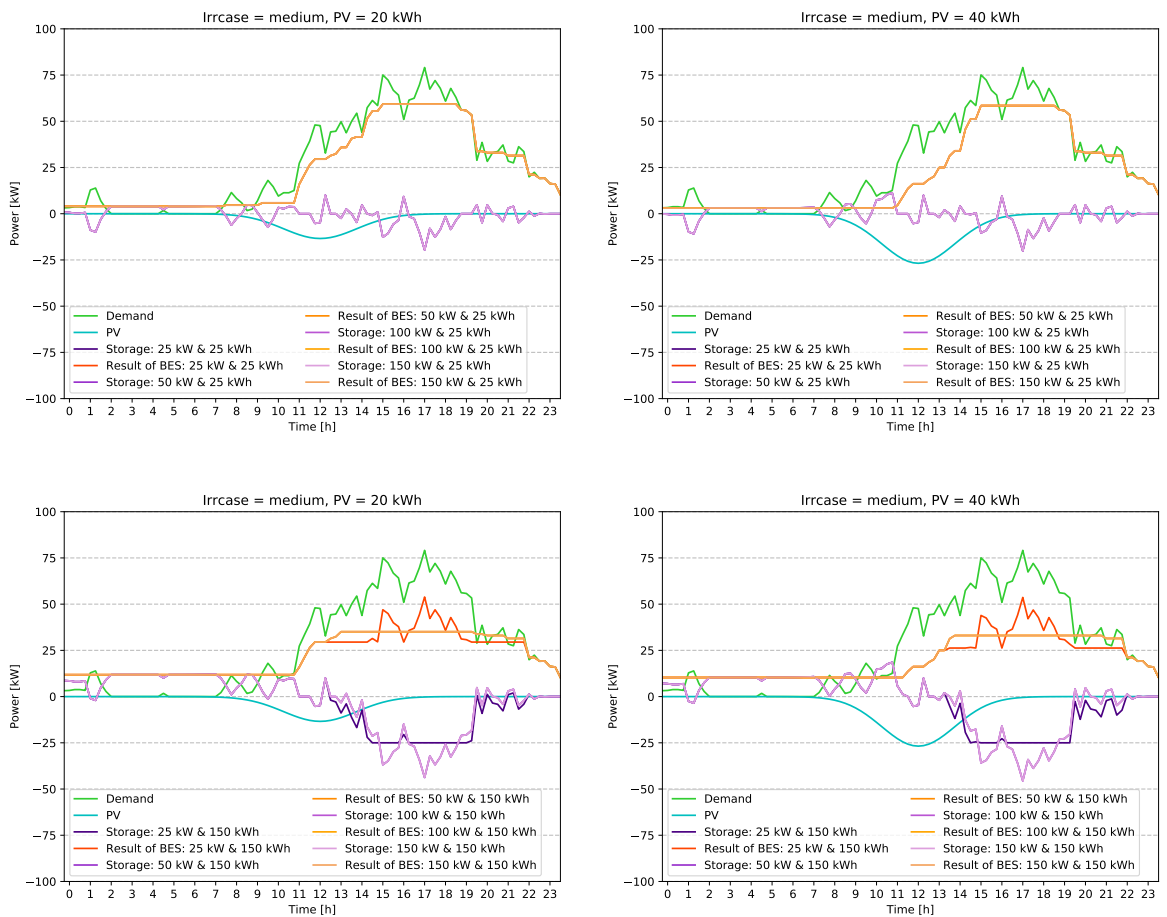


Figure A.16.: Monthly evaluation of the charging profiles with BES and PV system on a 24h basis (Charging Site B, medium PV power)

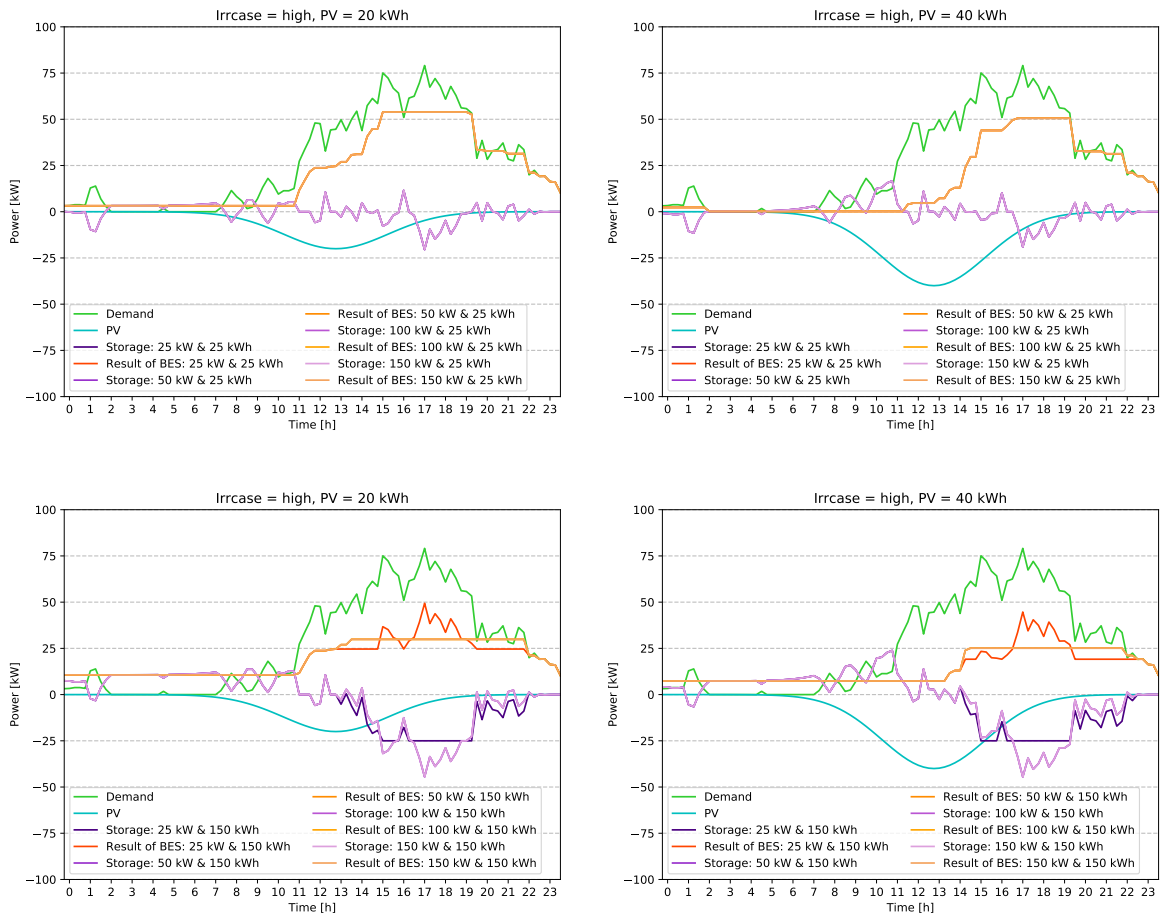


Figure A.17.: Monthly evaluation of the charging profiles with BES and PV system on a 24h basis (Charging Site B, high PV power)

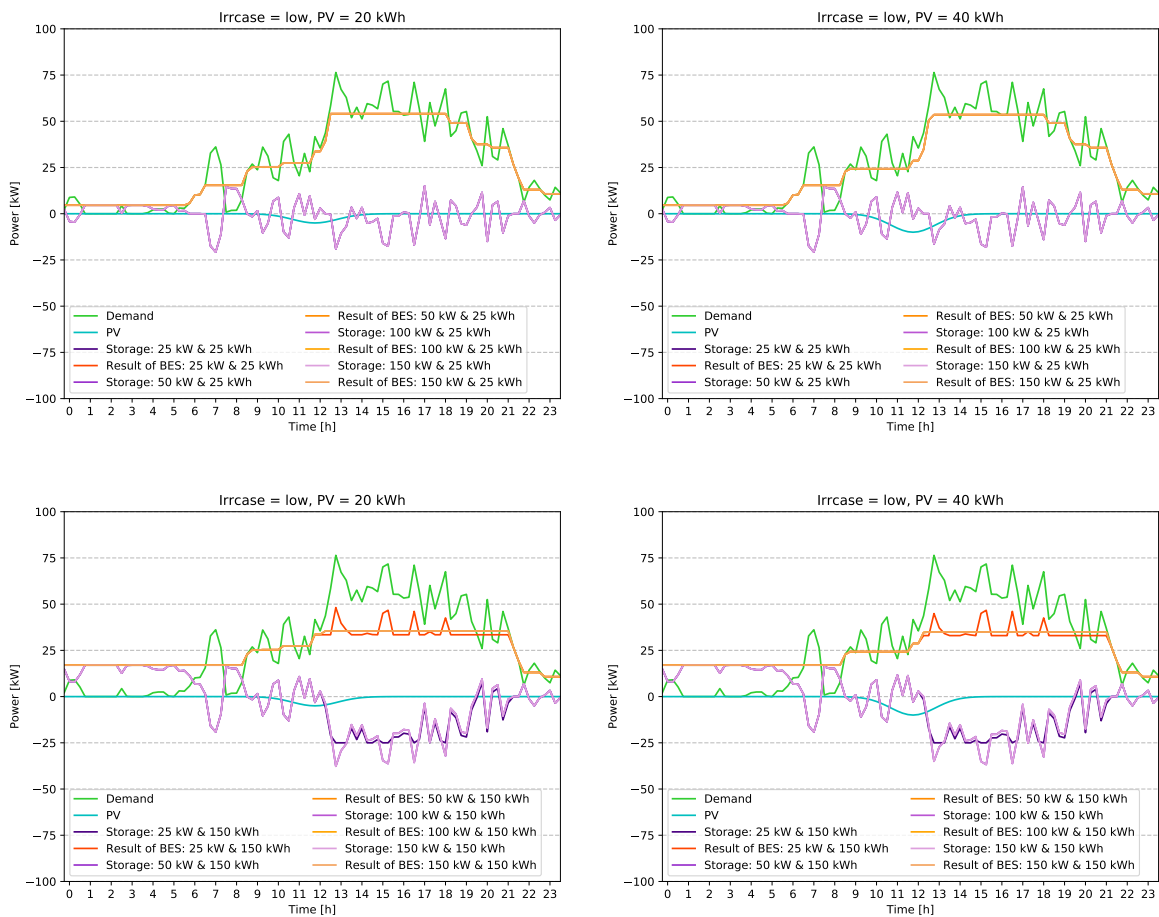


Figure A.18.: Monthly evaluation of the charging profiles with BES and PV system on a 24h basis (Charging Site A, low PV power)

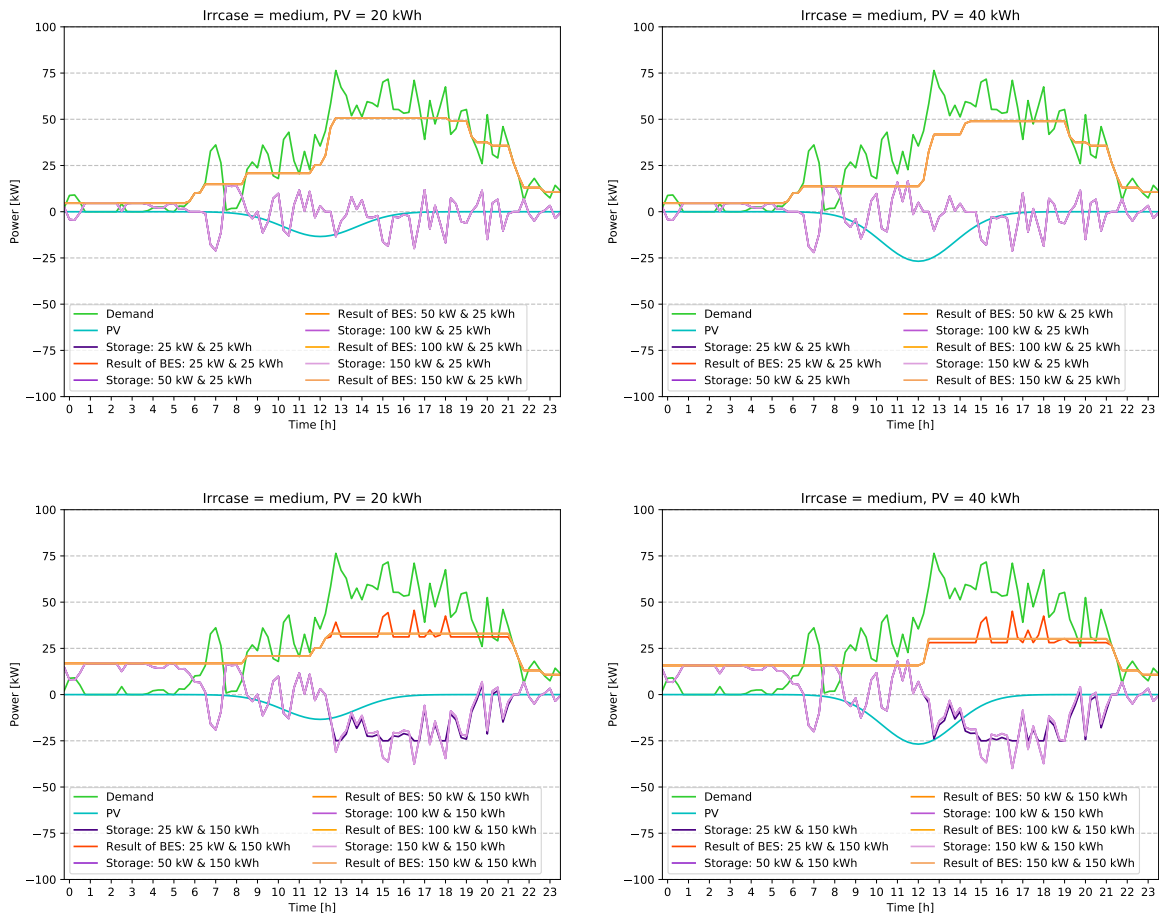


Figure A.19.: Monthly evaluation of the charging profiles with BES and PV system on a 24h basis (Charging Site A, medium PV power)

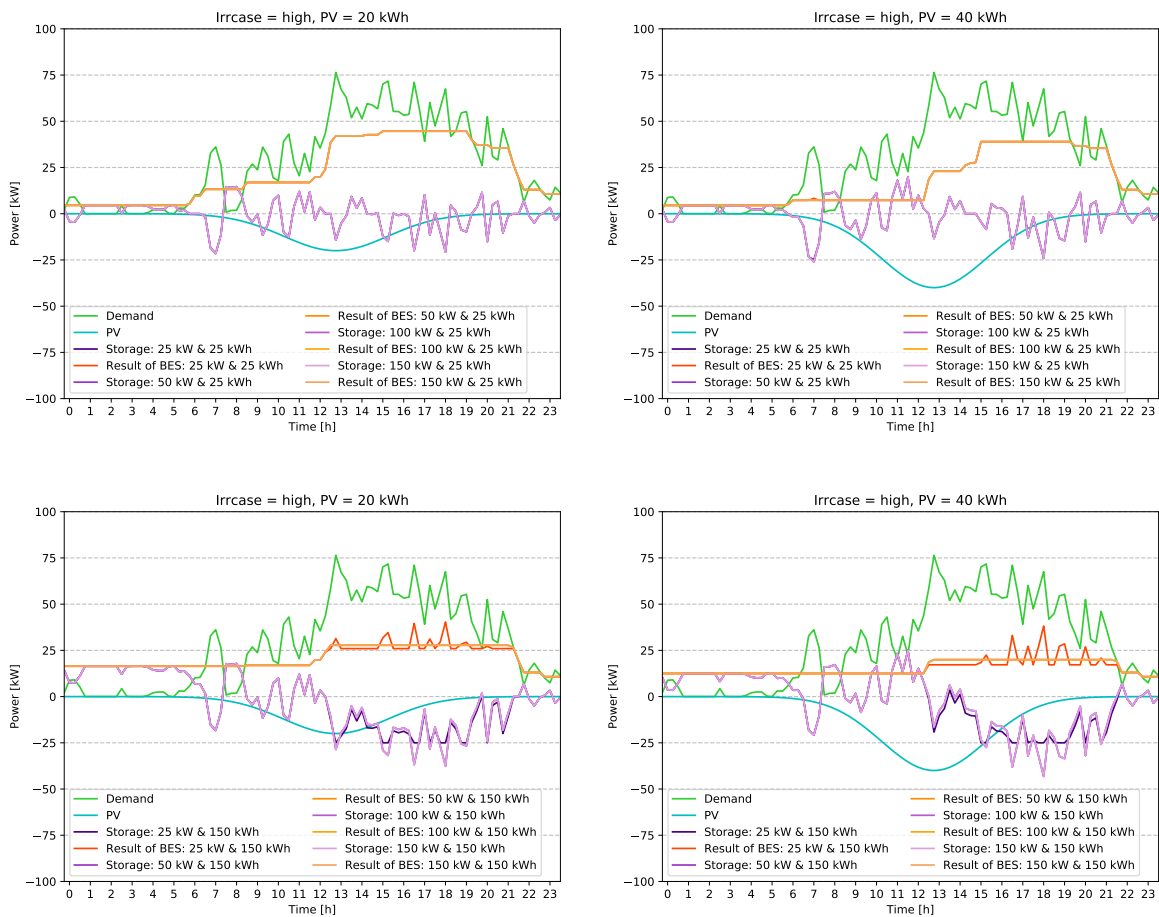


Figure A.20.: Monthly evaluation of the charging profiles with BES and PV system on a 24h basis (Charging Site A, high PV power)

Bibliography

- [1] Eu climate action. [Online]. Available: https://ec.europa.eu/clima/citizens/eu_en
- [2] B. S. R. of World Energy, “Bp statistical review of world energy 2019,” London. [Online]. Available: <https://www.bp.com/content/dam/bp/business-sites/en/global/corporate/pdfs/energy-economics/statistical-review/bp-stats-review-2019-full-report.pdf>
- [3] 3.1 what kind of energy do we consume in the eu? [Online]. Available: <https://ec.europa.eu/eurostat/cache/infographs/energy/bloc-3a.html>
- [4] A. J. Cheng, B. Tarroja, B. Shaffer, and S. Samuelsen, “Comparing the emissions benefits of centralized vs. decentralized electric vehicle smart charging approaches: A case study of the year 2030 california electric grid,” *Journal of Power Sources*, vol. 401, pp. 175–185, 2018.
- [5] M. Weiss, A. Zerfass, and E. Helmers, “Fully electric and plug-in hybrid cars - an analysis of learning rates, user costs, and costs for mitigating co2 and air pollutant emissions,” *Journal of Cleaner Production*, vol. 212, pp. 1478–1489, 2019.
- [6] Tesla model s. [Online]. Available: https://www.tesla.com/de_DE/models
- [7] Á. Cunha, J. Martins, N. Rodrigues, and F. P. Brito, “Vanadium redox flow batteries: a technology review,” *International Journal of Energy Research*, vol. 39, no. 7, pp. 889–918, 2015.
- [8] M. A. Quddus, M. Kabli, and M. Marufuzzaman, “Modeling electric vehicle charging station expansion with an integration of renewable energy and vehicle-to-grid sources,” *Transportation Research Part E: Logistics and Transportation Review*, vol. 128, pp. 251–279, 2019.
- [9] 2019 nissan leaf range, charging and battery. [Online]. Available: <https://www.nissanusa.com/vehicles/electric-cars/leaf/features/range-charging-battery.html>
- [10] M. Nicholas and D. Hall, “Lessons learned on early electric vehicle fast-charging deployments.”

- [11] E. Handschin, *Elektrische Energieübertragungssysteme*, ser. Eltex Studientexte Elektrotechnik. Heidelberg: Hüthig, 1992.
- [12] K. Smith, S. Galloway, and G. Burt, Ed., *Co-location of CHP units for High Power Charging of Battery Electric Vehicles: A comparison of the fuel efficiency for AC and DC coupled systems*, Glasgow, U.K., 2017.
- [13] M. Muratori, E. Elgqvist, D. Cutler, J. Eichman, S. Salisbury, Z. Fuller, and J. Smart, "Technology solutions to mitigate electricity cost for electric vehicle dc fast charging," *Applied Energy*, vol. 242, pp. 415–423, 2019.
- [14] F. Raulf, "Dc fast charging in oslo: Evaluating the charging behavior and the impact of a stationary battery," Master, TU Dortmund University, Dortmund, Germany, 2019.
- [15] Ac charging vs dc charging. [Online]. Available: https://newmotion.com/en_GB/ac-charging-vs-dc-charging
- [16] "Abb trafostationen schlÃ¼sselfertig aus einer hand."
- [17] L. Novoa and J. Brouwer, "Dynamics of an integrated solar photovoltaic and battery storage nanogrid for electric vehicle charging," *Journal of Power Sources*, vol. 399, pp. 166–178, 2018.
- [18] S. Singh, S. Jagota, and M. Singh, "Energy management and voltage stabilization in an islanded microgrid through an electric vehicle charging station," *Sustainable Cities and Society*, vol. 41, pp. 679–694, 2018.
- [19] J. A. Domínguez-Navarro, R. Dufo-López, J. M. Yusta-Loyo, J. S. Artal-Sevil, and J. L. Bernal-Agustín, "Design of an electric vehicle fast-charging station with integration of renewable energy and storage systems," *International Journal of Electrical Power & Energy Systems*, vol. 105, pp. 46–58, 2019.
- [20] H. Mehrjerdi and R. Hemmati, "Electric vehicle charging station with multilevel charging infrastructure and hybrid solar-battery-diesel generation incorporating comfort of drivers," *Journal of Energy Storage*, vol. 26, p. 100924, 2019.
- [21] Norway. [Online]. Available: <https://www.hydropower.org/country-profiles/norway>
- [22] C. Acar, "A comprehensive evaluation of energy storage options for better sustainability," *International Journal of Energy Research*, vol. 42, no. 12, pp. 3732–3746, 2018.
- [23] M. Hasanuzzaman, U. S. Zubir, N. I. Ilham, and H. Seng Che, "Global electricity demand, generation, grid system, and renewable energy polices: a review,"

- Wiley Interdisciplinary Reviews: Energy and Environment*, vol. 6, no. 3, p. e222, 2017.
- [24] O. Krishan and S. Suhag, “An updated review of energy storage systems: Classification and applications in distributed generation power systems incorporating renewable energy resources,” *International Journal of Energy Research*, vol. 36, no. 15, p. 40, 2018.
- [25] M. Resch, J. Bühler, B. Schachler, R. Kunert, A. Meier, and A. Sumper, “Technical and economic comparison of grid supportive vanadium redox flow batteries for primary control reserve and community electricity storage in germany,” *International Journal of Energy Research*, vol. 43, no. 1, pp. 337–357, 2019.
- [26] G. Kear, A. A. Shah, and F. C. Walsh, “Development of the all-vanadium redox flow battery for energy storage: a review of technological, financial and policy aspects,” *International Journal of Energy Research*, vol. 36, no. 11, pp. 1105–1120, 2012.
- [27] M. French, *Fundamentals of optimization: Methods, minimum principles, and applications for making things better*. Cham: Springer, 2018.
- [28] J. A. Snyman and D. N. Wilke, *Practical mathematical optimization: Basic optimization theory and gradient-based algorithms*, second edition ed., ser. Springer optimization and its applications. Cham: Springer, 2018, vol. Volume 133.
- [29] D. G. Luenberger and Y. Ye, *Linear and nonlinear programming*, 4th ed., ser. International series in operations research & management science. Cham: Springer, 2016, vol. 228.
- [30] J. A. Momoh, R. Adapa, and M. E. El-Hawary, “A review of selected optimal power flow literature to 1993. i. nonlinear and quadratic programming approaches,” *IEEE Transactions on Power Systems*, vol. 14, no. 1, pp. 96–104, 1999.
- [31] J. Mahmoudimehr and P. Sebghati, “A novel multi-objective dynamic programming optimization method: Performance management of a solar thermal power plant as a case study,” *Energy*, vol. 168, pp. 796–814, 2019.
- [32] J. Mahmoudimehr and L. Loghmani, “Optimal management of a solar power plant equipped with a thermal energy storage system by using dynamic programming method,” *Proceedings of the Institution of Mechanical Engineers, Part A: Journal of Power and Energy*, vol. 230, no. 2, pp. 219–233, 2016.

- [33] R. Bellman, "Dynamic programming," *Science (New York, N.Y.)*, vol. 153, no. 3731, pp. 34–37, 1966.
- [34] X. P. Chen, N. Hewitt, Z. T. Li, Q. M. Wu, X. Yuan, and T. Roskilly, "Dynamic programming for optimal operation of a biofuel micro chp-hes system," *Applied Energy*, vol. 208, pp. 132–141, 2017.
- [35] A. L. Facci, L. Andreassi, and S. Ubertini, "Optimization of chcp (combined heat power and cooling) systems operation strategy using dynamic programming," *Energy*, vol. 66, pp. 387–400, 2014.
- [36] M. Farrokhifar, "Optimal operation of energy storage devices with res to improve efficiency of distribution grids; technical and economical assessment," *International Journal of Electrical Power & Energy Systems*, vol. 74, pp. 153–161, 2016.
- [37] C. O. Onwubiko, *Introduction to engineering design optimization*. Upper Saddle River, NJ: Prentice-Hall, 2000.
- [38] C. T. R. Belegundu A. D., *Optimization Concepts and Applications in Engineering*. Prentice Hall, 1999.
- [39] S. J. Wright and J. Nocedal, *Numerical Optimization*. Springer New York, 2006.
- [40] J. B. Ekanayake, N. Jenkins, K. Liyanage, J. Wu, and A. Yokoyama, *Smart Grid: Technology and Applications*, 1st ed. UK: Wiley, 2012.
- [41] S. Chouhan, D. Tiwari, H. Inan, S. Khushalani-Solanki, and A. Feliachi, "Der optimization to determine optimum bess charge/discharge schedule using linear programming," in *2016 IEEE Power and Energy Society General Meeting (PESGM)*. IEEE, 7/17/2016 - 7/21/2016, pp. 1–5.
- [42] Linear programming algorithms. [Online]. Available: <https://www.mathworks.com/help/optim/ug/linear-programming-algorithms.html>
- [43] D. M. Pedroso, M. R. Bonyadi, and M. Gallagher, "Parallel evolutionary algorithm for single and multi-objective optimisation: Differential evolution and constraints handling," *Applied Soft Computing*, vol. 61, pp. 995–1012, 2017.
- [44] G. Chiandussi, M. Codegone, S. Ferrero, and F. E. Varesio, "Comparison of multi-objective optimization methodologies for engineering applications," *Computers & Mathematics with Applications*, vol. 63, no. 5, pp. 912–942, 2012.
- [45] W. F. Abd-El-Wahed, A. A. Mousa, and M. A. El-Shorbagy, "Integrating particle swarm optimization with genetic algorithms for solving nonlinear optimization

- problems,” *Journal of Computational and Applied Mathematics*, vol. 235, no. 5, pp. 1446–1453, 2011.
- [46] G. Squillero and P. Burelli, Eds., *Applications of evolutionary computation: 19th European conference, EvoApplications 2016, Porto, Portugal, March 30 - April 1, 2016, proceedings*, 1st ed., ser. LNCS Sublibrary: SL1 - Theoretical Computer Science and General Issues. [Switzerland]: Springer, 2016, vol. 9597-9598.
- [47] M. Alonso, H. Amaris, J. Germain, and J. Galan, “Optimal charging scheduling of electric vehicles in smart grids by heuristic algorithms,” *Energies*, vol. 7, no. 4, pp. 2449–2475, 2014.
- [48] M. Z. Daud, A. Mohamed, A. A. Ibrahim, and M. A. Hannan, “Heuristic optimization of state-of-charge feedback controller parameters for output power dispatch of hybrid photovoltaic/battery energy storage system,” *Measurement*, vol. 49, pp. 15–25, 2014.
- [49] J. A. Domínguez-Navarro, R. Dufo-López, J. M. Yusta-Loyo, J. S. Artal-Sevil, and J. L. Bernal-Agustín, “Design of an electric vehicle fast-charging station with integration of renewable energy and storage systems,” *International Journal of Electrical Power & Energy Systems*, vol. 105, pp. 46–58, 2019.
- [50] M. Motevasel, A. R. Seifi, and T. Niknam, “Multi-objective energy management of chp (combined heat and power)-based micro-grid,” *Energy*, vol. 51, pp. 123–136, 2013.
- [51] C. Liu, Y. Wang, L. Wang, and Z. Chen, “Load-adaptive real-time energy management strategy for battery/ultracapacitor hybrid energy storage system using dynamic programming optimization,” *Journal of Power Sources*, vol. 438, p. 227024, 2019.
- [52] Documentation. [Online]. Available: <https://pandas.pydata.org/pandas-docs/stable/#>
- [53] Overview. [Online]. Available: <https://wiki.python.org/moin/BeginnersGuide/Overview>
- [54] The python tutorial. [Online]. Available: <https://docs.python.org/3.7/tutorial/>
- [55] M. Lutz, *Learning Python*, fifth edition ed. Beijing and Boston and Farnham and Sebastopol and Tokyo: O’Reilly, 2017.
- [56] B. Slatkin, *Effective Python: 59 specific ways to write better Python*, ser. Effective software development series. Upper Saddle River, NJ: Addison-

-
- Wesley, 2015. [Online]. Available: <http://proquest.tech.safaribooksonline.de/9780134034416>
- [57] The python language reference. [Online]. Available: <https://docs.python.org/3.7/reference/>
- [58] Extending and embedding the python interpreter. [Online]. Available: <https://docs.python.org/3.7/extending/>
- [59] Documentation. [Online]. Available: <https://matplotlib.org/contents.html>
- [60] Numpy. [Online]. Available: <https://numpy.org/>
- [61] Scipy. [Online]. Available: <https://docs.scipy.org/doc/scipy/reference/>
- [62] sqlite3 - db-api 2.0 interface for sqlite databases. [Online]. Available: <https://docs.python.org/3.7/library/sqlite3.html>
- [63] Fahrzeuge & lade tipps. [Online]. Available: <https://support.fastned.nl/hc/de/sections/115000180588-Fahrzeuge-Lade-Tipps>
- [64] Ev models. [Online]. Available: <https://thedriven.io/ev-models/>
- [65] J. Usaola, X. Ayon, L. Verheggen, A. Supponen, and S. Repo, *Simulated benefits of active distribution network concept and applications*. Tampere University of Technology, 2016.
- [66] scipy.optimize.minimize. [Online]. Available: <https://docs.scipy.org/doc/scipy/reference/generated/scipy.optimize.minimize.html#rdd2e1855725e-12>

Eidesstattliche Versicherung (Affidavit)

Rohde, Lena

166565

Name, Vorname
(Last name, first name)

Matrikelnr.
(Enrollment number)

Ich versichere hiermit an Eides statt, dass ich die vorliegende Bachelorarbeit/Masterarbeit* mit dem folgenden Titel selbstständig und ohne unzulässige fremde Hilfe erbracht habe. Ich habe keine anderen als die angegebenen Quellen und Hilfsmittel benutzt sowie wörtliche und sinngemäße Zitate kenntlich gemacht. Die Arbeit hat in gleicher oder ähnlicher Form noch keiner Prüfungsbehörde vorgelegen.

I declare in lieu of oath that I have completed the present Bachelor's/Master's* thesis with the following title independently and without any unauthorized assistance. I have not used any other sources or aids than the ones listed and have documented quotations and paraphrases as such. The thesis in its current or similar version has not been submitted to an auditing institution.

Titel der ~~Bachelor-/~~Masterarbeit*:
(Title of the ~~Bachelor's/~~ Master's* thesis):

Electric vehicle fast charging with energy storage and generation capabilities

- Simulations based on real charging data

*Nichtzutreffendes bitte streichen
(Please choose the appropriate)

Dortmund, 31.01.2020

Ort, Datum
(Place, date)

Unterschrift
(Signature)



Belehrung:

Wer vorsätzlich gegen eine die Täuschung über Prüfungsleistungen betreffende Regelung einer Hochschulprüfungsordnung verstößt, handelt ordnungswidrig. Die Ordnungswidrigkeit kann mit einer Geldbuße von bis zu 50.000,00 € geahndet werden. Zuständige Verwaltungsbehörde für die Verfolgung und Ahndung von Ordnungswidrigkeiten ist der Kanzler/die Kanzlerin der Technischen Universität Dortmund. Im Falle eines mehrfachen oder sonstigen schwerwiegenden Täuschungsversuches kann der Prüfling zudem exmatrikuliert werden. (§ 63 Abs. 5 Hochschulgesetz - HG -).

Die Abgabe einer falschen Versicherung an Eides statt wird mit Freiheitsstrafe bis zu 3 Jahren oder mit Geldstrafe bestraft.

Die Technische Universität Dortmund wird gfls. elektronische Vergleichswerkzeuge (wie z.B. die Software „turnitin“) zur Überprüfung von Ordnungswidrigkeiten in Prüfungsverfahren nutzen.

Die oben stehende Belehrung habe ich zur Kenntnis genommen:

Official notification:

Any person who intentionally breaches any regulation of university examination regulations relating to deception in examination performance is acting improperly. This offense can be punished with a fine of up to €50,000.00. The competent administrative authority for the pursuit and prosecution of offenses of this type is the chancellor of TU Dortmund University. In the case of multiple or other serious attempts at deception, the examinee can also be unenrolled, section 63, subsection 5 of the North Rhine-Westphalia Higher Education Act (*Hochschulgesetz*).

The submission of a false affidavit will be punished with a prison sentence of up to three years or a fine.

As may be necessary, TU Dortmund will make use of electronic plagiarism-prevention tools (e.g. the "turnitin" service) in order to monitor violations during the examination procedures.

I have taken note of the above official notification:**

Dortmund, 31.01.2020

Ort, Datum
(Place, date)

Unterschrift
(Signature)



**Please be aware that solely the German version of the affidavit ("Eidesstattliche Versicherung") for the Bachelor's/ Master's thesis is the official and legally binding version.